Investigations on The Finite Size Effects of Some Inverse Spinels and Studies on Their Composites Based on Nitrile Rubber

Thesis submitted to
Cochin University of Science and Technology
In partial fulfilment of the requirements for the award of the Degree of

Doctor of Philosophy

By

Mathew George

Department of Physics
Cochin University of Science & Technology
Cochin – 686 022
Kerala
India

February 2004

CERTIFICATE

Certified that the thesis entitled **"Investigations on The Finite Size Effects of Some Inverse Spinels and Studies on Their Composites Based on Nitrile Rubber"** is based on the bonafide research work carried out by Mr. Mathew George under my guidance, at Department of Physics, Cochin University of Science and Technology, Cochin-682 022 and has not been included in any other thesis submitted previously for the award of any degree.

Dr.M.R.Anantharaman
(Supervising Guide)
Reader
Department of Physics
Cochin University of
Science &Technology
Cochin-682 022

Cochin-22
16-02-2004

DECLARATION

I hereby declare that the work presented in this thesis entitled **"Investigations on The Finite Size Effects of Some Inverse Spinels and Studies on Their Composites Based on Nitrile Rubber"** is based on the original research work done by me under the guidance of ***Dr. M.R.Anantharaman,*** Reader, Department of Physics, Cochin University of Science and Technology, Cochin-682 022 and has never been included in any other thesis submitted previously for the award of any degree.

Cochin - 22

16.02.2004

Mathew George

Acknowledgments

It is a matter of joy for me to present this thesis and I wish to express my grateful appreciation to all who have enabled me to accomplish this piece of work.

With immense pleasure, I express my sincere thanks and indebtness to Dr. M.R. Ananthiaraman, my research guide, for the excellent guidance, constant encouragement, personal attention, patience and friendly attitude, with out which I won't be able to complete this research work successfully.

I am thankful to Prof K.P. Vijayakumar, Head, Department of Physics, CUSAT, Prof K. Babu Joseph, Prof. M.Sabir, Prof K.P. Rajappan Nair, and Prof. Elizabeth Mathai, former Heads, for providing me the necessary facilities.

With pleasure I am thankful to all faculty members especially Dr. S. Jayalakshmi and all non teaching staff of Department of Physics for their help throughout the course of work.

I am grateful to Dr. Philip Kurian, Professor, Department of Polymer Science and Rubber Technology, CUSAT for fruitful discussions and help at various stages of this work. The help rendered from Dr.P. Mohanan, Department of Electronics, for conducting the microwave absorption studies is greatly appreciated. I am also thankful Dr.M.R Prathapachandra Kurup, Department of Applied Chemistry, for providing me necessary laboratory facilities.

Let me express my sincere gratitude to Dr. P.A Joy, Dr.S.K Date and Dr. S D Kulkarni, Physical Chemistry Division, National Chemical Laboratory, Pune for conducting the magnetic measurements. I also mention with thanks the help received from Mr. Jose, Mr. Murali and Mr. Joshi of Instrumentation Department.

I thankfully acknowledge UGC for providing me the fellowship under FIP scheme.

I extend my heartful thanks to my colleagues, Dr. K.A. Malini, Dr. S Sindhu, Dr. Asha Mary John, Dr. M.A Solomon, Mrs. K.H Prema Mr. S Saravanan, Mr. Sathosh D Shenoy, Mrs Veena Gopalan, Mr. S Sagar, Mr. Blesson Mathew, Mr. Francis Xavier P.A, Mrs. Smitha Thankachan, Ms. Vijutha Sunny, Mr. Rrajeev R, Ashokan, Mr. Sanoj M.A and Mr. Dineshan T for their affection, encouragement and valuable helps.

My warm appreciation goes to Dr. Joe Jacob and Dr. Saji Augustine for their help and encouragement received during various stages of my work. I am thankful to all the research scholars especially Mrs. T Nandini, Mr. Sunny Kuriakose, Mr. K.K. Vijayan and Mrs. Shyamalakumari of Department of Physics. I am also thankful to Miss. Litty Alen and Mr. Rajesh of Department of Polymer Science and Rubber Technology for their valuable help during the period of preparation of samples.

Words are insufficient to express my gratitude to Dr. E.M. Mohamed, Mr. E. Muhammed Abdul Jamal, Mr. Sajeev U.S and Ms. Swapna. S. Nair for their rewardless help and love during the period of my research work.

The support and encouragement received from the Principals and my colleagues at Maharajas College and Govt. Polytechnic College, Cherthala during the last few years is greatly acknowledged.

I express my sincere thanks to my family members, especially my mother, brothers and sisters and with the special note to my wife Princy, for all the support, encouragements and co-operation during the period of my research.

Let me not forget to mention the endurance shown by my little triplets Ananth, Aravinth and Abhijith.

Finally above all I thank the Almighty God for all the blessings showered upon me in my life.

Mathew George

Contents

Preface

"There is more room at the bottom". This is an epoch making statement made by the most renowned physicist of the century. He is none other than Richard Feynman. That statement turned out to be prophetic and farsighted. Now, with the dawn of the 21st century, scientists and engineers are beginning to look more and more into the 'bottom'. This has opened up new class of materials and technology which is widely known as nanomaterials / nanotechnology.

It is known that materials exhibit altogether different properties at the nanolevel. They show superlative chemical/physical/magnetic/electrical properties with respect to their coarser sized cousins. Engineering / tailoring of these materials for specific applications means understanding the physics and chemistry of these materials at the nano level or at the interfaces. Here phenomenon like wave function overlapping, quantum tunnelling, spin polarised tunnelling, quantum magnetisation have been known to influence the overall properties. Tailoring the properties requires a proper understanding of these phenomenon and effectively manipulating the properties for making useful devices. Fortunately, for science and technology, the understanding of these phenomenon is quite fast and has evolved, many useful technique to study these phenomenon.

Magnetism and magnetic materials have been an ever-attractive subject area for engineers and scientists alike because of its versatility in finding applications in useful devices. They find applications in a host of devices ranging from rudimentary devices like loud speakers to sophisticated gadgets like waveguides and Magnetic Random Access Memories (MRAM).

The one and only material in the realm of magnetism that has been at the centre stage of applications is ferrites and in that spinel ferrites received the lions share as far as practical applications are concerned.

It has been the endeavour of scientists and engineers to remove obsolescence and improve upon the existing so as to save energy and integrate in to various other systems. This has been the hallmark of material scientists and this has led to new materials and new technologies.

In the field of ferrites too there has been considerable interest to devise new materials based on iron oxides and other compounds. This means synthesising ultra fine particles and tuning its properties to device new materials. There are various preparation techniques ranging from top- down to bottom-up approaches. This includes synthesising at molecular level, self assembling,gas based condensation, low temperature co-precipitation, sol-gel process and high energy ball milling. Among these methods sol-gel process allows good control of the properties of ceramic materials. The advantage of this method includes processing at low temperature, mixing at the molecular level and fabrication of novel materials for various devices.

Composites are materials, which combine the good qualities of one or more components. They can be prepared in situ or by mechanical means by the incorporation of fine particles in appropriate matrixes. The size of the magnetic powders as well as the nature of matrix affect the processability and other physical properties of the final product. These plastic/rubber magnets can in turn be useful for various applications in different devices. In applications involving ferrites at high frequencies, it is essential that the material possesses an appropriate dielectric permittivity and suitable magnetic permeability. This can be achieved by synthesizing rubber ferrite composites (RFC's). RFC's are very useful materials for microwave absorptions. Hence the synthesis of ferrites in the nanoregime,

investigations on their size effects on the structural, magnetic, and electrical properties and the incorporation of these ferrites into polymer matrixes assume significance.

In the present study, nano particles of $NiFe_2O_4$, $Li_{0.5}Fe_{2.5}O_4$ and $CoFe_2O_4$ are prepared by sol gel method. By appropriate heat treatments, particles of different grain sizes are obtained. The structural, magnetic and electrical measurements are evaluated as a function of grain size and temperature. $NiFe_2O_4$ prepared in the ultrafine regime are then incorporated in nitrile rubber matrix. The incorporation was carried out according to a specific recipe and for various loadings of magnetic fillers. The cure characteristics, magnetic properties, electrical properties and mechanical properties of these elastomer blends are carried out. The electrical permittivity of all the rubber samples in the X – band are also conducted.

The thesis is divided in to **nine** chapters. ***Chapter 1*** gives a brief introduction about the history and classification of magnetic materials, ferrites in particular followed by a brief discussion on their fundamental physical properties. Relevance of magnetic fine particles and rubber ferrite composites (RFCs) are discussed. Superparamagnetism, and coercivity dependences of particle size are also discussed from a theoretical perspective.

An outline of the various experimental techniques employed for the preparation and characterisation of samples at various stages are discussed in **chapter 2**. Various analytical tools like X-ray diffraction, Vibrating sample magnetometer, Impedance analyser, Gottfert Elastograph, Universal testing machine and Network analyser which are employed to characterize and evaluate the properties of ferrites and their composites are discussed in detail in this chapter.

Structural and magnetic properties of nickel ferrite are evaluated. The pre- characterized powders are then incorporated in to nitrle rubber matrix at various loadings of 20phr, 40phr, 80phr and 120phr. The effects of grain size on the different properties are also discussed. The observed properties have been explained. These are dealt with in ***chapter 3.***

The electrical properties of nickel ferrites and its composites based on nitrile rubber are discussed in ***chapter 4.*** They are studied as a function of frequency and temperature. Dependence of grain size on the dielectric permittivity and ac conductivity of these samples are also studied in detail.

The mechanical properties and Cure characteristics of RFC's are dealt with in ***chapter5***. The cure parameters like maximum torque, scorch time; cure time and minimum torque are evaluated for samples of various loadings. The dependence of these parameters on the size and loadings of the fillers are also studied. Mechanical properties like tensile strength, 100% modulus, 200%modulus, 300%modulus and maximum strain are also evaluated and their dependence with loadings and grain size of the fillers are discussed. All the observed results are explained based on a theoretical model.

The dielectric permittivity and dielectric loss factor for all the composites are determined in the X –band. Dependence of these parameters on volume fraction and size of the ferrite filers are evaluated and are discussed in detail in ***chapter 6.***

The structural, magnetic and electrical properties of $Li_{0.5}Fe_{2.5}O_4$ heat treated at various temperatures are evaluated and are dealt with in ***chapter 7.*** The variation of magnetisation, coercivity, dielectric permittivity and AC conductivity with particle sizes are studied and correlated.

The structural, magnetic and electrical properties of nano ferrites of $CoFe_2O_4$ of various particle sizes are discussed in ***chapter 8***.The electrical and magnetic parameters are elucidated and variations of these parameters with particle sizes; temperature and frequency are included in this chapter.

Chapter 9 is the concluding chapter of the thesis and in this chapter the salient observations and the inferences drawn out are discussed and compared. The scope for further work is also discussed in this chapter.

Chapter 1

Introduction

The history of magnetism can be traced to a place in modern day Turkey, earlier called Magnesia. Earlier, around 800 B.C a piece of magnetite (Fe_3O_4) was discovered. This was called lodestone (leading stone). In China, the legendary ruler Huang-Ti used lodestone to win many battles against Barbarian tribesmen before 2600 BC [1]. This paved the way for great expeditions and laid the foundation for many great civilizations. Since then, magnetism and magnetic materials have been a keen subject of interest to the humankind.

The present day magnetism owes a great deal to Michael Faraday who classified magnetism into different categories namely diamagnetism, paramagnetism and ferromagnetism. It must be noted that magnetism derives its origin from the spinning and orbiting electrons and the different types of magnetism can be attributed to the total current constituted by the revolving/spinning electrons. In higher magnetism like ferro/ferri, it is the interaction of spins with one another that lead to this co-operative phenomenon.

Then magnetism can be broadly classified into five and they are the following.

1.1.Diamagnetism

It is a non-cooperative phenomenon and is universal in nature. Diamagnetism is caused by the orbital motion of electrons. In diamagnetic

materials the constituent atoms or molecules have all their electrons paired up in such a way that their magnetic dipole moments cancel each other. Hence there are no dipoles to be aligned by the applied magnetic field. In fact, an applied magnetic field is opposed by changes in the orbital motion of the electrons of a diamagnetic substance. The magnetic susceptibility in this class of material is negative and its magnitude is about 10^{-5}.

1.2.Paramagnetism

If the atoms or ions contain one or more unpaired electrons and this possesses a permanent magnetic moment the materials may be either paramagnetic or ferromagnetic. If there is no interaction between the adjacent magnetic moments, then the materials are called paramagnetic. In these materials, magnetic moments of the individual atoms or molecules line up in the direction of the applied magnetic field. This results in an overall magnetic moment that adds to the magnetic field. Paramagnets are governed by Curie law, which states that

$$\chi = \frac{C}{T} \qquad 1.1$$

T being the absolute temperature and C is the Curie constant

1. 3.Ferromagnetism

A ferromagnetic substance has a net magnetic moment even in the absence of an external magnetic field. This is because of the strong interaction between magnetic moments of the individual atoms or electrons in the magnetic substance and this align up parallel to one another. If the many individual magnetic dipole moments produced in a material are appreciable, there can be long-range interactions. This leads to large-scale

areas of magnetism called domains. In ferromagnetic materials, the dipoles within a domain are all aligned and the domains tend to align with an applied field. Ferromagnets can have a magnetic permeability of several thousands. The energy expended in reorienting the domains from the magnetized state back to the demagnetised state manifests itself as hysteresis. An important property of ferromagnets is the Curie temperature, θ. Above the Curie temperature ferromagnets become paramagnets, since there is sufficient thermal energy to destroy the interaction between atoms that creates domains. They then have a susceptibility given by the Curie–Weiss law as

$$\chi = \frac{C}{(T-\theta)} \qquad 1.2$$

1.4.Antiferromagnetism

Substances in which the magnetic moments interact in such a way that it is energetically favourable for them to line up antiparallel are called antiferromagnets. They exhibit a very small positive susceptibility. The response of antiferromagnetic substances to an applied magnetic field depends on the temperature. At low temperatures, the arrangement of the atomic dipoles is not affected, and the substance does not respond to an applied magnetic field. As the temperature is increased, some atoms are loosened and align with the magnetic field. This results in a weak magnetism in the substance. There is a temperature analogous to the Curie temperature called the Neel temperature, above which antiferromagnetic order disappears. Above the Néel temperature the effect decreases because of greater movement of the atoms. Oxides of Manganese, Cr_2O_3 etc are some examples of antiferromagnetic materials.

Susceptibility is given by

$$\chi = \frac{C}{(T + \theta)} \qquad 1.3$$

1.5.Ferrimagnetism

Ferrimagnetism is weak ferromagnetism in which the opposing dipoles are not equal and they do not cancel out. These materials display a spontaneous magnetization, very small compared to ferromagnets. Ferrimagnets are also good insulators, making them very useful in preventing energy losses due to eddy currents in transformers. Ferrites are typical examples of ferrimagnets and naturally occurring magnetite is a typical example of this category of materials.

There are other types of magnetism and a brief insight is provided in the ensuing sections. The descriptions are supplemented with a flowchart (Fig.1.1).

1.6.Other Types of Magnetism

Apart from the conventional classification of magnetism, eight other types of magnetic order were identified. These can be considered as derivatives and have relationship with one or more of the basic types [2]. They are superparamagnetism, Metamagnetism, Incipient ferromagnetism, Speromagnetism, Aspromagnetism, Helimagnetism, Spin glass, Mictomagnetism and Sperimagnetism. Materials like $FeCl_2$ and MnF_2, which are antiferromagnetic in large applied fields, and this type of ordering is termed metamagnetism. Due to decreasing influence of exchange and anisotropy effects in certain metals, no long range order of spins is possible, but some ferromagnetic alignment takes place over small region is called

paramagnon. Materials with paramagnons in them are said to exhibit incipient ferromagnetism. When cooled below a critical temperature, the spins can order speromagnettically and this effect is called spin glass freezing. A schematic is shown in Fig.1.1

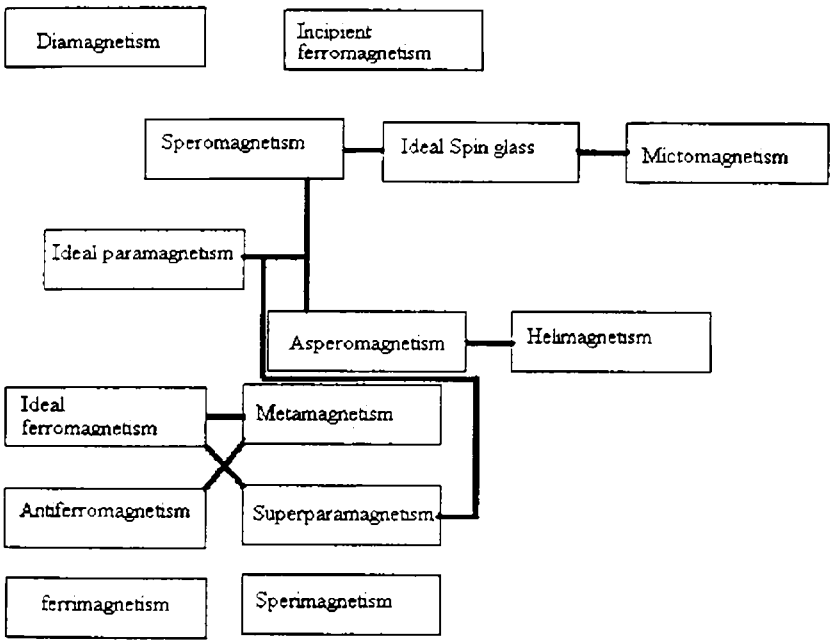

Fig.1.1. Flow chart depicting various types of magnetism

The focal theme of this thesis is nano ferrites and for continuity and clarity, a brief idea about ferrites is provided below.

1.7.Ferrites

The first magnetic material known to man was magnetite Fe_3O_4, which is known as ferrous ferrite. Though the saturation magnetisation of magnetite is low compared to ferromagnetic metals and alloys, the dc resistivity of magnetite is about 1000 times that of iron. This is useful in reducing eddy-current loses in inductors and transformers [2]. Hilpert prepared a large variety of ferrites in 1909. The breakthrough came after 1933 with the work of Snoek and his co-workers at the Philips Research Laboratories in Eindhoven the Netherlands. Snoek made a systematic investigation on ferrites, and produced materials having low hysteresis, high resistivity and high permeability suitable for use as magnetic cores up to a few megahertz.

Type	Structure	General formula	Example
Spinel	Cubic	$A^{2}Fe_2O_4$	A^{2} = Cd, Co, Mn, Mg, Ni, Zn.
Garnet	Cubic	$Ln_3^{3}Fe_2O_{12}$	Ln^{3}=Y, Sm, Eu, Gd, Dy, Ho, Er, Tm, Ln.
Magnetoplumbite	Hexagonal	$A^{2}Fe_{12}O_{19}$	A^{2} = Ba , Sr.

Table 1.1. General formulas for different Ferrites

He published a great way of original papers on magnetic and electrical properties of these compounds [3-5]. Bart and Posngak also made significant contributions to the understanding of the structural properties of ferrites. They carried out X-ray analysis on a large number of spinel type crystals, including ferrites. They found that in the case of ferrites, it was necessary to assume that the divalent and trivalent metal ions interchange positions in the lattice. Thus they discovered what is now called the inverted spinel, a structural prerequisite for the exhibition of ferromagnetism in ferrites. Extensive research work carried out by several researchers including Snoek, Bart and others led to a clear understanding and by then found that ferrites can be generally classified into three based on their crystal structure. They are depicted in Table 1.1

In any study involving ferrites, there is close intimacy .of the structure with the electrical and magnetic properties of these ferrites. In the following section the structure of spinel ferrites is described very briefly.

1.8.Crystal Structure of Spinel ferrites

Spinel ferrites have the general formula MFe_2O_4 where M is a divalent metal They resemble the structure of the naturally occurring mineral $MgAl_2O_4$. The oxygen anions have an fcc arrangement accommodating the smaller positive ions in the interstices. The available spaces are of two kinds. One is called tetrahedral or A site, because it is located at the centre of a tetrahedron whose corners are occupied by oxygen ions. The other is called octahedral or B sites, because the oxygen ions around it occupy the corners of an octahedron. In the mineral spinel Mg ion occupy the A site, known as tetrahedral site because it has four nearest

oxygen neighbours. The B site ions have six nearest oxygen ions and are called the octahedral site and is occupied by the Al ions [6-8].

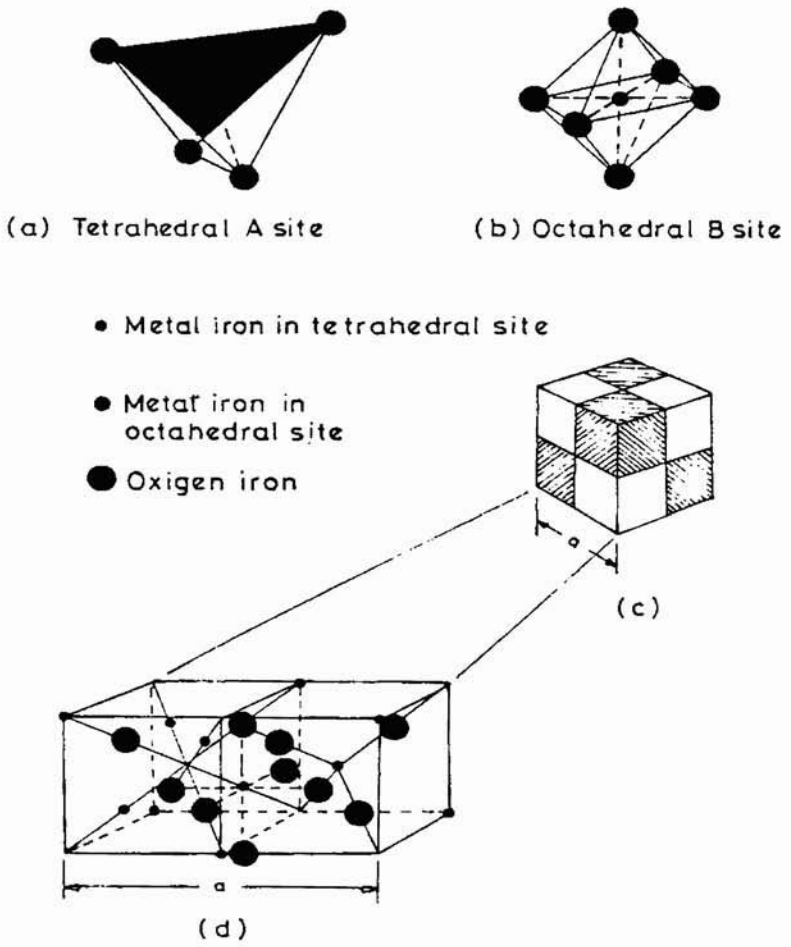

Fig.1.2.Crystal structure of a cubic ferrite

The crystal structure is best described by subdividing the unit cell into 8 octants with edge a / 2 where 'a' is the lattice parameter, as shown in fig.1.2. The location of oxygen ions and metal ions in every octant is

depicted in fig.1.2. The oxygen ions are arranged in identical manner in all octants. Each octant contains four oxygen ions in the body diagonal and they lie at the corners of a tetrahedron. Positions of metal ions are different in the two octants sharing a face. In the case of octants sharing only an edge the location is the same. The occupation is clearly illustrated in fig.1.2.d

The distribution of metal ions is very important for understanding the magnetic properties of these materials. Not all available sites are occupied by metal ions. Only one fourth of the A sites and one half of the B sites are occupied. In the case of mineral spinel, Mg^{2-} ions are in the A site and Al^{3-} ions are in B sites. Such an arrangement is called normal spinel structure in which the divalent ions are on B sites and trivalent ions are on the A sites. $ZnFe_2O_4$ is a normal spinel in the micron regime. The structure in which divalent ions are in the A sites and trivalent ions are equally distributed between A and B sites, is called an inverse spinel structure. $CoFe_2O_4$ and $NiFe_2O_4$ ferrites have inverse structure and they are all ferrimagnetics.

1.9. Exchange Interactions

In order to understand the magnetic ordering in a system, it is necessary to know the different interactions within the system. These interactions can be explained by Heisenberg's exchange integral. [6,9-11]

For example, in the case of a simple system with two atoms A and B, the total energy is expressed as

$$E = E_A + E_B + Q \pm J_{EX} \qquad 1.4$$

where 'E_A' and 'E_B' are energies of electrons when they revolve separate atoms. Q denotes the electrostatic coulomb interaction energy and 'J_{EX}'

denotes the exchange energy known as exchange integral. 'J_{EX}' is due to the exchange between electrons of the atoms, that is, when 'A' electron moves around the nucleus 'B' and 'B' electron moves around the nucleus 'A'. They are indistinguishable except for their spins. Therefore spin orientation is most important. Parallel spin will give positive 'J_{EX}' and antiparallel spins will result in negative 'J_{EX}'. This explains the formation of antiferromagnetic ordering and ferromagnetic ordering in materials.

In 1928 Heisenberg showed that the exchange energy can be expressed as

$$E_{EX} = -2J_{EX}S_i S_j \cos\theta = -2J_{EX}S_i S_j \qquad 1.5$$

'E_{EX}' is the exchange energy, 'S_i' and 'S_j' are the total spins of adjacent atoms and 'J_{EX}' is the exchange integral which represents the probability of exchange of electron.

If $J_{EX} > 0$, ferromagnetic order results in an energy minimum and $J_{EX} < 0$ antiparallel spin is favoured. Having discussed the various interactions in ferrites, it is imperative that a brief theory on ferrimagnetism is discussed with particular reference to Neel's sublattice model.

1.10.Neel's two sublattice theorem of Ferrimagnetism

Strong quantum mechanical forces of interaction exist between the spinning electrons in the neighbouring metal ions [6,7]. According to Neel, this interaction is negative in ferrites, that is: the forces acting between ions on A site and B site are negative. This means that the force acting to hold the neighbouring atomic magnetic axes are antiparallel or opposite in direction..

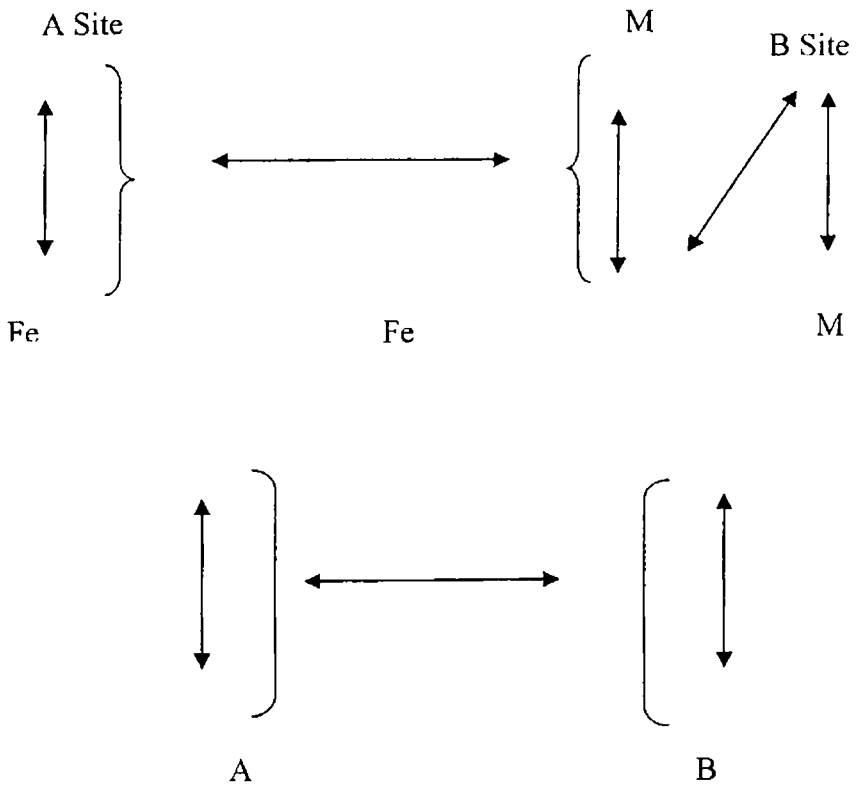

Figure 1.3 Exchange interactions

Three sets of interactions namely, A-A, B-B and A-B are possible in ferrites. A-A and B-B interactions are weak and A-B interaction is predominant in ferrites. The result is that the magnetic moments on A sites are held antiparallel to those on B sites and the spontaneous magnetization of the

domain is therefore due to the difference of moments on A and B sites respectively. In ferrimagnets however the A and B sublattice magnetizations are not equal and hence this results in a net spontaneous magnetization

The exchange forces between the metal ions in a ferrimagnet will be through the oxygen ions by means of the super exchange mechanism. However molecular field theory for ferrimagnet is inherently complicated, because A and B sites are crystallographically different for ferrimagnets. That is, the AA interaction in ferrimagnets will be different from the BB interaction eventhough the ions involved are identical. The basic reason is that an ion in the A site has different number and arrangement of neighbours than the identical ion in the B site.

Fig.1.3 shows the exchange interactions that would have to be considered in a rigorous treatment of an inverse spinel $MOFe_2O_3$. These interactions are five in all. To simplify this problem Neel replaced the real ferrimagnet with a model composed of identical magnetic ions divided unequally between A and B sublattices. This still leaves three different interactions to be considered.

Let there be 'n' identical magnetic ions per unit volume with a fraction λ located on A sites and a fraction $\nu = 1-\lambda$ on B sites. Let μ_A be the average moment of an A ion in the direction of the field. Eventhough A and B sites are identical , μ_A is not equal to μ_B because these ions are exposed to different molecular fields. Then magnetization of A sublattice is

$$M_A = \lambda n \mu_A \qquad 1.6$$

by Putting $n\mu_A = M_a$.

Then $M_A = \lambda M_a$ and $M_B = \lambda M_b$

Neel defined the interaction within the material from the Weiss Molecular field viewpoint. The magnetic field acting upon an atom or ion is written in the form $H=H_o+H_m$ where H_o is externally applied field and H_m is internal or molecular field which arises due to interaction.

When molecular field concept is applied to ferrimagnetic materials we have

$$H_A = H_{AA} + H_{AB} \qquad 1.7$$

and $$H_B = H_{BB} + H_{BA} \qquad 1.8$$

The molecular field components may be written as

$$H_{AA} = \gamma_{AA} M_A \qquad 1.9$$

$$H_{AB} = \gamma_{AB} M_B \qquad 1.10$$

$$H_{BB} = \gamma_{BB} M_B \qquad 1.11$$

$$H_{BA} = \gamma_{BA} M_A \qquad 1.12$$

Where γ's are molecular field coefficients and M_A and M_B are magnetic moments of A and B sublattices.

$\gamma_{AB} = \gamma_{BA}$ but $\gamma_{AA} \neq \gamma_{BB}$ unless the two sublattices are identical. Neel showed that $\gamma_{AB} < 0$ favours antiparallel arrangement of M_A and M_B and gives rise to ferrimagnetism.

If all the magnetic moments of the ions were aligned parallel, it would be possible to calculate the saturation magnetisation of a ferrite in Bohr magnetons per molecule simply by adding together the magnetic moments of the ions. However, if this is done, the values obtained are larger than those obtained experimentally. Neel suggested that a magnetic dipole on a tetrahedral site is aligned antiparallel to a magnetic dipole on an octahedral site [12]. Then the total magnetisation is given by the difference in magnetisation of the ions on the two sites, which agrees well with experiments.

Magnetic fine particles are known to behave differently with respect to micronsized counterparts. They exhibit superparamagnetism, finite size effects and quantum tunneling of magnetisation. In the subsequent sections, a brief idea on magnetic nanoparticles with special emphasis on superparamagnetism is provided.

1.11.Nanostructured Magnetic Materials

The term "Nanostructured Materials" was introduced into literature soon after the conference on "Materials with Ultrafine Microstructures" held in Atlantic City in the year1990. One of the main features of nanomaterials is the fact that their microscopic structure affects the macroscopic properties, giving rise to a wide variety of new phenomenon.

Owing to the extremely small dimensions of nanostructured materials, a major portion of the atoms lie at the grain boundaries, which in turn is responsible for superior magnetic, dielectric and mechanical properties in these materials compared to their conventional coarse sized grains. The reduced dimension of nano-crystalline materials can lead to novel properties compared to their conventional counterparts [13-19]

Materials in the nanolevel possess altogether different magnetic properties. The magnetic properties are substantially changed when the size becomes very small. Below a certain size, the magnetic materials are single domain and they exhibit superparamagnetism. The superparamagnetism of materials are determined by the magnetic anisotropy and the volume factor, which comes from electron spin-orbital angular momentum, coupling at lattice sites in the crystal structure. These materials have potential application in diverse areas such as information storage, colour imaging, ferrofluids and magnetic refrigeration [20-24].

The magnetic behaviour of the particles at the surface differs from that corresponding to the core, because of the distinct atomic coordination, compositional gradients and concentration and nature of the defects present in both regions. Thus, whereas the core usually displays a spin arrangement similar to that of the bulk material, a much higher magnetic disorder is present in the surface, giving rise to magnetic behaviours which cover from that of non-collinear surface to that of a spin glass like behaviour [25-26]

New synthesis routes to produce nanomaterials and the emergence of new measurement/analytical techniques have resulted in the discovery of exotic and novel nanomaterials. Magnetic fine particles have been successfully prepared by numerous chemical routes such as self-assembling, gas condensation, reverse micelle synthesis, coprecipitation, thermal decomposition, solgel and aerogel process. High energy ball milling is also used as an alternate route to obtain novel materials through solid state reactions. Among these methods sol-gel process allows good control of the properties of ceramic materials. The advantage of this method includes

processing at low temperature, mixing at the molecular level and fabrication of novel materials for various devices.

Particles below a critical size displays single domain characteristic and exhibit superparamagnetism. A brief treatment on the considerations of superparamagnetism is reproduced here for continuity.

1.12.Superparamagnetism and grain size dependence of Coercivity

Superparamagnetism is a unique feature of magnetic nanoparticles and has great relevance to modern technologies, including, data lifetime in high density information storage, ferrofluid technology and in magnetic refrigeration [27,28]. As the particle diameter decreases to the order of lattice parameter, the intrinsic magnetic properties such as the spontaneous magnetization, mangetocrystalline anisotropy and magnetostriction will become size dependent [6].The reasons for the particle size dependence of the magnetization are (i) The probability of thermally activated magnetisation increases as the particle volume decreases. As soon as the energy barrier for irreversible magnetization changes, KV is of the order of magnitude of kT, then hysteresis vanishes (ii) Surface effects become increasingly important as the particle volume decreases. This is particularly strong in cases where the spin systems of the particles are coupled by exchange interaction to other spin systems along the particle surfaces. This phenomenon is known as exchange anisotropy and this will cause a shift in the hysteresis curve. (iii). The condition for reversal of magnetization as well as the reversal mechanism depend on the particle dimension as well as the particle shape. The general character of the hysteresis loop is not affected, but the coercivity is greatly affected.

To find the effect of particle size and temperature on the coercivity and magnetisation, consider an assembly of uniaxial single domain particles each with anisotropic energy density E= K $\sin^2\theta$ where K is the anisotropy constant and θ is the angle between Ms and the easy axis of magnetisation. If the volume of each particle is V then energy barrier ΔE that must be overcome before a particle reverses its magnetization is KV ergs. In every material fluctuations due to thermal energy are continuously occurring at a microscopic level. If the single domain particle becomes small enough,KV will become comparable with thermal energy and fluctuations could overcome the anisotropy forces and spontaneously reverse the magnetization from one direction to another. Each particle has a magnetic moment $\mu=M_sV$ and if a field is applied it will tend to align the moments along the field. But the thermal fluctuations will promote randomization. This is similar to the behaviour of a normal paramagnet with the exception that the moments involved are enormously high compared to the moment in paramagnetism.

Hysteresis will appear and superparamagnetism disappears when particles of certain size are cooled to a particular temperature or particle size at certain temperature is increased beyond a critical size. To obtain the conditions for superparamagnetism, consider an assembly of uniaxial particles, which is in an initial state of magnetization M_i by an applied field. Now the field is reduced to zero at a time t=0. Some particles in the assembly will reverse their magnetization as their thermal energy is larger and the magnetization of the assembly tend to decrease. The rate of decrease at any time is given by

$$-\frac{dM}{dt} = f_0 M e^{\frac{-KV}{kT}} = \frac{M}{\tau} \qquad 1.13$$

The proportionality factor is called the frequency factor and it has a value of $10^9 sec^{-1}$.

The constant τ is called the relaxation time.

Rearranging the above equation and integrating we arrive at

$$M_r = M_i e^{\frac{-t}{\tau}} \qquad 1.14$$

and hence relaxation time τ can be defined as the time for remanence M_r to decrease to 1/e of its initial value. From equation 1.13, we can write

$$\frac{1}{\tau} = f_0 e^{\frac{-KV}{kT}} \qquad 1.15$$

Thus it is clear that τ is strongly dependent on V and T.

If we put relaxation time as 100sec, then from equation 1.15 we arrive at

$$\frac{KV}{kT} = 25 \qquad 1.16$$

Hence transition to stable state occurs when energy barrier equals 25kT and also the upper limit of the particle volume for superparamagnetism for uniaxial particles is given by

$$V_p = \frac{25kT}{K} \qquad 1.17$$

For a particle assembly of constant size there will be particular temperature called the superparmagnetic blocking temperature, below which magnetisation will be stable. For a uniaxial particle assembly,

$$T_B = \frac{KV}{25k} \qquad 1.18$$

Now we can consider the effect of an applied field on the approach to equilibrium. Assume an assembly of particles with their easy axis parallel to the z axis. Let it be initially saturated in the +z direction and let us now apply a field in the –z direction. Then the Ms in each particle will make an angle θ with the z axis. Then the total energy per particle is

$$E = V(K \sin^2 \theta + HM_s \cos \theta) \qquad 1.19$$

The energy barrier for reversal is the difference between the maximum and minimum values of E and it can be obtained as

$$\Delta E = KV\left(1 - \frac{HM_s}{2K}\right)^2 \qquad 1.20$$

The particles with sizes larger than D_p are stable in zero field and will not thermally reverse in 100s. But when the field is applied the energy barrier can reduce to 25kT. This will be the coercivity and is given by

$$\Delta E = KV\left(1 - \frac{H_{ci}M_s}{2K}\right)^2 = 25kT \qquad 1.21$$

$$H_{ci} = \left(\frac{2K}{M_s}\right)\left[1 - \left(\frac{25kT}{KV}\right)^{1/2}\right] \qquad 1.22$$

When V is very large or T is zero, $H_{ci} = (2K/Ms)$

Putting this limiting value as

$H_{ci,0}$ and substituting for 25kT/K as V_p, we get

$$h_{ci} = \frac{H_{ci}}{H_{ci,0}} = 1 - (\frac{V_p}{V})^{1/2} = 1 - (\frac{D_p}{D})^{3/2} \quad 1.23$$

Similarly equation 1.22 can also be used for variation of coercivity with temperature for particles of constant size. For this we assume that particle with critical size V_p have zero coercivity at their blocking temperature T_B.

We get

$$h_{ci} = \frac{H_{ci}}{H_{ci,0}} = 1 - (\frac{T}{T_B})^{1/2} \quad 1.24$$

Particles larger than V_P have finite retentivity as thermal energy cannot reverse their magnetization in 100s. To find a relation between retentivity and size we can combine equations 1.14 and 1.15 to get

$$\ln\frac{M_r}{M_i} = -\frac{t}{\tau} = -10^9 e^{-KV/kT} \quad 1.25$$

substituting equation 1.10 and putting t=100s we get

$$\ln\frac{M_r}{M_i} = -10^{11} e^{-25V/V_P} \quad 1.26$$

Thus the above equations predict the dependence of magnetic properties of the fine particles on their size.

In cubic crystals like $NiFe_2O_4$ there are more than one easy axis of magnetization there by reducing the magneto crystalline anisotropy. But in a hexagonal crystal like Cobalt, there is only one magnetic easy axis, which is

directed along the hexagonal 'c' axis. So the anisotropy and hence the coercivity is very high in case of a uniaxial crystal like cobalt.

AC susceptibility measurements are an important tool in the characterization of small ferromagnetic particles, which exhibit superparamagnetism, the theory of which was originally propounded by Neel and Brown. In the Neel-Brown theory, the particles are assumed to be non-interacting and the blocking temperature is given by

$$T_B = \frac{\Delta E}{\ln(\tau / \tau_0) k_B} \qquad 1.27$$

Where ΔE is the energy barrier to magnetization reversal in a single particle, τ is the measurement time, τ_o is the attempt frequency and k_B is the Boltzmann's constant. .

1.13.Nitrile Rubber

A brief description about the nitrile rubber and its properties are provided in this section, nitrile rubber being the matrix selected for the preparation of composites. Nitrile rubber, otherwise known by the generic name Buna-N or NBR, is a special purpose synthetic rubber. It is a copolymer of butadiene and acrylonitrile. The basic polymer reaction in the production of nitrile rubber is

$$CH_2=CH-CH=CH_2 + CH_2=CH \longrightarrow -[-CH_2-CH=CH-CH_2-CH_2-CH(CN)-]-$$

butadiene acrylonitrile copolymer unit

Oil resistance is the most important property of nitrile rubber. NBR has good resistance to oils, greases, petroleum hydrocarbons and other non-polar solvents. Hence it is used in the manufacture of products like oil seals, O-rings, gaskets, fuel and oil hoses, including high pressure hoses, for hydraulic and pneumatic applications, friction covering, linings, containers, work boots, shoe soling and heels, conveyor belts, in membranes, etc. The presence of the nitrile group (C N) on the polymer is responsible for this property. Nitrile rubbers are sometimes blended with plastics to obtain useful products [29-31].

Commercially available nitrile rubber is further graded depending on the acrylonitrile content, temperature of polymerization and Mooney viscosity. It must be noted that the amount of acrylonitrile content is the single determining factor in most of the cases that divides the properties of nitrile Rubber as an oil resistor and fuel resistant.

Increasing the acrylonitrile (ACN) content increases the oil resistance of the polymer. The amount of ACN also improve the mechanical and cure properties of the polymer. With increasing ACN content, cure rate is fast and having a better heat resistance.

Basically nitrile rubbers are compounded much like natural rubber [32,33]. The compounding ingredients used are the same though they differ slightly in the amount. Vulcanisation of nitrile rubber is usually accomplished with sulphur, accelerator and zinc oxide and fatty acid as activator. In special cases peroxide may also be used. Sulphur is less soluble in NBR than in NR and only small amounts are used.

NBR shows no self-reinforcing effect, as there is no stress induced crystallisation. Since it does not crystallise, reinforcing fillers are necessary

to obtain optimum tensile strength, tear strength and abrasion resistance. Fillers like carbon black, precipitated silica, calcium carbonate are incorporated in nitrile rubber to enhance the mechanical and other properties.

The important industrial applications of NBR include the manufacture of cables for the petroleum, coal-mining and quarrying industries, transport, shipbuilding, power distribution, domestic and miscellaneous applications [34-36]. The other fields that account for most of the uses of NBR are the automobile, aircraft, oil, textile and printing industries.

1.14.Rubber Ferrite Composites (RFCs)

The magnetic powders of ferrites can be incorporated in various elastomer matrixes to produce flexible magnets or rubber ferrite composites RFCs [37-40]. The incorporation of these ferrite powders can be carried out in various matrixes to produce RFCs, both in natural and synthetic rubber. RFCs have unique advantage of mouldability into complex shapes, which is not easily possible by conventional ceramic magnets. The addition of magnetic fillers in an elastomer matrix modifies the physical properties of the matrix considerably, in that they modify the dielectric properties and impart magnetic properties to the matrix [41-42]. When preparing RFCs, the choice of compounding ingredients, compounding conditions and their processability are important. Also factors like percolation limit and nature of the matrix like saturated/unsaturated polar/non polar rubber, all influence the final properties of the composites.

In magnetic polymers, the magnetic powder as well as the polymer chosen affect the processability and other physical properties of the final product. In tailoring composites for various applications it is necessary, to select the proper filler and matrix. The polymer matrix must have

appropriate mechanical and chemical properties. The macroscopic properties of the composite magneto-polymers is influenced by the interactions between the filler and the matrix.

The microwave absorbing properties of elastomer warrants an appropriate dielectric strength and a desirable magnetic property[3,46]. This can be achieved by synthesizing RFC where appropriate amount of fillers are incorporated into the rubber matrix. In principle, the macroscopic parameters of the composites would be influenced by the interaction between the filler and the matrix. The effect of fillers in modifying the properties is to be understood properly in explaining the various properties of the composites.

Rubber Ferrite Composites find applications in microwave and stealth devices. They are found to be very good microwave absorbers and are useful for EMI shielding. Here their lightweight, low cost and flexibility are added advantages. Depending on the filler characteristics as well as filler loading, one can vary the properties of these composites.

1.15.Proposed Study

In the earlier sections, it has been stated that spinel ferrites can broadly divided in to three categories. They are the normal, inverse and random spinels. This can easily be described by the chemical formula $\{(M)_{\delta}(Fe)_{1-\delta}\}[(M)_{1-\delta}(Fe)_{1-\delta}]O_4$. The divalent metal ion M (eg:- Zn, Mg, Mn, Fe, Co, Ni or a mixture of them) can occupy either tetrahedral(A) or octahedral(B) sites as depicted by curled and square brackets respectively. In the above formula when $\delta = 1$, it is called normal spinel and when $\delta = 0$, it is called inverse spinel. When $\delta = 1/3$, it is called a random spinel. $C = 1-\delta$ represents the inversion parameter.

Factors like ionic size, charge, madelung energy, lattice energy and crystal field stabilization effects all influence the formation of spinels and their respective forms, namely, inverse, normal and random. Another factor, which determines the occupation of cations, is the site preference energy. For example, cations like nickel and cobalt have a strong preference for octahedral site while zinc and cadmium have strong tetrahedral site preference .In the micron regime the occupation of the cations can be easily predicted provided information of the site preference energy of cation, their radii and charge are available. This can be effectively utilized to manipulate the synthesis of these ferrites with optimum magnetic and electrical properties. Another factor, which influences the cation distribution in the spinel ferrite, is the temperature. In the ultra fine regime, these thumb rules are no longer hold. For instance, in the case of fine particles of zinc ferrite, a small amount of Zn is found to occupy B-site instead of A-site and in nickel ferrite, a small amount of Ni occupies the tetrahedral site instead of the preferred octahedral site (25,47). Various theories have been propounded to explain the anomalous behaviour of normal and inverse spinels in the ultrafine regime. It has been known that ultra fine magnetic particles below a certain critical size exhibit superparamagnetism and spin glass behaviour.

From the fundamental point of view various theories have been put forwarded to explain the anomalous behaviour of ultra fine ferrites. Shell-core effect, cation redistribution and surface spins are widely thought to be responsible for this phenomenon. It must be noted here that not a single model is capable of explaining the anomalous behaviour of ferrites in the nano regime. Different models are invoked at different stages to explain the properties in the ultra regime. So it is natural that one does a systematic

study on the preparation and characterisation of spinel ferrites like nickel, lithium and cobalt ferrites.

$NiFe_2O_4$, $Li_{0.5}Fe_{2.5}O_4$ and $CoFe_2O_4$ are important group of pure ferrites. These ferrite systems belong to the category of inverse spinels in which the divalent ions often occupy the B-sites. Nickel and lithium ferrites belongs to the category of soft ferrites and they find great scope in the high frequency applications Nanoparticles of these materials are widely used in improving the quality of magnetic resonance imaging, replacement of radioactive materials used as tracers, ferrofluids and delivery of drugs to specific areas of the body. Single domain particles of cobalt ferrites are prospective materials for isotropic permanent magnets, magnetic recording and magnetic fluids. Cobalt ferrite thin films are of great interest for magneto- optical recording because of their large faraday rotation and their good chemical stabilities. From the application point of view, the most significant properties of magnetic ceramic materials namely magnetic saturation, coercivity, magnetization and loss, change drastically as the size of the particles move down into the nanometre range. The addition of nickel ferrite in nitrile rubber matrix modifies the physical properties of the matrix considerably, in that they modify the dielectric properties and impart magnetic properties to the matrix. This composite is a powerful tool for electromagnetic absorption.

In the proposed work, nano particles of $NiFe_2O_4$, $Li_{0.5}Fe_{2.5}O_4$ and $CoFe_2O_4$ are to be prepared by sol gel method. By appropriate heat treatments, particles of different grain sizes can be obtained. The structural evaluation of these samples will be carried out by using X-ray diffraction, in order to calculate the grain size and other structural parameters. XRD

will also be used to identify the phase of the nano-samples. Finite size effects on the magnetic parameters namely saturation magnetisation, and coercivity, will be studied. Electrical properties like dielectric permittivity and ac conductivity will be studied in detail as a function of frequency, temperature and grain size.

The fine particles of $NiFe_2O_4$ heat treated at varying temperature and possessing varying grain sizes, will then be incorporated to nitrile rubber matrix for the preparations of rubber ferrite composites. The mixing is to be carried out for various loadings of the filler. The cure characteristics will be evaluated by employing Gottfert elastogram. The magnetic properties of the composites will also be carried out and dependence of these properties will be studied with respect to loading and particle size of the filler. The electrical properties of the composites based on nitrile rubber will be studied as a function of frequency and temperature. Dependence of grain size on the dielectric permittivity and ac conductivity of these samples will also studied in detail. The mechanical properties of RFC's like tensile strength, 100% modulus, 200%modulus, 300%modulus, maximum strain and the tensile strength will be evaluated and their dependence with loadings and grain size of the fillers will be studied.

The dielectric permittivity for all the composites will be determined in the X –band using Network analyser. This is intended to shed light on the permittivity data at high frequency experiments in the X-band. These data together with permeability data will be very useful in modelling microwave absorbers for microwave applications. Dependence of these parameters on volume fraction and size of the ferrite filers can be evaluated and studied.

Thus the objectives of the proposed work can be summarised as follows

- Preparation of nano particles of $NiFe_2O_4$, $Li_{0.5}Fe_{2.5}O_4$ and $CoFe_2O_4$ by solgel method
- Investigations on the structural, magnetic and electrical properties of these nanoferrites and to study the finite size effects.
- Incorporation of nanoparticles of $NiFe_2O_4$ in to nitrile rubber matrix to form rubber ferrite composite (RFCs).
- Processability and Mechanical Studies of the RFCs.
- Electrical and Magnetic Characterisation of RFCs
- Permittivity studies of the RFCs in the X-band

References

1. Chin-Wen Chen, Magnetism and Metallurgy of Soft Magnetic Materials1997, North Holland Publishing Company Amsterdam.
2. C.Radhakrishnamurty, Magnetism and Basalts, Geological Society of India, Banglore, 1993.
3. Snoek J.L, Magnetic and electrical properties of ferrites, Physica,3,463.
4. Snoek, J.L, Philips Tech.Rev.1946, 353.
5. Snoek J.L, New developments in ferromagnetic materials, (Elsevier, 2nd.edn, 1949)
6. B.D.Cullity,Introduction to Magnetic Materials Addison-WeiseleyPublishingCompany, Inc (1972).
7. S.Chikazumi, "Physics of Magnetism", John Wiley and Sons
8. Valenzuela R, 'Magnetic Ceramics', 1994, Cambridge, Cambridge University Press.
9. Smit. J and H.P.J.Wijn, 'Ferrites', 1959, Philips Technical library
10. Hadfield D, 'Permanent Magnets and Magnetism', 1962, John Wiley and sons, Inc., London.
11. Murthy V.R.K and B.Viswanathan, 'Ferrite Materials', 1990, Science and Technology, Narosa Publishing House
12. NeelL,"Properties magnetiques des ferrites, ferrimagnetisme et antiferromagnetisme",Ann.Phys., **3** (1948), 137.
13. D.Ravichandran, R.Roy, P.Ravindrananthan and W.B. White, J.Am.Ceram.Soc. **82** (1999), 1082.
14. T.Tsuzuki and P.G. McCormick, Acta Mater. **48** (2000), 2795.
15. J.G.Li and X.D.Sun, Acta Mater. **48** (2000), 3101.

16. B.L.Shen, T.Itoi, T.Yamasaki and Y.Ogino, *Scripta Mater.* **42** (2000), 893.

17. H.J. Hoffler and R.S.Averback, Scripta Metall. Mater, **24** (1990), 240.

18. L.E.Mc Candlish, B.H.Kear and B.K.Kim, Nanostruct. Mater. **1** (1992), , 119.

19. G. Skandan, H.Hahn, M.Roddy and W.R.Cannon, J.Am.Ceram.Soc, 77 (1994), , 1706

20. L.Gunther, Physics World, December 1990, 28.

21. R.G.L Aurdran and A.P.Huguenard, U.S Patent 4 302 523, 1981.

22. R.F.Ziolo, U.S. Patent 4 474866 1984.

23. R.E.Rosenweig, ferrohydrdynamics (MIT Press, Cambridge, 1985)

24. R.D.McMichael, R.D.Shull,, L.J.Swartzendruder,L.H. Bennett and R.E.Watso, J, Magnetism and Magnetic materials, III, 29 (1992)

25. C.N.Chinnasamy,A.Narayanasamy,N.Ponpandian,K.Chatopadhya, K.Shinoda B.Jeyaadevan,K.Tohji, nakatsuka,T.Furubayashi and I.Nakatani, Phy.Rev. B,.**63**, 18 4108.

26. H.Kodama and A.E. Berkowitz, E.J.McNiff and S.Foner, Phy.Rev. Lett.77, (1996) 394.

27. Qi Chen,Adam J. Rondinone, Bryan C. Chakoumakos, Z.John Zhang,J. Magnetism and Magnetic Materials **194** (1999) 1.

28. J.Popplewell,L Sakhnini, J. Magnetism and Magnetic Materials 149 (1995) 72.

29. Muller K.H, G. Krabbes, J. Fink, S. Grub. A. Kirchner, G. Fuchs, L. Schultz, J. Magn. Magn. Mater, **226-230** (2001) 1370.

30. Maurice Morton, 'Rubber Technology', 3rd edition, 1987, Van Nostrand Reinhold Company, New York.

31. Fred W Billmeyer Jr, 'Textbook of Polymer Science', 2nd edition, 1971, John Wiley & Sons, Inc., New York.

32. Brydson J. A, 'Plastic Materials',4th edition, 1982, Butterworth Scientific, London.

33. Werner Hofmann, 'Rubber Technology Handbook', Hanser Publishers, Munich Vienna, New York.

34. Colin W. Evans, 'Developments in Rubber and Rubber Composites – 2', 1983, Applied Science Publishers Ltd, London and New York.

35. Penn W. S, 'Synthetic Rubber Technology', **1**, 1960, Staples Printers Limited.

36. S.Blow, Handbook of Rubber Technology , Galgotia Publishing, 1998.

37. Georgeg Winspear (Edt), The Vanderbilt Rubber Handbook R.T.Vanderbilt Company Inc.New York , 1958

38. Safari Ardi M ,Dick W and McQueen D.H, Plastic Rubber and Composites Processing Applications, **24**(1995) 157.

39. Anantharaman M.R, S.Jagatheesan, S.Sindhu, K.A.Malini, C.N. Chinnasamy, A.Narayanasamy, P.Kurian and Vasudevan, Plastic Rubber and Composites Processing Applications,**27**,2,(1998) 77.

40. Anantharaman M.R, S.Sindhu, S.Jagatheesan, K.A.Malini and Philip Kurian, Journal of Physics D Applied Physics **32**(1999) 1801.

41. Katz H.S and J.V.Milweski, 'Handbook of Reinforcement of Plastics',1978,Vannostrand Reinhold.New York.

42. Praveen Singh & T.C.Goel:Indian J.Pure and Appl Phys.,**38**(2000) 213.

43. Anantharaman M.R, P.Kurian, B.Banerjee, E.M.Mohammed, and M.George, Kautschuk Gummi Kunstsoffe, (Germany),**49**,6 (1996),424.

44. Anantharaman M.R, K.A.Malini, S.Sindhu, E.M.Mohammed, S.K Date, S.D.Kulkarni, P.A.Joy, and Philip Kkurian, Bull.Mater.Sci., **24**,6(2001) 623.

45. Y. Naito and K. Suetaki, " Application of ferrite to electromagnetic wave absorber and its characteristics , " IEEE transactions, Microwave Theory, Tech, volume **MTT- 19**. (Jan 1971). 65

46. H M Musal. Jr. and HT Hahn. IEEE Transactions on Magnetics, **25** no 5 , (Sept 1989)3851.

47. S.D.Shenoy, P.A. Joy, MR Anantharaman, J. Magnetism and Magnetic Materials **269** (2004) 217.

Chapter II

Experimental Techniques

No investigation in Material Science is complete without the synthesis of materials and the appropriate /thorough characterisation of the synthesised materials. This is being ritualistically carried out to ensure/detect the purity of the material/impurities present. Sometimes phase pure materials are very much necessary to test some hypotheses/models and at other times, the history of the samples vis a vis heat treatment/pressure treatment etc are very much essential for the correct interpretation of the results. Hence a detailed description of the various experimental techniques employed for the preparation and characterisation of samples at various stages are discussed. Various analytical tools like X-ray diffraction, Vibrating sample magnetometer, Impedance analyser, Gottfert Elastograph, Universal testing machine and Network analyser which were employed to characterize and evaluate the properties of ferrites and their composites at various stages are discussed in this chapter.

2.1.Preparations of nanoferrites.

Innumerable techniques/ methods for the synthesis of samples are described in the literature, from the conventional ceramic techniques to the sol-gel/cold co- precipitation methods [1-3]. In this study, the focal theme of the present investigation is on delving the finite size effects on the magnetic, and electrical properties of ultra fine ferrites. Hence sol-gel method is adopted for the preparation of samples. The details of the experimental techniques are described in this section. The sol-gel method allows good control of the structural and magnetic characteristics of fine particles of ferrites. With the sol-gel process, a solid ceramic can be synthesised from a

solution with viscosity similar to that of water. Broadly the solgel method can be defined as the transformation of a solution through series of chemical reactions to a solid gel. The advantages of this method includes processing at low temperatures and intermixing at the molecular level.

To prepare ultra fine particles of nickel ferrite, analytical grades of $Fe(NO_3)_3.9H_2O$ and $Ni(NO_3)_2.6H_2O$ in the 2:1 ratio were dissolved in ethylene glycol at about 40°C. After heating the sol of the metal compounds to around 60°C a wet gel is obtained. The obtained gel when dried at about 100°C self ignites to give a highly voluminous and fluffy product. A certain amount (sample a) of the as prepared powder obtained through the sol-gel method was kept as such and nanosized particles of $NiFe_2O_4$ with varying particle sizes were obtained by heat treating different portions of the as prepared powder separately for 12 h at 300°C, 600°C and 900°C.

Fine particles of $CoFe_2O_4$ and $Li_{0.5}Fe_{2.5}O_4$ were also synthesised employing similar methods. The raw materials for the preparation of $CoFe_2O_4$ are $Fe(NO_3)_3.9H_2O$ and $Co(NO_3)_2.6H_2O$ and that for $Li_{0.5}Fe_{2.5}O_4$ are Li NO_3 $3H_2O$ and $Fe(NO_3)_3.9H_2O$

2.2. Structural evaluation of ferrite samples

The X ray diffractograms of these powder samples were recorded on a X-ray diffractometer (Rigaku D max-C) using Cu K_α radiation (λ = 1.5418 A^0). This was carried out to ensure the formation of exact phase/ and to detect any impurity present in the material and to confirm that there is no impurity phase present in the prepared samples. Lattice parameter was calculated from the X-ray diffractogram by employing the relation

$$d_{h,k,l} = \frac{a}{\sqrt{h^2 + k^2 + l^2}} \qquad 2.1$$

The average particle size was determined from the measured width of their diffraction curves by using Debye Scherrer formula [4,5]

$$D = \frac{0.9\lambda}{\beta \cos \theta} \qquad 2.2$$

Here λ is the wavelength of Cu K_α radiation (λ = 1.5406 A^0), β is the angular width in radians which is equal to the full width at half maximum.

The X- ray density of the prepared ceramic samples were calculated using the relation [6,7]

$$\rho_x = \frac{nM}{a^3 N} \qquad 2.3$$

where n is the no. of molecules/unit cell, M is the molecular weight, a is the lattice parameter and N is the Avogadro number.

The apparent density is calculated by considering the cylindrical shape of the pellets and by using the relation

$$\rho_a = \frac{m}{V} = \frac{m}{\pi r^2 h} \qquad 2.4$$

where m is the mass r the radius and h the thickness of the pellet.

Porosity P of the ferrite samples were then determined by employing the relation

$$P = \frac{\rho_x - \rho_a}{\rho_x} \qquad 2.5$$

The surface area in m^2/ g was obtained using the relation

$$S = \frac{6000}{D\rho} \qquad 2.6$$

where 'D' is the diameter of the particle in nm and 'ρ' the density of the particle in g/cc. [8,9].

2.3. Incorporation of $NiFe_2O_4$ fillers in rubber matrix

The magnetic fillers were then incorporated in nitrile rubber matrix according to a specific recipe[10]. Compounds were prepared for various loadings of 20phr, 40phr, 80phr and 120phr. The compounding ingredients of a typical matrix is cited in table 2.1. The mixing is carried out in a Brabender Plasicorder.

Table 2.1.

Typical Recipe for compounding of nitrile rubber with nickel ferrite

Nitrile rubber	100.0
Zinc oxide	5.0
Stearic acid	1.5
Sulphur	1.5
CBS	1.5
Antioxidant (SPS)	1.0

A brief description of Brabender Plasticorder is provided below. Brabender Plasticorder is a device for measuring the processability and determining the rheological and blending properties of the polymers. The heart of the torque rheometer is a jacketed chamber with horizontal split rotors connected to a shaft. The resistance put up by the test material against the rotors in the mixing chamber is made visible with the help of a dynometer balance. A mechanical gear is used to control the speed of rotation (rpm) of the rotor. The rpm of the rotor can be varied from 0 to 150. A tachometer is attached to measure the rpm of the rotor. An oil bath is used to maintain constant temperature inside the mixing chamber. A digital temperature controller is used to change the mixing temperature. The temperature can be varied between 30^0C to 300^0C. A constant torque of 460

Nm is maintained throughout the mixing of the compound. The rubber was charged into the mixing chamber after setting the test conditions. When the nerve of the rubber had disappeared, the compounding ingredients were added as per the sequence given in ASTM D 3182 (1982) [11]. The mixing of the ingredients are carried out according to the order of the recipe keeping the temperature at 60^0C and the rpm of the rotor was maintained at 50. The compound was discharged after completion of the mixing.

2.4.Determination of Cure Characteristics

After the mixing, in Brabender plasicorder, it is passed 4 to 5 times through the two roller mill to ensure complete homogenisation. This compounded blend can be cured after a time interval of 24 hours. Cure characteristics of the vulcanisable rubber compounds is to be studied before moulding the compound into sheets. Knowledge of these cure characteristics also throws light on the processability and mechanical properties of the composites[10,12]. The cure characteristics of the composites were determined using a Goettfert elastograph model 67.85. It is a microprocessor controlled rotorless cure meter with a quick temperature control mechanism and well defined homogeneous temperature distribution in the test chamber. Cure characteristics gives information of parameters like minimum torque, scorch time, cure rate, maximum torque and cure time. Cure temperature is fixed at 150^0C and the cure time required for each RFC samples is determined from the respective cure characteristics. It is the time required for the optimum cure of the sample .

Maximum torque is a measure of the stiffness or shear modulus of fully vulcanised test specimen at the vulcanisation temperature. Minimum torque is the stiffness of the unvulcanised test specimen at the lowest point

of the cure curve. Cure time is the time required for 90% cure of the test specimen.

The time required to obtain the cure curve is characteristic of the rubber compound and of the test temperature. Further, from the cure curve, the cure parameters are extracted. Using these parameters the compounds are then vulcanized at 150^{0}C on an electrically heated laboratory hydraulic press up to their respective cure times to make sheets of the sample. The entire test is carried out according to the ASTM standards [12-14]

2.5.Evaluation of Mechanical properties

Tensile properties of the RFCs are determined as per ASTM D 412 (1980) using dumb-bell shaped specimens on an Instron Universal Testing Machine, Model 4411 Test System. Specimens for the tests are punched out of compression moulded sheets along the mill grain direction using a standard die. The thickness of the narrow portion is measured by bench thickness gauge. The sample is held between the two grips on the UTM, the upper grip of which is fixed. The rate of separation of the power actuated lower grip is fixed at 500 mm/min. The tensile strength, elongation at break and modulus at different elongations which are some of the important indications of the strength of the material[15-21] are recorded and evaluated after each measurement by the microprocessor. Fig shows a representative shape of the tensile testing specimen used in the present study.

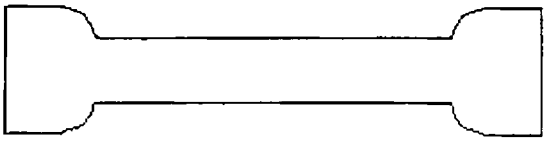

Fig2.1Test Specimen for tensile measurements

Dumb-bell shaped samples were cut from the prepared RFCs containing $NiFe_2O_4$ at various loadings of 20,40,80 and 120phr. Tensile strength, 100% modulus,200% and elongation at break were determined for the RFCs of various loadings.

2.6. Magnetic Characterization

The magnetic characterization of both nickel ferrite powder samples and rubber ferrite composites (RFC) are carried out using a Vibrating Sample Magnetometer (VSM), model: EG & G Par 4500. A simplified block diagram of the VSM is given in Fig.(2.2) and the main parts of the VSM are shown in and Fig.(2.3). Parameters like Saturation magnetization (M_s) and coercivity (H_c) were evaluated from the hysteresis loops obtained at room temperature.

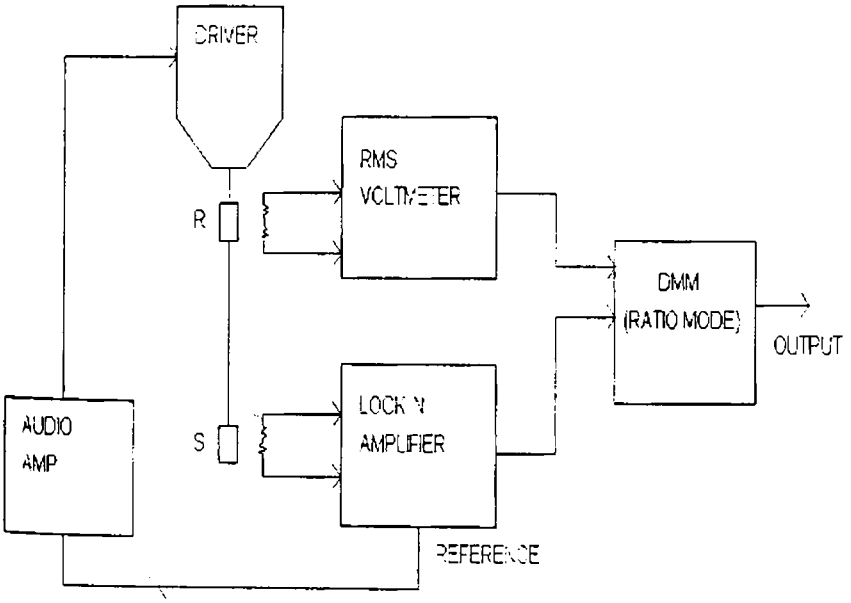

Fig. 2.2. Block diagram of VSM.

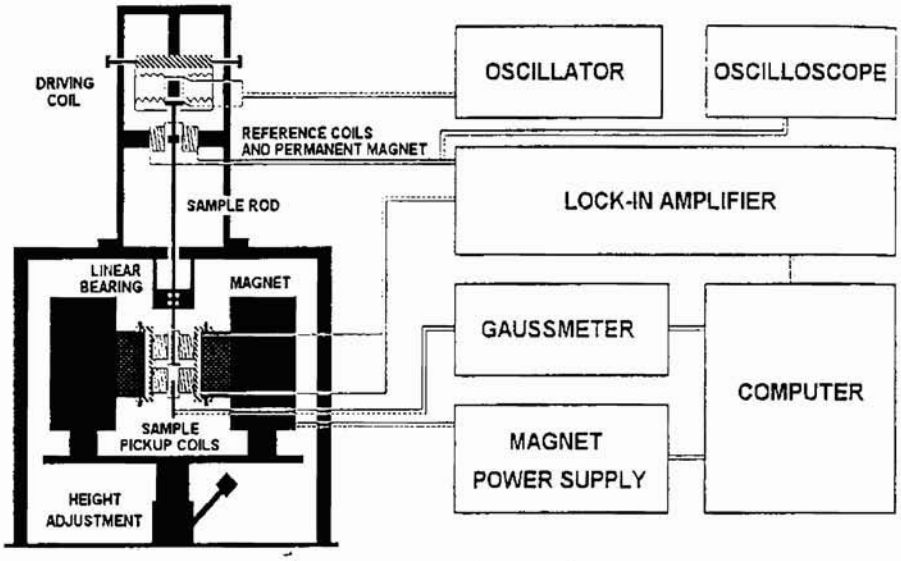

Fig. 2.3. Main parts of the VSM

2.6.1.Principle & Theory Involved in VSM

When a magnetic material is placed in a uniform magnetic field, a dipole moment is induced which is proportional to the susceptibility of the sample and the applied field. If the sample is vibrated periodically, it can induce an electrical signal in a pickup coil. The position of the pickup coil is adjusted in such a way as to give the maximum induction with minimum noise. The induced signal in the pickup coil will be proportional to the magnetic moment produced in the sample and the vibrating frequency of the sample. This is the basic principle used in the design of a VSM to measure the magnetic properties

The amount of magnetic flux linked to a coil placed in the vicinity of the magnetic field is given by

$$\phi = \mu_0 n \alpha M \qquad 2.7$$

μ_0 – permeability of free space, n - number of turns per unit length of coil, M– magnetic moment of the specimen and $\varkappa$- Geometric moment decided by position of moment with respect to coil as well as shape of coil. Anharmonic oscillator of the type

$$Z = Z_0 + A \exp(j\omega t) \qquad 2.8$$

induces an emf in the stationary detection coil. The induced emf is given by

$$V = -\frac{d\phi}{dt} = -j\omega\mu_0 nMA\left(\frac{\partial\alpha}{\partial z}\right)e^{j\omega t} \qquad 2.9$$

If amplitude of vibration (A), frequency and $\frac{\partial\alpha}{\partial z}$ are constant over the sample zone then induced voltage is proportional to the magnetic moment of the sample[22,23].

A transducer is used to convert the electrical oscillations into mechanical vibrations. An electronic oscillator circuit produces a constant frequency and it is applied to the transducer to vibrate the sample rod. The vibrating sample in the uniform magnetic field induces a signal in the pickup coils mounted to it. Vibration amplitude and frequency also will have some contributions to the induced emf in addition to the contributions of the magnetic moment. A servomechanism is used to stabilize the amplitude and frequency of the drive so that the output accurately tracks the moment level without degradation due to variation in the amplitude and frequency of the oscillator.

The servomechanism uses a vibrating capacitor located beneath the transducer to generate an ac control signal that varies solely with the vibration amplitude and frequency. The signal, which is at the vibration frequency is fed back to the oscillator where it is compared with the drive signal so as to maintain constant drive output. It is also phase adjusted and

routed to the signal demodulator where it functions as the reference drive signal. The signal developed in the pick up coils is then buffered, amplified and applied to the demodulator. There it is synchronously demodulated with respect to the reference signal derived from the moving capacitor assembly. The resulting dc output is an analog signal, which depends only on the magnitude of the magnetic moment, and not influenced by the amplitude and frequency drift. The cryogenic setup attached to the sample assembly can be used to study the magnetisation of samples at low temperatures.

2.7.Dielectric and ac conductivity studies

Dielectrics are basically insulators having the property of storing and dissipating electrical energy when subjected to electromagnetic fields. The dielectric permittivity is defined as the ratio of the filed strength in vacuum to that in the material for the same distribution of charges. Dielectric permittivity is dependent on parameters like temperature, orientation, grain size, molecular structure of the material and frequency of the applied field [24-28].

When a parallel plate capacitor with a dielectric in between is charged, then the capacitance is given by

$$C = \frac{\varepsilon_0 \varepsilon_r A}{d} \qquad 2.10$$

where A is the area of the sample, d is the separation between the plates and ε_0 is the permittivity of free space and ε_r is the dielectric permittivity of the material between the plates. HP 4285A was employed for the evaluation of dielectric permittivity. The acquisition of data was automated by interfacing HP 4285A with a computer. For this a virtual instrumentation package, based on graphical programme was employed. This package is called LabVIEW, a base software package developed by National Instruments for

implementing virtual instrumentation. It is object oriented and uses a graphical language called 'G' resembling the first principles of flowcharting.

Figure 2.3 shows a schematic diagram of the fabricated dielectric cell. The dielectric measurements have been carried out for both powder samples and rubber ferrite composites. For this, pellet shaped samples were used with diameter 1cm. The behaviour of the dielectric permittivity of these samples is investigated in the frequency range of 100 KHz to 8 MHz and in the temperature range of 300K to 393K.

The dielectric permittivity is complex in nature of the form

$$\varepsilon = \varepsilon' - j\varepsilon'' \qquad 2.11$$

with imaginary part indicates the absorption in the medium.

The loss factor or dissipation factor in any dielectric is given by the relation

$$\tan\delta = \frac{\varepsilon''(\omega)}{\varepsilon'(\omega)} \qquad 2.12$$

In Polar dielectrics, the absorption is caused by the orientation and relaxation of dipoles. Dipoles rotate under the action of an external electric field overcoming the forces of internal friction of matter, which is attended by the expenditure of a part of dielectric energy as heat which is the dielectric loss [29]. Tan δ is the measure of dielectric loss

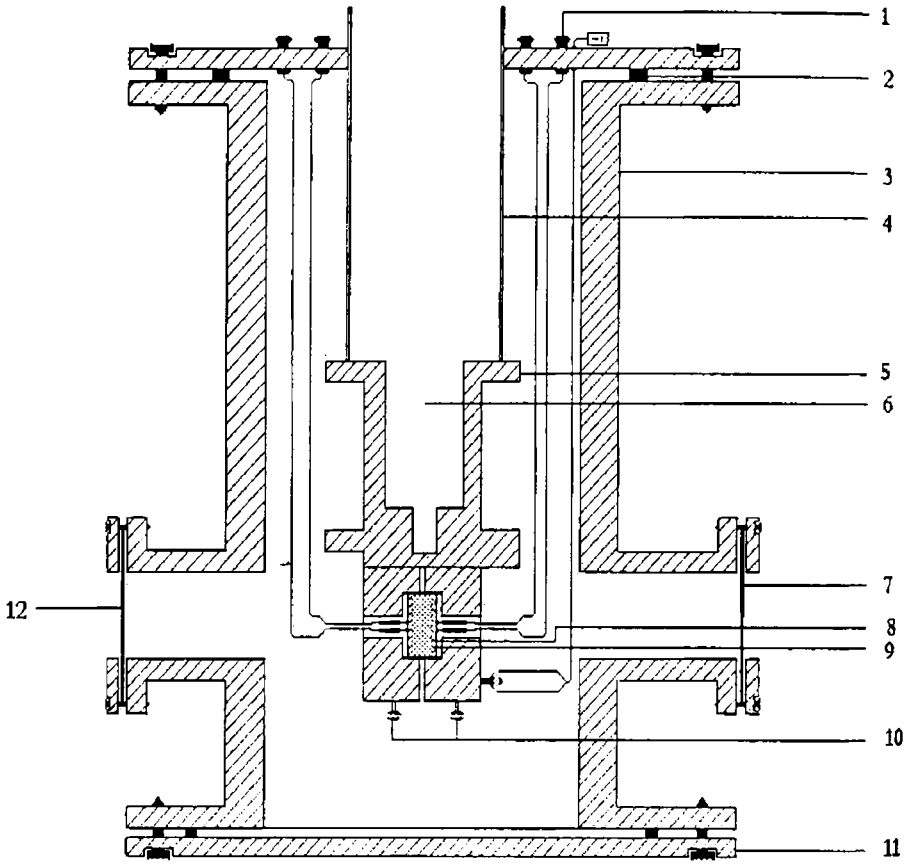

1. BNC
2. Neoprine O Ring
3. MS Chamber
4. SS Pipe
5. Sample Holder
6. Liq. Nitrogen Cavity
7. Glass Window
8. Copper Electrodes
9. Sample
10. Fixing Screws
11. MS Flange
12. To Vacuum pump

Fig. 2.3. Schematic representation of dielectric cell

2.8.Ac conductivity

The theory involved for the evaluation of ac conductivity from dielectric constant values is explained in this section. Any capacitor when charged under an ac voltage will have a loss current due to ohmic resistance or impedance by heat absorption.

For a parallel plate capacitor of area of cross section A and separation d, the ac conductivity is given by the relation

$$\sigma_{ac} = \frac{J}{E} \qquad 2.13$$

Here J is the current density and E is the field density. But we know that the electric field vector

$$E = \frac{D}{\varepsilon} \qquad 2.14$$

where D is the displacement vector of the dipole charges, ε is the complex permittivity of the material. Also the electric field intensity (E) for a parallel plate capacitor is the ratio of potential difference between the plates of the capacitor and the inter plate distance.

$$\text{i.e. } E = \frac{V}{d} \qquad 2.15$$

V is the potential difference between the plates of the capacitor, d is the inter plate distance.

Since the current density $J = \frac{dq}{dt}$ and q is given by $\frac{Q}{A} = \frac{V\varepsilon}{d}$, where Q is the charge in columns due to a potential difference of V volts between two plates of the capacitor.

$$J = \frac{dq}{dt} = \frac{d}{dt}\left(\frac{V\varepsilon}{d}\right) = \frac{\varepsilon}{d}\frac{dV}{dt}$$

$$J = \frac{\varepsilon}{d}\frac{dV}{dt} = \frac{\varepsilon}{d} V j\omega \qquad 2.16$$

Substituting for E and J from the equations 2.13 and 2.14 we get

$\sigma_{ac} = \frac{J}{E} = \varepsilon j\omega$, Considering ε as a complex entity of the form

$\varepsilon^{*} = \varepsilon^{'} - j\varepsilon^{''}$ and neglecting the imaginary term in the conductivity we can write

$$\sigma_{ac} = \omega\varepsilon^{''} \qquad 2.17$$

But the loss factor or dissipation factor in any dielectric is given by the relation

$$\tan\delta = \frac{\varepsilon''(\omega)}{\varepsilon'(\omega)} \qquad 2.18$$

Hence from the dielectric loss and dielectric constant, ac conductivity of these samples can be evaluated using the relation

$$\sigma_{ac} = 2\pi f \varepsilon_0 \varepsilon_r \tan\delta \qquad 2.19$$

where f is the frequency of the applied field and tanδ is the loss factor.

The ac electrical conductivity of both powder samples and RFC.s is calculated utilizing the dielectric parameters. The ac conductivity is calculated by using the relation $\sigma_{ac} = 2\pi f \varepsilon_0 \varepsilon_r \tan\delta$. After obtaining capacitance and dielectric loss from the instrument, LabVIEW software first calculates the dielectric constant and then evaluates the ac conductivity of the ferrites and RFC's.

1.9.Microwave measurements

The measurements in microwave frequency region are required not only for scientific but also for industrial applications. Different methods including cavity resonant and cavity perturbation are employed for microwave measurements. But cavity perturbation method has been widely used to study the dielectric and magnetic parameters in the X-band. In this technique it is assumed that the fields externals to the ferrite body remains unchanged from those of the empty cavity and it is the fields in the ferrite body which is different. Also it is assumed that the ferrite makes only a small perturbation to the fields existing in the unperturbed activity [30].

2.10.1.Theory for the measurement of permittivity in the X-band using rectangular waveguide cavity

When a small sample is inserted in a cavity which has the electric field E_0 and magnetic field H_0 in the unperturbed state, the fields in the interior are E and H. Beginning with Maxwell's equation, the variation of the resonant frequency is given as [31]

$$\frac{\omega - \omega_0}{\omega} = \frac{\int (\Delta\varepsilon\ E.E^* + \Delta\mu\, H.H_0^*) d\tau}{\int (\varepsilon\, E.E_0^* + \mu\, H.H_0^*) d\tau} \qquad 2.20$$

Where ε and μ are the permittivity and permeability of the medium in the un perturbed cavity respectively Δ ε and Δ μ are the changes in the above quantities due to introduction of the samples in the cavity.

The complex frequency shift is due to the samples given by [31]

$$\frac{-\delta\Omega}{\Omega} = \frac{(\bar{\varepsilon}_r - 1)\varepsilon_0 \int_{V_s} E.E_0^* dV + (\bar{\mu}_r - 1)\mu_0 \int_{V_s} H.H_0^* dV}{\int_{V_c} (D_0.E_0^* + B_0.H_0^*) dV} \qquad 2.21$$

Two approximations are made in applying equation 2.20, based on the assumption that the fields in the sample are uniform over its volume. Both these assumptions can be considered valid if the object is sufficiently low relatively to the resonant wave length. The negative sign in equation 2.20 indicates that by introducing the sample the resonant frequency is lowered. Since the pemittivity is complex, the resonant frequency should also be considered as complex. V_c and V_s are the volumes of the cavity and the sample respectively. In terms of energy, the numerator of equation 2.20 represents the energy stored in the sample and the denominator represents the total energy stored in the cavity. The total energy W=Wc+Wm. When a dielectric sample is introduced at the position of maximum electric field only the first term in the numerator is significant, since a small change in ε at a point of zero electric field or a small change in μ at a point of zero magnetic field does not change the resonance frequency. The equation 2.20 can be reduced to

$$\frac{-\delta\Omega}{\Omega} \approx \frac{(\varepsilon_r - 1)\int_{V_s} E\,E_0^{*}{}_{max}\, dV}{2\int_{V_c} |E_0|^2 dV} \qquad 2.22$$

Let Q_o be the quality factor of the cavity in the unperturbed condition and Q_s the Q-factor of the cavity loaded with the object. The complex frequency shift is related to measurable quantities by

$$\frac{\delta\Omega}{\Omega} \approx \frac{\delta\omega}{\omega} + \frac{j}{2}\left[\frac{1}{Qs} - \frac{1}{Q_0}\right] \qquad 2.23$$

Equating the real and imaginary terms of equations 2.21 and 2.22, we get

$$\frac{-f_s - f_0}{f_s} = \frac{(\varepsilon'_r - 1)\int_{Vs} E.E_0{}^*{}_{max}\, dV}{2\int_{VC} |E_0|^2\, dV} \qquad 2.24$$

$$\frac{1}{2}\left[\frac{1}{Qs} - \frac{1}{Q_0}\right] = \frac{\varepsilon''_r \int_{Vs} E.E_0{}^*{}_{max}\, dV}{2\int_{Vc} |E_0|^2\, dV} \qquad 2.25$$

We may assume that $E=E_o$ and the value of E_o in TE_{10p} as $Eo=Eo_{max}$ Sin (mπx/a) Sin (pπz/d) where a is the broader dimension of the waveguide and d the length of the cavity. Integrating and rearranging the above equations, we get

$$\varepsilon'_r - 1 = \frac{f_0 - f_s}{2 f_s}\left[\frac{V_C}{V_s}\right] \qquad 2.26$$

$$\varepsilon''_r = \frac{V_C}{4V_s}\left[\frac{1}{Qs} - \frac{1}{Q_0}\right] \qquad 2.27$$

If the frequency shift is measured from the resonance frequency f_1 of the cavity alone, the above equations become

$$\varepsilon'_r - 1 = \frac{f_t - f_s}{2 f_s}\left[\frac{V_C}{V_s}\right] \qquad 2.28$$

$$\varepsilon''_r = \frac{V_C}{4V_s}\left[\frac{1}{Qs} - \frac{1}{Q_t}\right] \qquad 2.29$$

Q_l is the quality factor of the loaded with empty tube. f_s and Q_s are the resonance frequency and quality factor of the cavity loaded with capillary tube containing the sample material.

2.10.2.Measurement of complex permittivity

The block diagram of the experimental set-up is shown in fig.2.5. The material whose permittivity is to be measured is taken in a capillary tube. The resonance frequency f1 and unloaded Q-factor Q1 of the cavity resonator are measured with the empty

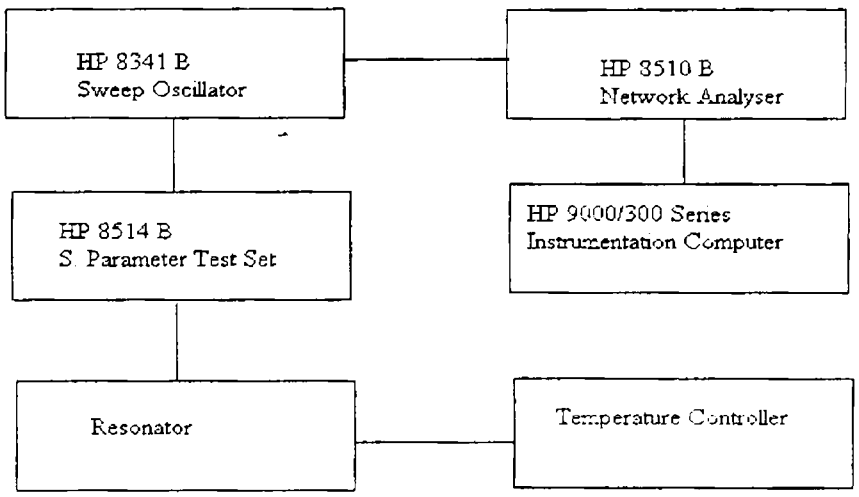

Fig.2.5.Block diagram of the experimental set-up

capillary tube inserted in the cavity at the position of maximum electric field. The sample material is filled in the capillary tube and is positioned at the maximum electric field. The resonance frequency f_s and loaded quality factor Q_s are measured. From these data's, ε' and ε'' of the material can be computed.

Reference.

1. Chen D.H and Y.Y.Chen, *J.Colloid Interface Sci.*, **235** (2001). , 9.
2. J. J.Kingsley, K.Suresh and K.C.Patil, *J.Mater. Sci.*, **25** (1990). , 1305.
3. Chen D.H. and X.R.He, *Bull. Mater.Res.*, **36** (2001), , 1369
4. Ph.D Thesis ,K.A.Malini, Cochin University of Science and Technology, Cochin, 2001
5. H.V.Keer Principles of Solid State Phys, Willey Eastern Ltd. NewDelhi ,1993
6. C.Kittel, Introductions to Solid State Physics, John Wiley and Sons, New York, 1997.
7. Cullity B.D Elements of X-ray Diffraction ,1978, Philippines, Addison-Weisley Publishing Company, Inc.
8. Solid Sstate Physics, (India), **42** ,(1999) Edited Mukhopadhyay,B K Godwal and S M Yusuf
9. S.Blow. Handbook of Rubber Technology, Galgotia Publishing, 1998.
10. ASTM D3182 (1982).
11. George Winspear (Edt), The Vanderbilt Rubber Handbook, R.T. Vanderbilt Company Inc .New York ,
12. Vishu Shah, Handbook of Plastic TestingTtechnology, John Wiley and Sons Inc ,USA 1998.
13. A.W. Allen, Natural Rubber and the Synthetics, Granda Publishing Ltd.1972.
14. Charles A Harper, Handbook of Plastic, Elastomers and Composites (Second Edition) McGraw Hill Inc.1992.
15. R.D.Shull. J.J.Ritter and L.J.Swartzendruder, J. Appl .Phys .**69,** (1991) ,5414.
16. A.Gravin and C.L.Chein, J.Appl.Phys.**67,** (1990), 938.
17. K.A Malini, P. Kurian, M.R. Anantharaman., Mater. Letter **57,** (2003), 3381.
18. E.M. Mohammed, K.A.Malini, Philip Kurian, M.R. Anantharaman, Materials Research Bulletin **37** ,(2002), 753.
19. M.A.Soloman, Philip Kurian, M.R.Anantharaman, Progress in Rubber, Plastics and Recycling Technology, **18** No.4, (2002), 269.
20. Roberts.A.D, Natural Science and Technology, (1998), Oxford University Press, New York 556.
21. Simon Foner, Rev. Sci. Instrum. **30,** no.7, (1959), 548.
22. Joseph A. Pesh .Rev. Sci .Instrum **70,** No.1,(1999) ,85
23. S.Jankowski, Journal of American Ceramic Society, (1988),176.

24. F.C.Brockman, R.T.White, J. of American Ceramic Society 54,(1971), 109.
25. P.V.Reddy, R.Sathyanarayana, T.S.Rao, Phys. Stat. Sol A, **78,** (1983) ,109.
26. A.Verma, T.C.Goyal, R.G.Mindiretta, R.G.Gupta, Journal of Magnetism and Magnetic Materials, **192,** (1999), 271.
27. M.A.El Hiti, Jof Magnetism and Magnetic materials **164,** (1996), 187
28. Ramasastry C and Syamasundra Rao, J.Phys.E.Sci.Instrum.**12**, (1979) ,1023
29. Physics of Dielectric Materials, B. Tareev, Mir Publishers Moscow
30. VRK Murthy, Microwave materials, (Methods of Measurement of Dielectric Constant and Loss in the Microwave Frequency Region), Narosa Publishing House, New Delhi.
31. Ferrites at Microwave Frequencies, A. J. Baden Fuller, Peter Peregrinus Ltd. U.K, 1987.

Chapter III

Structural and Magnetic properties of Nanosized $NiFe_2O_4$ and their Composites

3.1. Introduction

Synthesis of advanced ceramics as nanoparticles is currently gaining widespread interest in material processing technology [1-5]. Owing to the extremely small dimensions of nanostructured materials, a major portion of the atoms lie at the grain boundaries, which in turn is responsible for superior magnetic, dielectric and mechanical properties in these materials compared to their conventional coarse grained counterparts [6-8]. The different chemical processes currently in vogue for the synthesis of nanoparticles include co-precipitation [9], combustion method [10], sol gel process [11], spray pyrolysis [12], micro emulsion technique [13] and hydrothermal process [14]. Among these methods, sol gel process allows good control of the structural and magnetic properties of ceramic materials. The advantages of this method include processing at low temperatures, mixing at the molecular level and fabrication of novel materials.

Nanosized magnetic particles exhibit unique properties and have promising technological applications in high-density recording, color imaging, ferrofluids, high frequency devices and magnetic refrigerators, [15-16]. Nanoparticles of magnetic ceramic materials are also widely used as contrasting agents in magnetic resonance imaging (MRI), replacement of radioactive materials used as tracers and delivery of drugs to specific areas of the body. From the application point of view, the most significant properties of magnetic ceramic materials namely magnetic

saturation, coercivity, magnetization and loss, change drastically as the size of the particles move down into the nanometre range [17-19]. Among the different ferrites, which form a major constituent of magnetic ceramic materials, nanosized nickel ferrite possess attractive properties for application as soft magnets and low loss materials at high frequencies [20]. Moreover, there are numerous reports wherein anomaly has been reported in the structural and magnetic properties of spinel ferrites in the nanoregime [21-23]. A typical example is zinc ferrite, which is a normal spinel exhibiting antiferromagnetism with a Neel temperature of ~ 10.5 K in the micron regime[24]. However nanoparticles of zinc ferrite prepared by different techniques show ferrimagnetic characteristics with ordering temperatures above room temperature. Nickel ferrites in the ultrafine form, is an inverse spinel exhibiting noncollinear spin structure and the magnetic moment at low temperatures is appreciably lower than the value for the bulk material [25].. Chinnasamy et al found a mixed spinel structure for nickel ferrite when the grain size is reduced to a few nanometers [26]. They deducted this with the help of Mössbauer spectroscopy, magnetisation and EXAFS. They observed that in addition to the canting of surface spins because of the broken exchange bonds, the core spins could also have canted spin structure, resulting from the occupation of the tetrahedral sites by Ni^{2+} ions. Kodama et al [27-28] observed anomalous magnetic properties for their organic coated nickel ferrite nanoparticles. Hence, the synthesis of nickel ferrites as nanoparticles and the investigation of their various physical properties depending on the grain size continue to be an active area of research in the field of material science.

Rubber ferrite composites (RECs) are composite materials with ferrite as one of the constituents and natural or synthetic rubber as the base

matrix. The size of the magnetic powder as well as the polymer will affect the processability and other physical properties of the final product [29]. These plastic magnets can in turn be useful for various applications in different devices. The addition of magnetic fillers in an elastomer matrix modifies the physical properties of the matrix considerably, in that they modify the dielectric properties and impart magnetic properties to the matrix. In applications involving ferrites at high frequencies it is essential that the material posses an appropriate dielectric constant and suitable magnetic permeability. This can be achieved by synthesizing rubber ferrite composites (RFC). The microwave absorbing properties of elastomers warrant an appropriate dielectric strength and a desirable magnetic property [30-34]. Nickel ferrites and its composites, which absorb energy from electromagnetic waves and are widely used in stealth technology have attracted much attention. [35]. The preparation of RFCs and evaluation of various properties such as magnetic, dielectric and mechanical assumes significance not only in tailor making compounds but also in understanding the fundamental aspects that govern these properties.

It is customary that pre characterised magnetic fillers are incorporated in to matrix. This will ensure a proper understanding of the composite and the properties exhibited it after incorporation, curing and moulding. Here the evaluation of the structural and magnetic properties serves the twin objective of correlating the properties of the filler plus the correlation of the properties of the matrix. The results are presented here in this chapter.

3.2.Structural Studies of Nickel Ferrites

Ultrafine nickel ferrites were prepared by sol-gel method. The details are cited in chapter 2.The resulting gel when dried at about 100°C self

ignites to give a highly voluminous and fluffy product. A certain amount (sample a) of the as prepared powder obtained through the sol-gel method, was kept as such and nanosized particles of $NiFe_2O_4$ with varying particle sizes were obtained by heat treating different portions of the as prepared powder separately for 12 h at 300°C (sample b), 600°C (sample c) and 900°C (sample d).

The structural characterisation of all the four samples were carried out by X-ray diffraction (XRD) technique on a Rigaku D_{max} 2C diffractometer with nickel filter using Cu-Kα radiation (wavelength λ= 1.5418 Å). The lattice parameters were evaluated from the X-ray diffraction data assuming cubic symmetry. The line broadening during X-ray diffraction can be mainly due to particle size effect, temperature effect and strain. The grain size and/or microstrain developed during the synthesis/ heat treatment is related by the equation,

$$\beta = \beta' + \beta'' = \lambda/d_g \cos\theta + 4\varepsilon \tan\theta \qquad 3.1$$

where β' and β'' are the contributions of grain size and strain respectively, to line broadening, θ is the Bragg angle, ε is the strain and d_g is the grain size. When the strain term (β''= 4ε tan θ) is negligible, then the line width (β) is given by

$$\beta \sim \lambda/d_g \cos\theta \qquad \text{or} \qquad d_g \sim \lambda/\beta\cos\theta \qquad 3.2$$

and the value of grain size calculated from different XRD lines will be approximately the same. However, when the strain is not negligible as in the case of $NiFe_2O_4$ synthesized by the sol-gel method, the grain size calculated from different XRD lines will be different. Thus to evaluate strain, β is measured for different XRD lines and equation [1] may be rewritten as

$$\beta\cos\theta = \varepsilon(4\sin\theta) + \lambda/d_g \qquad 3.3$$

This gives an equation of a straight line between $\beta \cos \theta$ and 4 sin θ. Plotting $\beta \cos \theta$ (y axis) and 4 sin θ (x axis), the slope of the line gives the strain (ε) and the particle size (d_g) can be calculated from the intercept (= λ/d_g) of this line on the y axis.

Assuming all the particles to be spherical, the specific surface area was calculated from the relation

$$S = 6000/d_g \rho \qquad 3.4$$

Where ρ is the measured density in gm/cc and d_g the grain size in nm. The porosity was calculated from the observed and theoretical density for all the four samples.

The X-Ray diffraction pattern of the four samples of $NiFe_2O_4$ powders synthesized by the sol-gel technique is depicted in Fig.3.1. All the characteristic peaks of $NiFe_2O_4$ are present in the diffraction pattern. The XRD data agrees well with the standard JCPDS values [36]. However, a sharp increase in the crystalline nature of the nickel ferrite powders is observed as the firing temperature was increased which is recorded as a decrease in the broadening of the peaks in the diffraction pattern. This clearly indicates that the grain size has increased with increase of firing temperature. The grain size of the four samples heated at different temperatures is calculated using equation 3.2 and the results are given in table 1.

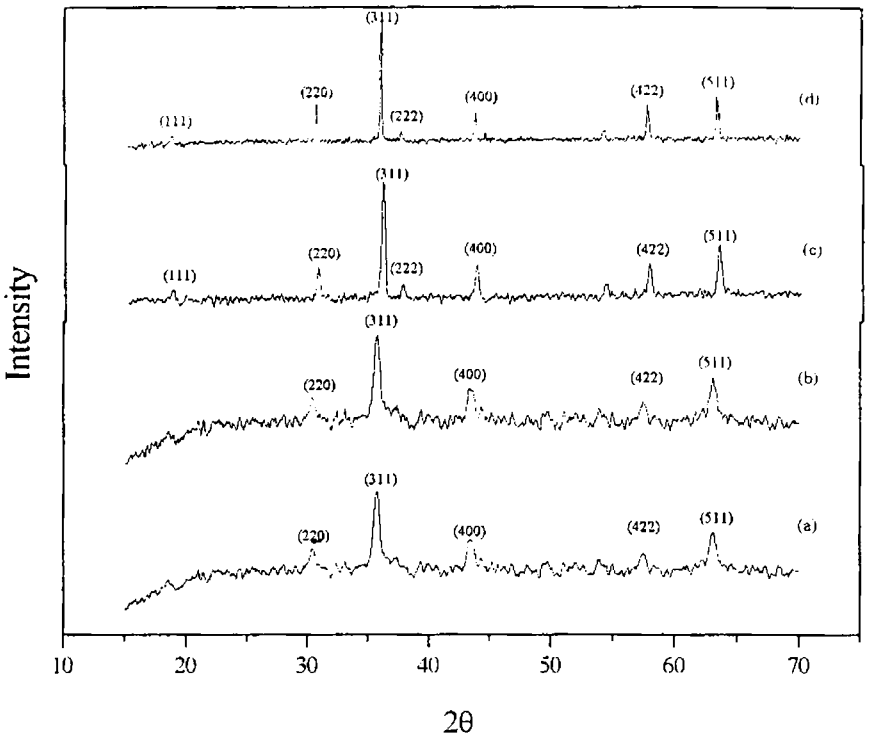

Figure3.1: X-ray diffraction pattern of the (a) as prepared $NiFe_2O_4$ powder, (b) the $NiFe_2O_4$ powder heated at 300°C, (c) at 600°C and (d) 900°C all for a duration of 12 h.

Table3.1

Structural parameters of sol-gel synthesized $NiFe_2O_4$

Firing Temperature (^oC)	Particle Size (nm)	Specific surface area (m^2/gm)	Theoret-ical Density (gm/cc)	Experimental Density (gm/cc)	Porosity (%)
As prepared	9.17	182.7	5.38	3.585	33.36
300	12.44	124.6	5.41	3.871	28.5
600	14.94	91.3	5.53	4.38	20.79
900	21.95	54.56	5.537	5.01	9.51

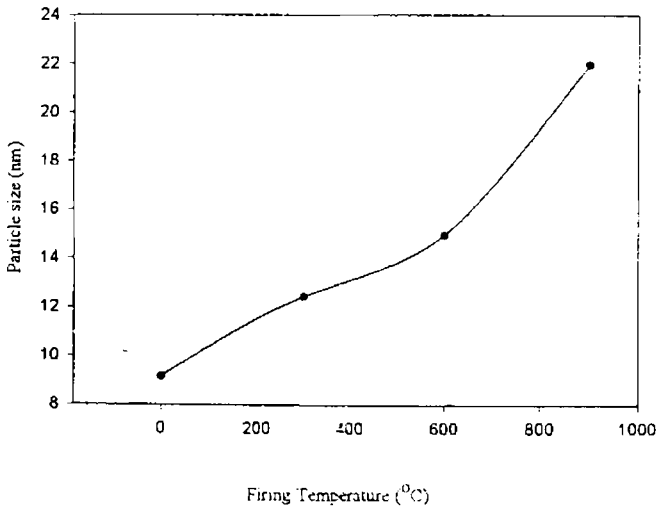

Figure3. 2: Variation of grain size with firing temperature for the sol gel synthesized $NiFe_2O_4$

Figure 2 shows the variation of particle size calculated from the hundred percent intensity peak with firing temperature for all the four samples. From fig.3.2, it is clear that the grain size increases with increase of firing temperature. It is also observed that the value of d_g determined from XRD lines at different θ values differs, indicates the presence of strain. Hence, equation 3 is used to calculate the grain size and the strain factor from the line width values.

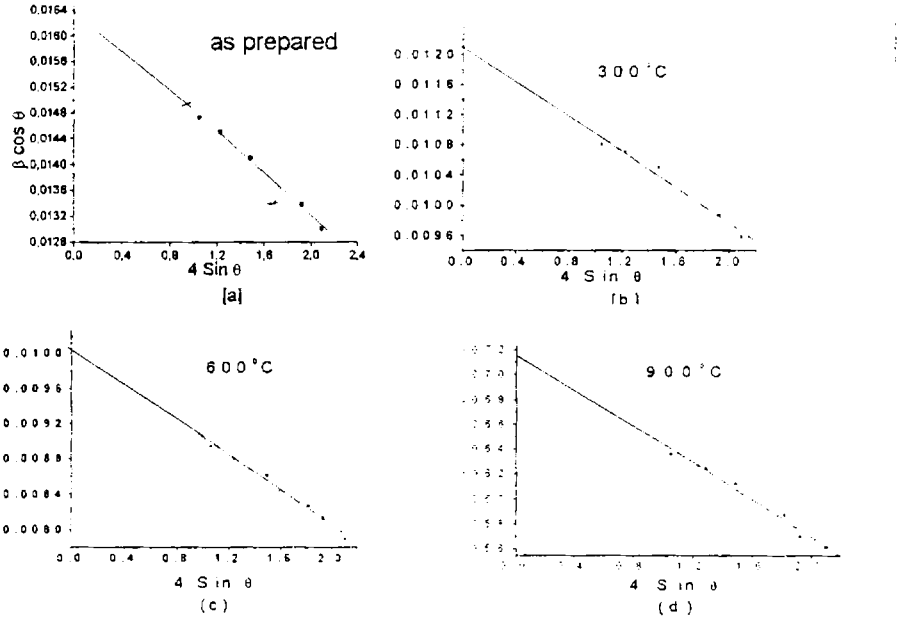

Figure3.3: Strain graphs for the sol-gel synthesized (a) as prepared $NiFe_2O_4$ (b) $NiFe_2O_4$ sample heated at 300°C (c) 600°C and (d) 900°C all for a duration of 12 h

Figures 3.3 shows the strain graphs for all the four samples. It is observed that the strain (value of slope) decreases with increase in firing temperature. The grain size is calculated from the intercept (λ/d_g) and it is observed that the grain size increases with increase of firing temperature.

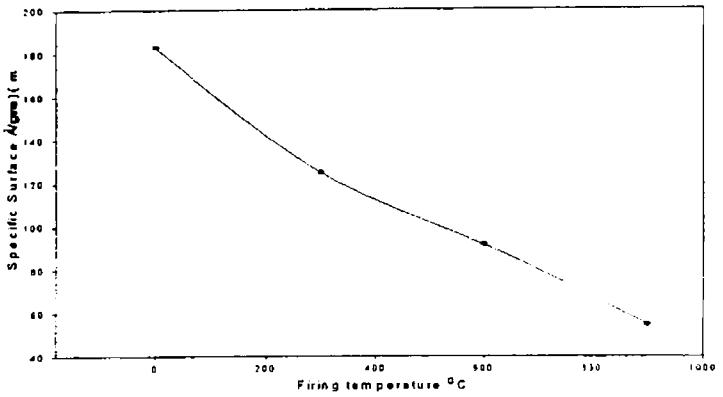

Fig. 3.4: Variation of specific surface area with temperature

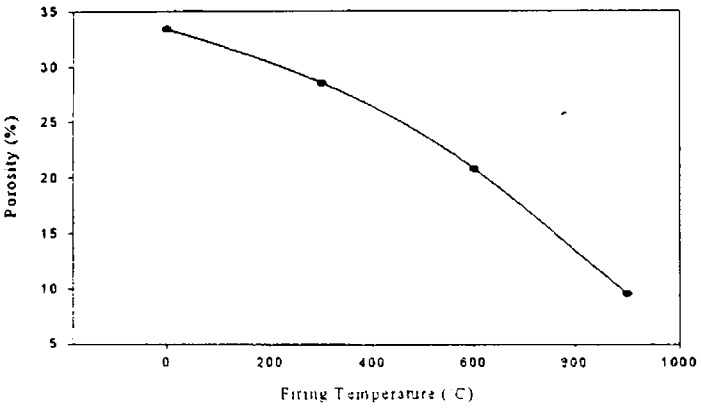

. Figure 3. 5: Variation of porosity with firing temperature for samples.

Figure3.4 shows the graph between firing temperature and specific surface area .The Specific surface area of the particles decreases as the firing temperature increases, indicating the increase of grain size. The porosity of the samples were calculated from apparent density and x-ray density values; and shown in fig. 3.5. The porosity was found to decrease as the firing temperature increases. It may be noted that the density of the sample heat treated at 900°C is with only 90% theoretical density.

3.3.Magnetic measurements

3.3.1.$NiFe_2O_4$ Powder samples

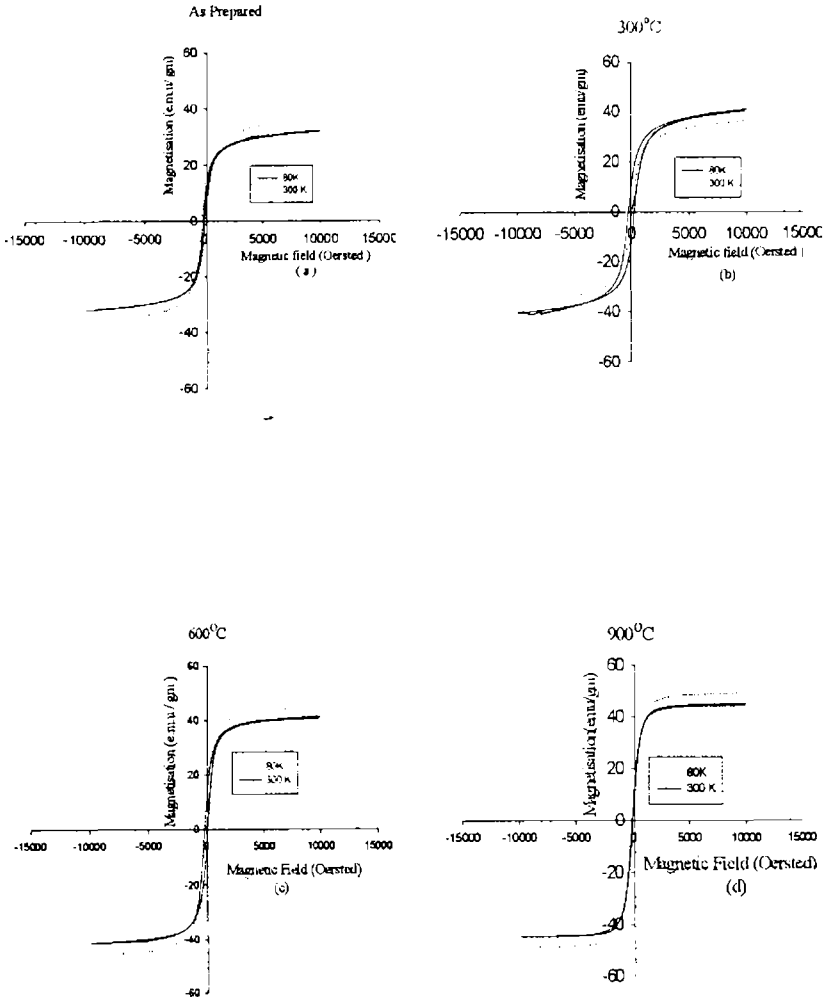

Fig. 3.6: Hysteresis curve (a) as prepared $NiFe_2O_4$ powder (b) $NiFe_2O_4$ powder heat treated at 300°C (c) 600°C and (d) 900°C measured at room temperature and at 80K

Magnetic measurements are carried out using a Vibrating Sample Magnetometer (EG & GPAR 4500) for all the four samples at room temperature (300 K) and liquid nitrogen temperature (80 K). The various magnetic properties like saturation magnetization and coercivity are estimated from the hysteresis curve. Figure 3.6 shows the hysteresis curve for the $NiFe_2O_4$ nanoparticles measured at 300 K and at 80K

Table 2

Magnetic parameters of sol gel synthesized $NiFe_2O_4$

Particle size (nm)	Saturation magnetization (M_s) (emu/gm)		Coercivity (H_c) (Oersted)	
	300 K	80 K	300K	80 K
9.17	32.1	36.2	59	183
12.44	36.2	40.6	90	263
14.94	41.2	45.4	130	172
21.95	44.7	49.1	50	65

The specific saturation magnetization (σ_s) of the nanosized nickel ferrite is observed to decrease with decreasing particle size (table 3.2). The linear decrease in saturation magnetization is accompanied by an increase in specific surface area as shown in fig. 3.7.

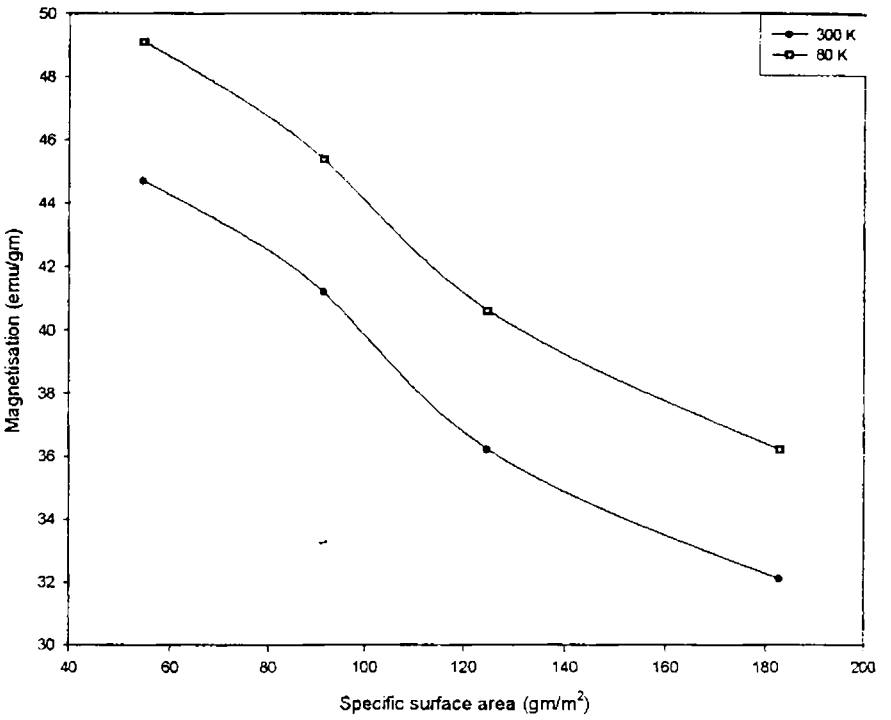

Figure 3.7: Variation of saturation magnetization with specific surface area for $NiFe_2O_4$

In the bulk $NiFe_2O_4$, Ni exhibits a strong octahedral site preference and these ferrites crystallise in the inverse spinel structure. However, in the ultrafine regime, the findings of various researchers as regard the saturation magnetisation are at variance [26,27,28,37]. Some researchers have reported increase in saturation magnetisation with decrease in particle size [26], while others observed a decrease in M_s with decrease in particle size [27,28]. The observed increase or decrease can be due to many factors. Cation redistribution, the existence of surface spins or the formation of spin glass structure can all influence the magnetic properties at the submicron sizes. The presence of a dead layer has also been thought to be one of the reasons

for the reduced magnetisation in the ultrafine regime [37]. The saturation magnetisation of $NiFe_2O_4$calculated using Neel's sublattice theory is 50 emu/g and the reported value for the bulk sample is 56 emu/g [22]. The sample fired at 900°C shows a maximum value of 49 emu/g, is by and large in tune with the reported values of M_s for nickel ferrite.

Several researchers [37] invoked the theory of dead layer to explain the reduction in magnetisation with particle size reduction. However, Kodama and Berkowitz [27,28] with the help of Mössbauer spectroscopy ruled out the possibility of the existence of dead layer in magnetisation. The exhibition of lower saturation magnetisation at fine particle sizes can be attributed to the following. The ferrite can be thought to possesses collinear ferrimagnetic structure. In the usual structural model for a ferrimagnetic ferrite the magnetization of tetrahedral (A) sublattice is antiparallel to that of octahedral (B) sublattice. However, ultrafine nickel ferrites have non-collinear magnetic structure on the surface layer [25]. The decreasing particle size causes an increase in the proportion of non-collinear magnetic structure, in which magnetic moments are not aligned with the direction of external magnetic field. The increase in the proportion of non-collinear structure decreases the saturation magnetization

Figure 3. 8 shows the variation of coercivity with average grain size of the sol gel synthesized nickel ferrite at 300K and at 80K. It is evident from the graph that as the particle size increases, the value of coercivity increases, reaches a maximum value and then decreases at room temperature as well as at 80K. This variation of H_c with particle size can be explained on the basis of domain structure, critical diameter and the anisotropy of the crystal [38-40]. A crystallite will spontaneously break up into a number of domains in order to reduce the large magnetization energy it would have if it

were a single domain. The ratio of the energies before and after division into domains varied as $\sqrt{d}$, where d is the particle diameter. Thus as d becomes smaller, the reduction in energy becomes smaller and this suggests that for very small d the crystallite prefers to remain in the single domain.

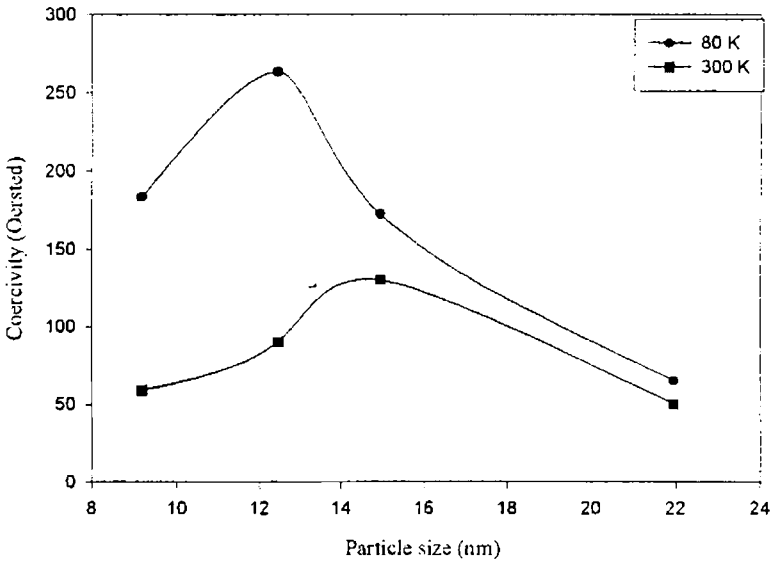

Fig.3.8: Variation of coercivity with particle size for the sol-gel synthesized $NiFe_2O_4$

In the single domain region as the particle size decreases the coercivity decreases because of thermal effects. The coercivity H_c in the single domain region is expressed as

$$Hc = g - \frac{h}{D^2} \qquad 3.5$$

Where g and h are constants

In the multi domain region the variation of coercivity with particle size can be expressed as in [22],

$$H = a + \frac{b}{D} \qquad 3.6$$

where 'a' and 'b' are constants and 'D' is the diameter of the particle. Hence in the multi domain region the coercivity decreases as the particle diameter increases. For magnetic nanoparticles having no interaction between them, the coercivity Hc is given by [42,43]

$$Hc = Hco\left(1 - \frac{T}{T_B}\right)^{1/2} \qquad 3.7$$

Where H_{co} is the coercivity at T=0 K, T the temperature of measurement and T_B the critical blocking temperature, below which hysteresis appears and superparamagnetism disappears and this explain the decrease of coercivity of nano nickel ferrites as the temperature increases.

It can be seen that for $NiFe_2O_4$, a critical particle size 15 nm is obtained at 300K At the same time the variation of H_c with particle size at 80K though similar, has a different critical size, 13 nm corresponding to the formation of single domain particles. This behaviour is in accordance with the equation [39]

$$\left(\frac{D_S}{D}\right)^{\frac{3}{2}} = \left(\frac{T}{T_B}\right)^{\frac{1}{2}} \qquad 3.8$$

As per 3.8, the temperature of measurement (T) decreases, the critical particle size (D_s) of the fine particles decreases. Hence in fig.3.8, the peak value of coercivity shifted to lower particle size region when the temperature decreases from 300 K to 80 K. This clarifies the decrease of the critical particle size of the ultra fine nickel ferrites as the temperature of measurements decreases from 300 K to 80 K

3.3.2.Composite Samples

The magnetic parameters of these rubber ferrite composites were evaluated using VSM. Representative hysteresis loops for rubber ferrite composites are shown in Figure. [9-12].

From these figures it can be seen that the same behavior is obtained for both power samples and RFC. While calculating the M_s of the rubber ferrite composites it was assumed that only single magnetic component is contributing to the magnetic properties of the matrix.

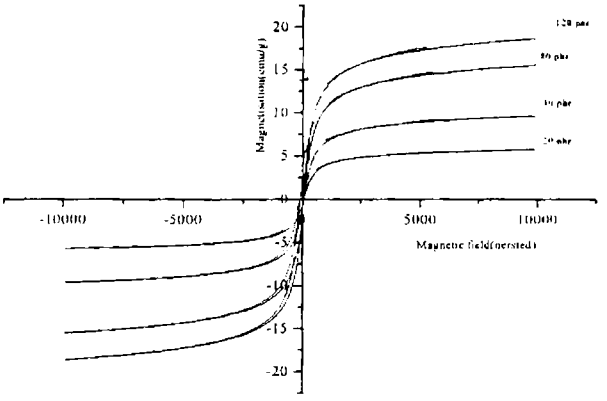

Figure3.9: Hysteresis curve for the as prepared nickel ferrite in 20phr , 40 phr, 80 phr and 120phr nitrile rubber.

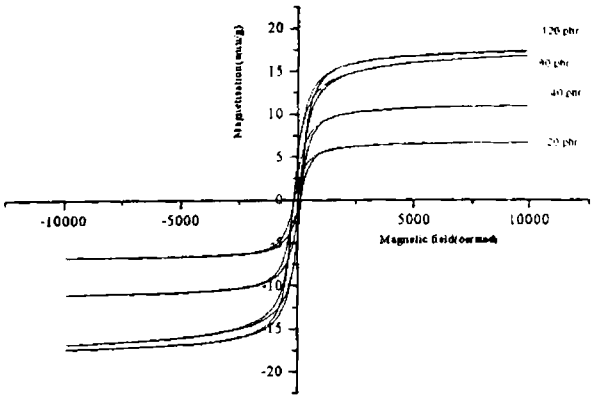

Figure 3.10: Hysteresis curve for the nickel ferrite powder heat treated at 300°C in 20phr , 40 phr, 80 phr and 120phr nitrile rubber.

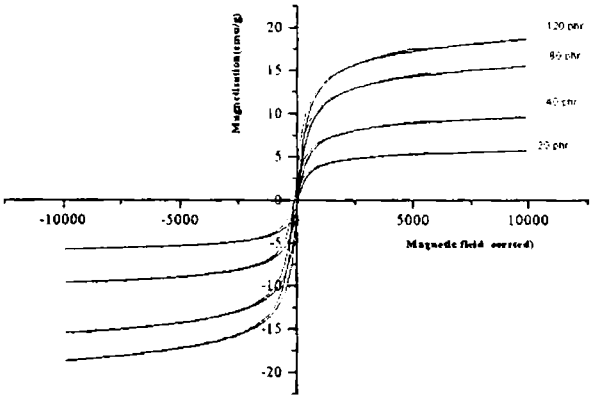

Figure 3.11: Hysteresis curve for the nickel ferrite powder heat treated at 600°C in 20Phr, 40 phr, 80 phr and 120phr nitrile rubber.

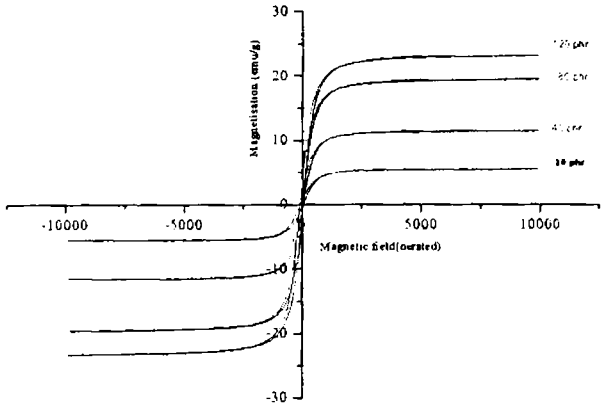

Figure 3.12: Hysteresis curve for the nickel ferrite powder heat treated at 900°C in 20Phr 40 phr, 80 phr and 120phr nitrile rubber.

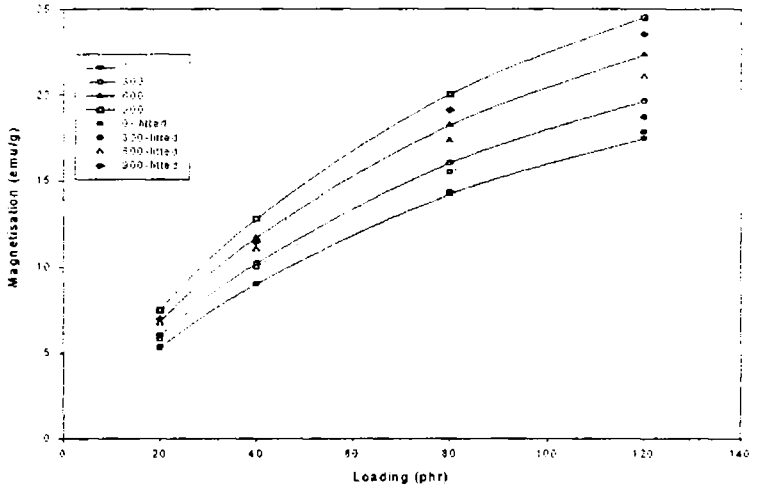

Figure3.13: Variation of saturation magnetisation with loading

From the hysteresis curves it was observed that the magnetization increases with loading for each composition The variations of magnetisation with loading for different compositions are shown in Fig.3. (13).

If saturation magnetisation (Ms) values of the ceramic fillers are known, a simple mixture equation of the general form involving the weight fractions of the filler can be employed to calculate the Ms of the composite samples as.

$$M_{rfc} = W_1 M_1 + W_2 M_2 \qquad 3.7$$

Where W_1 is the weight fraction of filler, M_1 is the magnetisation of the filler, W_2 is the weight fraction of matrix (NBR), M_2 is the magnetisation of the matrix.

Since NBR is nonmagnetic this equation can be reduced to the following form

$$M_{rfc} = W_1 M_1 \qquad 3.8$$

The Ms values were calculated using 3.8 and the measured and calculated values of Ms are plotted with loading and is shown in Fig. 3.13.The measured values tallies well with the fitted data.

The variation of magnetization and coercivity of the composites is the same for the powder (filler) samples. This similarity implies that there is no possible interaction between the filler and the matrix at the macroscopic level. But it may be noted that the coercivity remains more or less same for different loadings of each composition, this value of coercivity tallies well with the value of coercivity obtained for the corresponding powder samples

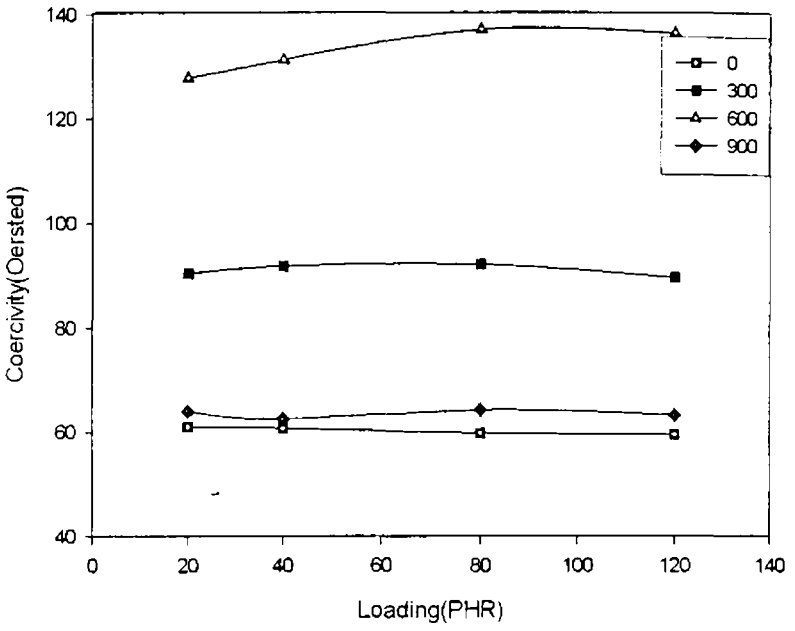

Figure.5. 14: Variation of coercivity with loading.

The variation of coercivity with different loading of nickel ferrite and at various particle sizes are shown in the fig (14). The coercivity is almost independent of the loadings. The slight variation in coercivity from the powder samples and the composites can occur due to the particle size reduction that takes place during compounding and mixing. This also confirms the findings on RFC prepared with butyl rubber [43] and with natural rubber [44]. These results suggest that the magnetic property of the matrix can be suitably modified by appropriate loading of the ferrite.

3.4.Conclusion

The X-Ray diffraction studies showed that the $NiFe_2O_4$ prepared has the inverse spinel structure and the x-ray data agreed well with the reported data. It was observed that in addition to change in the particle size, strain is also induced during the firing process. The magnetic studies carried out using the Vibrating Sample Magnetometer showed that the specific saturation magnetization (σ_s) of the nanosized $NiFe_2O_4$ decreased as the particle size was decreased. As the particle size was increased by the annealing process, the coercivity was found to increase, attain a maximum value and then decreased. The nanosized particles of $NiFe_2O_4$ synthesized by the sol-gel method could be sintered at a lower temperature when compared to its solid-state counterpart. The sintering behaviour of $NiFe_2O_4$ nanoparticles is much superior compared to coarse-grained powder obtained through the solid-state reaction process.

The nano nickel ferrites were then incorporated into a nitrile rubber matrix to produce rubber ferrite composites. Magnetisation measurements on rubber ferrite composites suggest that their saturation magnetisation can be modified by the addition of ferrites. The coercivity of the samples remains as that of the corresponding powder samples and which is independent of loadings. Fundamentally, these results indicate that there is no possible interaction between the filler and the matrix because, if there were an interaction it would have affected the nature of the domain and hence would have disturbed the coercivity. In making composites, M_s can easily be manipulated by fixing the loading percentage of the magnetic filler. Since H_c of the composites is the same as that of the overall magnetic properties of the composites can be tuned. These results also indicate that mouldable complex shaped device based on nitrile rubber and nickel ferrite can be fabricated.

Chapter 3

Nitrile rubber being oil resistant and offers optimum mechanical properties, the contribution of nitrile rubber and nickel ferrite looks promising for high frequency applications, especially, for microwave absorption and other microwave devices. The easier in tuning the saturation magnetisation by varying the particle size provides leverage in manipulating the overall magnetic properties of the composites.

References

1. Skandan, Y.J.Chen, N.Glumac and B.H.Kear, *Nanostructured. Material* **11,**(1999),149.
2. D. Ravichandran, R.Roy, P.Ravindrananthan and W.B. White. *J.Am.Ceram.Soc.* **82**, (1999), 1082.
3. T.Tsuzuki and P.G. McCormick, *Acta Mater.* **48**, (2000), 2795.
4. J.G.Li and X.D.Sun,. *Acta Mater.* **48**, (2000), 3101.
5. B.L.Shen, T.Itoi, T.Yamasaki and Y.Ogino, *Scripta Mater.* **42**, (2000), 893.
6. H.J. Hoffler and R.S.Averback, *Scripta Metall. Mater*, **24**, (1990), 240.
7. I.E. Candlish, B.H.Kear and B.K.Kim, *Nanostruct. Mater.*, **1**, (1992), 119.
8. G. Skandan, H.Hahn, M.Roddy and W.R.Cannon, *J.Am.Ceram.Soc.*, 77, (1994), 1706.
9. Chen D.H and Y.Y.Chen, *J.Colloid Interface Sci.*, **9,** (2001), 235.
10. J.J.Kingsley, K.Suresh and K.C.Patil, *J.Mater. Sci.*, **25**, (1990), 1305.
11. Chen D.H. and X.R.He, *Bull. Mater.Res.*, **36**, (2001), 1369.
12. S.Z Zhang and G.L Messing, *J.Am.Ceram.Soc.*, **73**, (1990), 61.
13. Chen D.H. and Y.Y.Chen, *J.Colloid Interface Sci.*, **41,** (2001), 236,.
14. Sridhar Komarneni, Maria Cristina D'Arrigo, Cristins Leonelli, Gian Carlo Pellacani and Hiroaki Katsuki, *J.Am.Ceram.Soc.*, **81**, (1998), 3041.
15. J.L. Dorman, D. Fiorani (Eds), Magnetic Properties of Fine Particles, North-Holland.
16. M.Kishimoto, Y.Sakurai, T.Ajima, *J. Appl. Phys.* **76**, (1994), 7506.
17. I.M.L. Billas, A.Chatelain, W.A. de Heer, *Science*, **265**, (1994), 1682.
18. D.D. Awschalom, D.P.D. Vincenzo, *Physics Today*, April, **43** ,(1995),.
19. J.Shi, S.Gider, K.Babcock, D.D.Awschalom, *Science*, **271**, (1996), 937.
20. S.Son, M.Taheri, E.Carpenter, V.G.Harris and M.E.McHenry, *J.Appl.Phys.*, **91** ,(2002), , No: 10, 7589.
21. H.Ehrhardt, S.J.Campbell and M.Hofmann, *Journal of Alloys and Compounds*, **339,** (2002) 255.
22. V. Sepelak, K. Tkacova, V.V. Boldyrev, S. Wibmann and K.D. Becker, *Physica B* **617,** (1997), 234-236
23. Qi Chen, Z.John.Zhang, *Appl.Phys.lett.*, **73,** (1998) 3156

24. S.D. Shenoy, P.A. Joy, M.R Anantharaman, J. Magnetism and Magnetic Materials **269,** (2004) 217-226.

25. A.H.Morrish and K.Haneeda, *J.Appl. Phys.* **52**, (1981), 2496

26. C.N.Chinnasamy, A.Narayannasamy, N.Ponpandian, K.Chatopadhyay, K.Shinoda, B. Jeyaadevan, K. Tohji, K. Nakatsuka, T. Furubayashi and I.Nakatani, Phy.Rev B,.**63**,184108.

27. R.H. Kodama and A.E. Berkowitz, E.J. McNiff and S. Foner, *Phy Rev. Lett.* 77, (1996) 394

28. R.H.Kodama and A.E. Berkowitz, *Phy.Rev.B* 59, (1999), 6321

29. KA Malini, E.M Mohammed, S. Sindhu, P.A. Joy, S.K. Date, S.D Kulkarni, P. Kurian, M.R. Anantharaman *J.of Material Science*, **36**,(2001) ,5551

30. D.Y. Kim, Y.C. Chang, T.W .Kang, H.C. Kim *IEEE Transactions On Magnetics,*

31. Y. Naito and K. Suetaki, " Application of Ferrite to Electromagnetic Wave Absorber and its characteristics," *IEEE Transactions, Microwave Theory,* Tech, volume MTT- 19. No1., (Jan 1971). 65-72

32. H M Musal. Jr. and HT Hahn. *IEEE Transactions On Magnetics,* **25**.No **5** (September 1989) 3851,

33. H M Musal. Jr. and DC Smith. *IEEE Transactions On Magnetics*,**26**,1462-1466, September 1990.

34. Yung Do Choi, Hwan Woo Shim, Kwang Yun Cho, Hyuk Jace Lee, *Journal of Applied Polymer Science,* Vol 72, (1999) .75-83

35. Sung- Soo Kim and Dae- Hee Han *IEEE Transactions On Magnetics,* volume 30 No. 6 November 1994.

36. *ASTM* 10-325 (Ni-ferrite) *Nat.Bur. Stands (U.S)* cir. 539-1044 (1960).

37. M.Zheng, X.C. Wu, B.S. Zou and Y.J. Wang, *J. Magn.& Magn. Mater.*, **183** (1998) ,152.

38. George C.Hadjipanayis and Richard W.Siegel (Edited), *Nanophase Materials-Synthesis-Properties-Applications*, Kluwer Academic Publishers

39. B.D.Cullity, *Introduction to Magnetic Materials*, Addison-Weiseley Publishing Company.Inc (1972).

40. S. Chikazumi, Physics of Magn. John Wiley and Sons, Inc, New York, 1959

41. E.H.Frei, S.htrikman,D.Treves.*Phys.Rev.* **106**, (1957)

42. S.Banerjee,S.Roy,J.W.Chen,D.Chakravorty, J.Magnetism and Magnetic Materials , **219** (2000) 45

43. M R Anantharaman, S Jagatheesan, S Sindhu, K A Malini, C N Chinnasamy, A Narayanasamy, P Kurian And K Vasudevan, *Plastic Rubber and Composites Processing Applications* **272** *(1998),77*

44. M R Anantharaman, K A Malini, S Sindhu, E.M. Mohammed, P.A joy, S.K. Date and P Kurian, *Bull. Mater. Sci.*, **24**, No. 36, (December 2001), 623.

Chapter IV

Electrical Studies On Nickel-Ferrites And Composites Based On Nitrile Rubber.

4.1. Introduction

Ferrites, which are magnetic oxides, belong to the class of magnetic dielectrics, because of their high resistivity and low loss. They find vast technological applications over a wide range of frequencies. These include the applications in circuits, high quality filters, antennas, transformer cores, read/write heads for high-speed digital tape and operating devices [1 – 3]. Dielectric behaviour is one of the most important properties of ferrites, which markedly depends on preparative conditions, chemical composition, method of preparation, grain size, ratio of Fe^{2+}/Fe^{3+} ions and defects in lattices [4,5]. The study of the effect of temperature, frequency and grain size on the dielectric behaviour and ac electrical conductivity offers much valuable information on the behaviour of localized electric charge carriers leading to greater understanding of the mechanism of electric conduction and dielectric polarization in ferrite systems. Nickel ferrite and nickel-zinc ferrites are well-known for their high frequency applications. The dielectric behaviour was previously studied for poly crystalline nickel and its mixed ferrites in the micro regime [6-11]. But no comprehensive study was carried out for nickel ferrites in the nano regime.

Many theories and semiimperical relationships exist, which explain the role of different fillers in various matrixes. Further more, from the dielectric and magnetic measurements, it is possible to gather valuable information regarding the matrix filler interaction, dispersion of filler and percolation threshold, which are important and play a significant role in

determining the gross physical properties of the composites. The evaluation of structural, magnetic, and dielectric properties of both the ferrites and their rubber ferrite composites (RFC) are also important since the interrelationship of the properties of the filler and the matrix will help in the design of devices for various applications. The frequency dispersion characteristics of the polymer ferrite composites are important because of their application as electromagnetic wave absorbers and EMI shielding materials [12-17] .The modification of the dielectric properties of the lossy dielectric materials by the addition of magnetic fillers is of interest to various researchers in understanding the fundamental aspects governing the properties of these materials. So the incorporation of pre-characterized ferrite powders into various matrixes assumes significance. The dependence of these parameters on the dielectric properties of ferrite fillers will also have a profound influence on the overall physical properties of the composites incorporated with the filler [18]

The electrical properties are important for ferrites and composites containing ferrites not only from the application point of view but also from the fundamental point of view [18-23]. Evaluation of ac conductivity reveals wealth of information as regard the usefulness of these materials for various applications. Moreover the study of ac electrical conductivity sheds light on the behaviour of charge carriers under an ac electric field, their mobility and the mechanism of conduction [24-26]. The conductivity studies on ferrites carried out by various researchers prove its semi conducting behaviour and also prove the dependence of electrical conductivity on preparation condition, sintering time, temperature and the type of impurities present.

Pre characterized nickel ferrites prepared by sol-gel method were incorporated into a nitrile rubber matrix according to specific recipe to yield RFC's. The dielectric permittivity and ac conductivity of nickel ferrite and the RFC's have been studied as a function of frequency, temperature, particle size and loading of the fillers. These results are discussed in this chapter.

4.2. Dielectric Measurements of $NiFe_2O_4$

The dielectric measurements of nickel ferrite samples and the composite samples were carried out by using a homemade cell and an LCR meter HP 4285A. The cell was standardized by using test samples of teflon, lead and fringe capacitance was eliminated by employing a procedure suggested by Ramasasthry *et al* [27].

Pellet shaped samples were employed for the evaluation of the dielectric permittivity. The dielectric permittivity (ε_r) of the samples were calculated using the relation

$$\varepsilon_r = \frac{Cd}{\varepsilon_0 A} \qquad 4.1$$

Where 'C' is the measured value of capacitance of the sample, 'd' is the thickness, 'A' is the surface area, and 'ε_o' is the dielectric permittivity of air. The complete experimental set-up and details of the dielectric measurements are explained in Chapter II.

4.3. $NiFe_2O_4$-Samples

4.3.1. Frequency Dependence

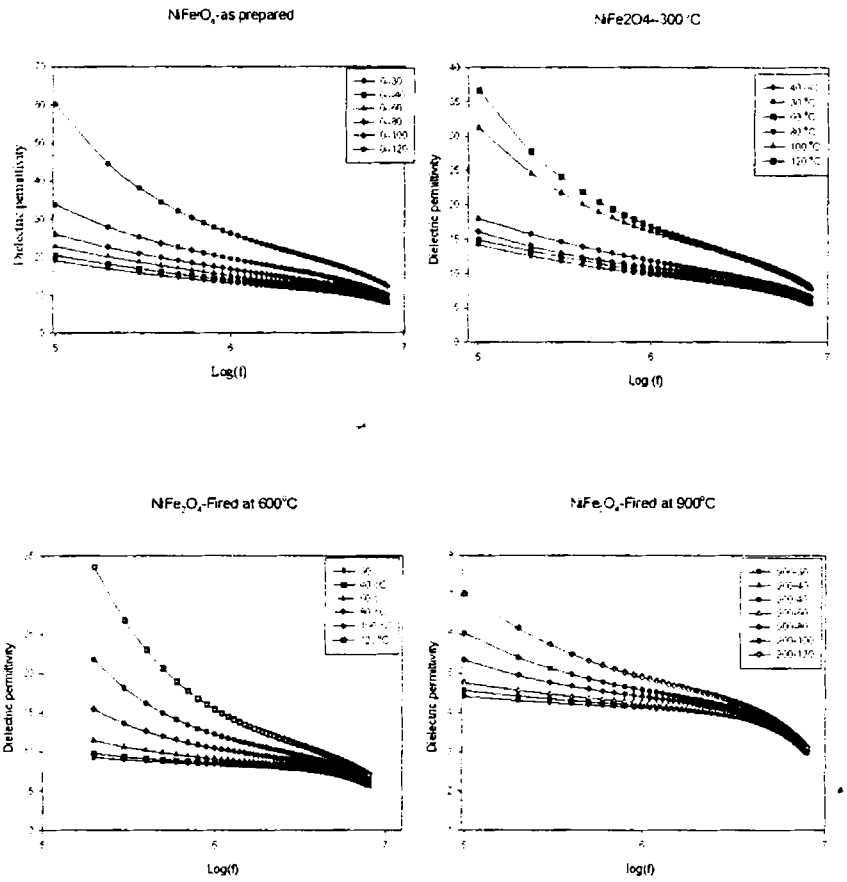

Fig.4.1 Variation of dielectric constant with frequency for $NiFe_2O_4$ samples.

Fig.4.1.shows the variation of dielectric permittivity with frequency in the frequency range 100kHz to 8MHz.The variation of dielectric permittivity with frequency reveals the dispersion due to Maxwell-Wagner

type [28,29] interfacial polarisation in agreement with Koops phenomenological theory of dielectric dispersion [30]. The variation of dielectric permittivity with frequency for the powder samples of nickel ferrite heat treated at various temperatures are shown in fig.4.1. The dielectric permittivity decreases with increasing frequency reaching a constant value for all the samples. The mechanism of dielectric polarisation in ferrites is similar to that of conduction process [31]. By electron exchange between $Fe^{2+} \leftrightarrow Fe^{3+}$, one obtains local displacement of electrons in the direction of applied field and these electrons determine the polarisation. The polarisation decreases with increase in frequency and then reaches a constant value due to the fact that, beyond a certain frequency of external field the electronic exchange $Fe^{2+} \leftrightarrow Fe^{3+}$ cannot follow the alternating field.

The large values of the dielectric permittivity at low frequencies are due to the predominance of the species like Fe^{2+} ions, interfacial dislocation pile ups, oxygen vacancies, grain boundary defects etc[28,29], while the decrease in dielectric permittivity with frequency is natural because of the fact that any species contributing to polarisability is bound to show lagging behind the applied field at higher and higher frequencies.

Koops [30] was among the first to study the frequency dependence of dielectric constant and dispersion of ferrites. He interpreted the result by considering the dielectric as an inhomogeneous medium of a Maxwell-Wagner type. The high values of ε could be explained on the basis of Maxwell- Wagner theory, which is a result of the inhomogeneous nature of dielectric structure. This dielectric structure is supposed to be composed of two layers [30]. The first layer is the large ferrite grains of fairly well conducting materials, which is separated by the second thin layer (grain

boundaries) of relatively poor conducting grains. The grain boundaries are found to be effective at lower frequencies, while the ferrite grains are more effective at higher frequencies [31,32]. Maxwell-Wagner model thus explain the decrease of permittivity as the frequency increases.

A general relation of the following form explains the variation of dielectric permittivity with frequency

$$\varepsilon'' = (r - r')(\varepsilon' \times \omega) \qquad 4.2$$

where ε' and ε'' are the real and imaginary parts of the dielectric permittivity and r and r' are the ac and dc conductivity respectively and ω is the frequency.

4.3.2. Temperature dependence of Dielectric permittivity

Fig.4.2. shows the variation of permittivity with temperature. From these figures it can be seen that the dielectric constant increases slowly with temperature in the beginning up to about 373K and above this temperature, permittivity increases rapidly and sharply for all samples.

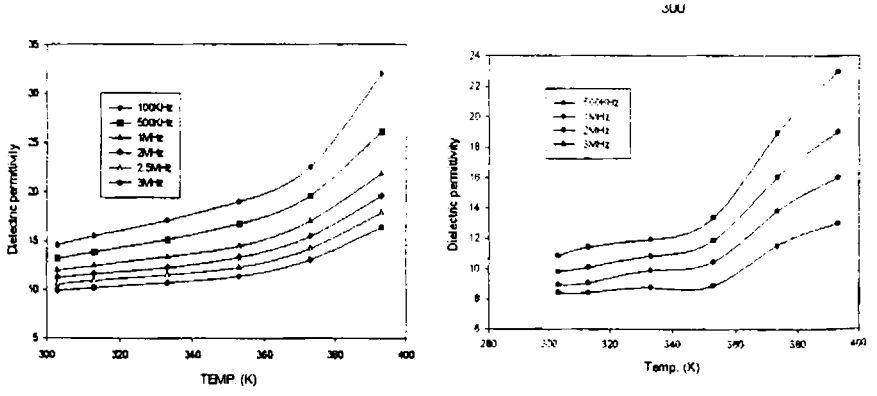

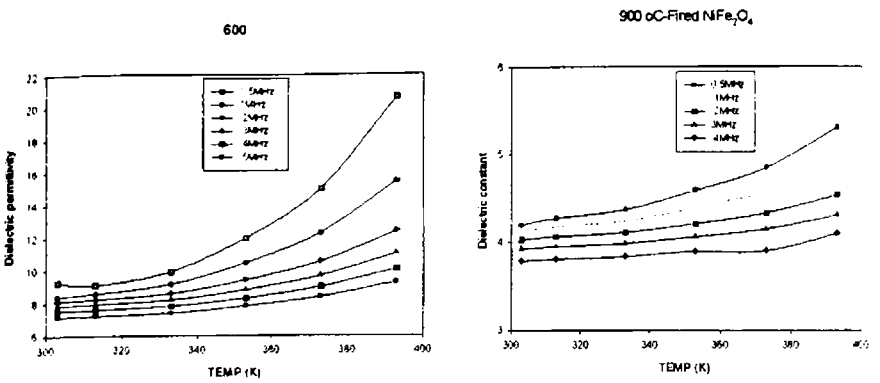

Fig.4.2.Variation of dielectric permittivity with temperature of $NiFe_2O_4$ powder samples heat treated at various temperatures.

The resistivity of ferrites decrease with increase in temperature. Anantharaman et al reported the same variations of dielectric constant with temperature in Ni-Zn ferrites [33]. According to Koops, the dielectric permittivity is inversely proportional the square root of resistivity. Therefore the increase in dielectric constant with temperature is expected.

The high dielectric permittivity at lower frequencies found at high temperature may be explained in presence of the permanent dipole moments indicating a small effective charge separation. Such a small charge separation must be due to asymmetry in the fields experienced by either oxygen ion or metallic ions. This could arise in the case of oxygen ions three B-site and one A-site neighbours, or in the case of A-site ion through a distortion of its surrounding oxygen tetrahedron [35]. Similar results have been also reported by Josyulu et al[36] in case of mixed ferrites.

At very high temperatures the chaotic thermal oscillations of molecules are intensified and the degree of orderliness of their orientation is diminished, thus the permittivity passes through a maximum value. It is found that the variation of dielectric permittivity with temperature at low frequencies (100kHz) is much more pronounced than at higher frequencies.

At lower frequencies, an equation of the form

$$\varepsilon=\varepsilon_0 +Aexp(BT) \qquad 4.3$$

where ε and ε_0 are the dielectric permittivity at temperature T and 0K and A and B are constants [37]. This relation holds good only at lower frequencies. For higher frequencies the ε variation is nominal since the dipoles are not free to orient at a higher frequency and hence the orientation polarization will be less at higher frequencies. Thus the total increase in polarisation will be less with the rise in temperature at higher frequencies. This explains the changes in dielectric constant with temperature at higher frequencies.

4.3.3.Particle size dependence.

Resistivity of ferrites is known to depend upon the purity of the starting compounds and the preparation details such as sintering temperature and atmosphere, which also influence the micro structure and the composition of the prepared samples. The grain size, grain boundaries, porosity and stochiometry are important factors in this regard. It has been reported [37,38] that the resistivity of a polycrystalline material in general increases with decreasing grain size; smaller grains imply larger number of insulating grain boundaries which acts as barriers to the flow of electrons. Smaller grains also imply smaller grain- grain surface contact area and therefore a reduced electron flow. As expected, increase in grain is observed with increase in temperature.

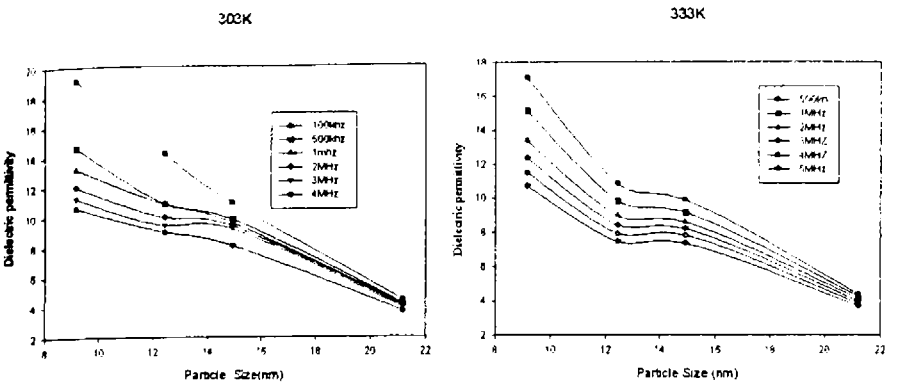

Fig.4.4.grain size dependence of dielectric permittivity

According to the above arguments, the resistivity of the ferrites is expected to decrease with increase in sintering temperature or the increase in grain size. However, a reverse trend is observed in the present work for sintering the samples up to 900^{0}c. This indicates that some factors other than those considered above are important in determining the resistivity of the ferrites. The comparatively lower value of resistivity or higher value of permittivity in samples sintered at lower temperatures are possibly due to the presence of localised stage in the forbidden energy gap which arises due to lattice imperfections. The presence of this states effectively lowers the energy barriers to the flow of electrons. Increase in resistivity or decrease of permittivity with sintering temperature can be explained in terms of increasing structural improvement. Increased sintering temperature results in more uniform crystal structures with reduced imperfections there by increasing the sample resistivity. The above discussion suggests that the effect of structure has an influence which is more significant than that of the anticipated effect of grain size. A similar trend in resistivity was reported by Van Uitert [39], who also explain it in terms of increased homogeneity and structural perfection with increase in sintering temperature.

4.4.Blank Nitrile rubber

The dielectric properties of gum nitrile rubber vulcanisate were evaluated in the frequency range100 kHz to 8MHz.A dielectric permittivity of 9.5 was observed for nitrile rubber at 100 kHz and at 303 KHz. The high dielectric permittivity of the nitrile rubber indicates that it is superior in dielectric properties compared to natural rubber [40]. The dielectric permittivity is almost independent of frequency at low frequencies and decreases at high frequencies. The variation is given in fig. (4.4.a)

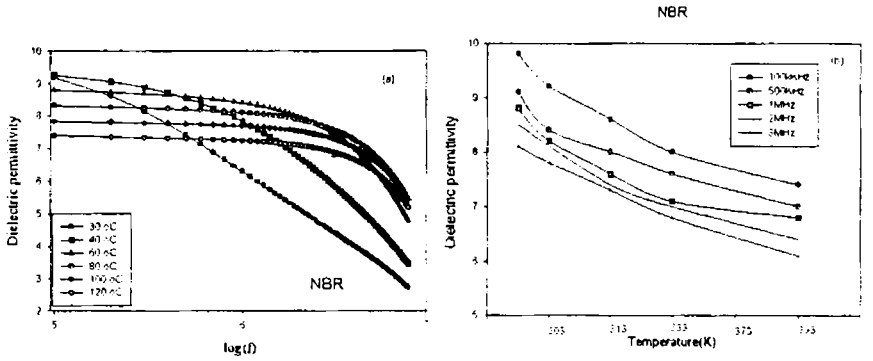

Fig.4.4.Variation of dielectric permittivity (a) with logarithmic frequency and (b) with temperature.

The dependence of dielectric permittivity with temperature is shown in fig.4.4 (b). The dielectric permittivity decreases with increase in temperature. This is because as the temperature increases the polymer density will be reduced which in turn will cause a decrease in dielectric permittivity. Solomon et al [40] also reported similar dielectric properties for nitrile rubber.

4.5.Dielectric properties of Rubber ferrite composites

4.5.1.Frequency dependence.

The dielectric behaviour of RFC containing nitrile rubber with change in frequency is depicted in fig.4.5. This shows almost similar behaviour as that of the ceramic component in the matrix.

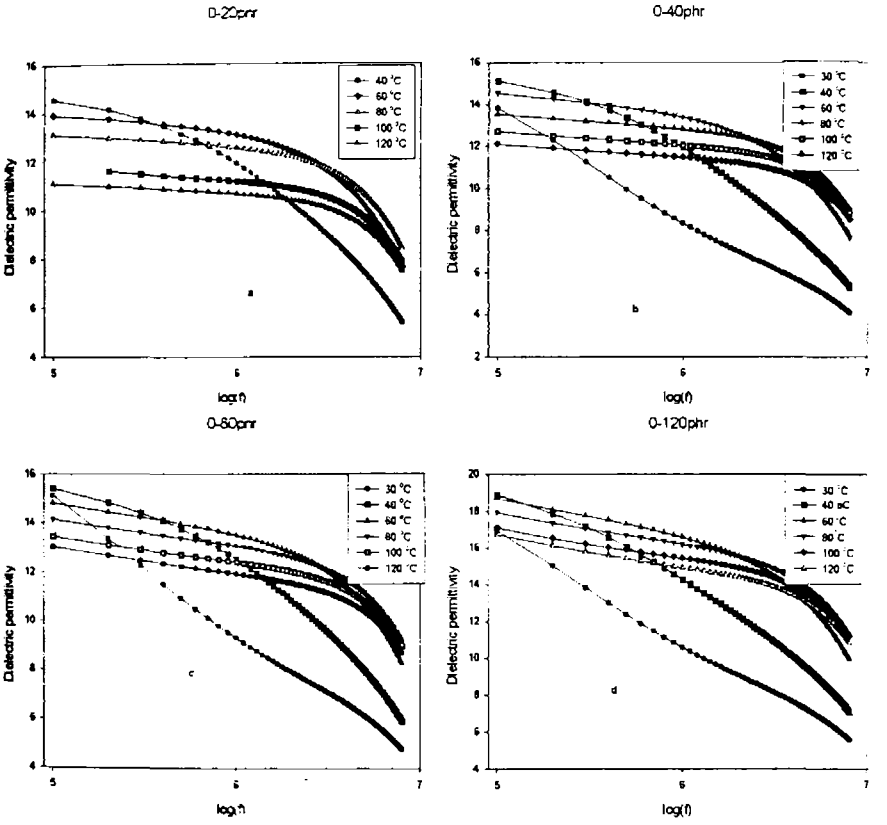

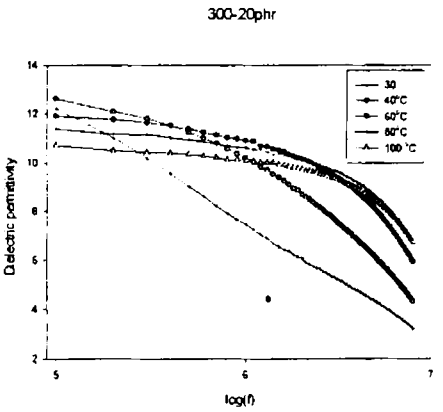
300-20phr
30
40°C
60°C
80°C
100 °C
Dielectric permittivity
log(f)

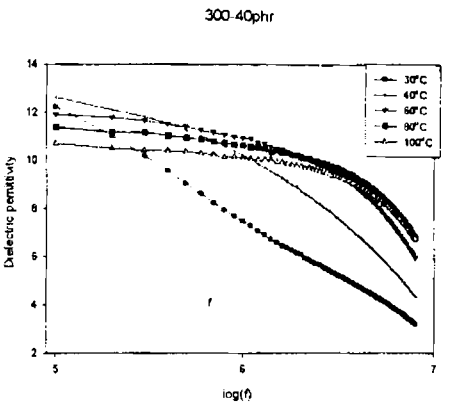
300-40phr
30°C
40°C
60°C
80°C
100°C
Dielectric permittivity
log(f)

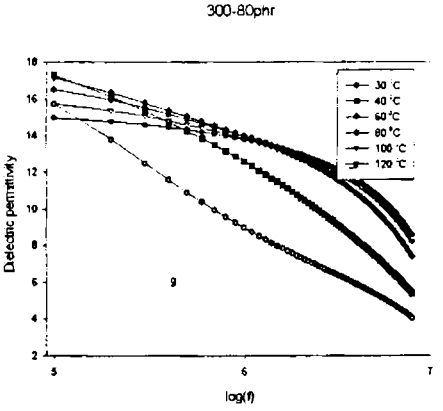
300-80phr
30 °C
40 °C
60 °C
80 °C
100 °C
120 °C
Dielectric permittivity
log(f)

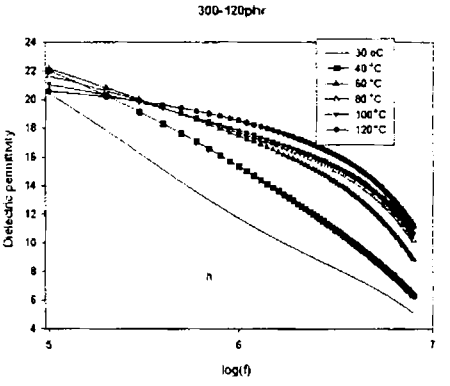
300-120phr
30 oC
40 °C
60 °C
80 °C
100 °C
120 °C
Dielectric permittivity
log(f)

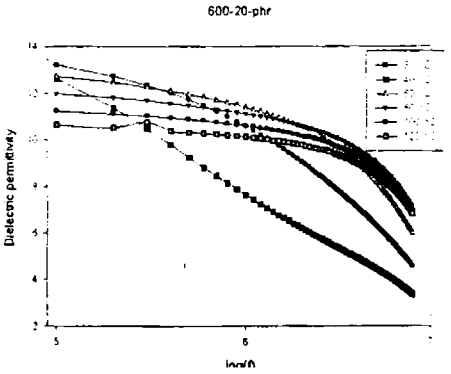
600-20-phr
Dielectric permittivity

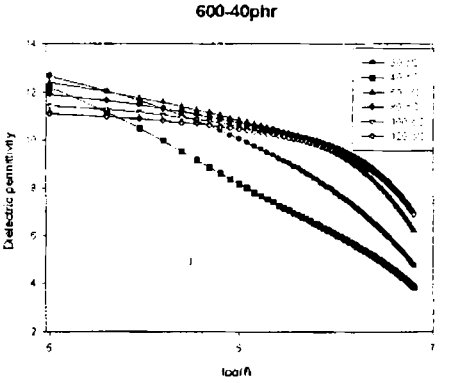
600-40phr
Dielectric permittivity

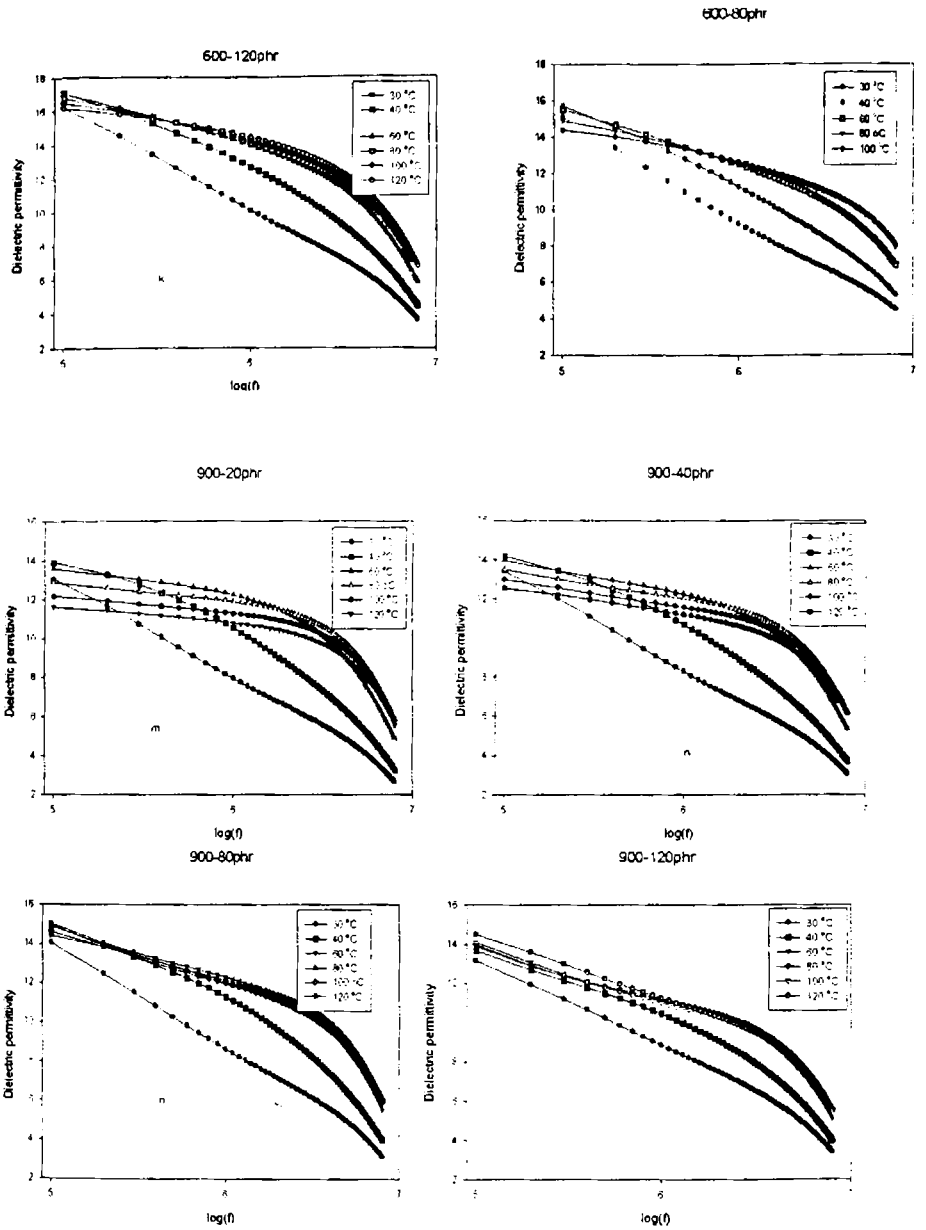

Fig.4.5 (a-o). Variation of dielectric permittivity of RFCs with logarithmic frequency

The absolute values of the dielectric permittivity of the composite are found to be greater than that of the blank NBR, but less than that of the ceramic component. Maximum dielectric constant is observed for the maximum loading of 120phr. Thus it is clear that addition of the filler is modifying the dielectric properties and the required dielectric constant can be achieved by varying the loading of the filler.

4.5.2. Temperature dependence.

The effect of temperature on the dielectric permittivity of rubber ferrite composites at various loadings of the fillers were studied in the range 303K to 393K. The variations are given in fig.4.6.

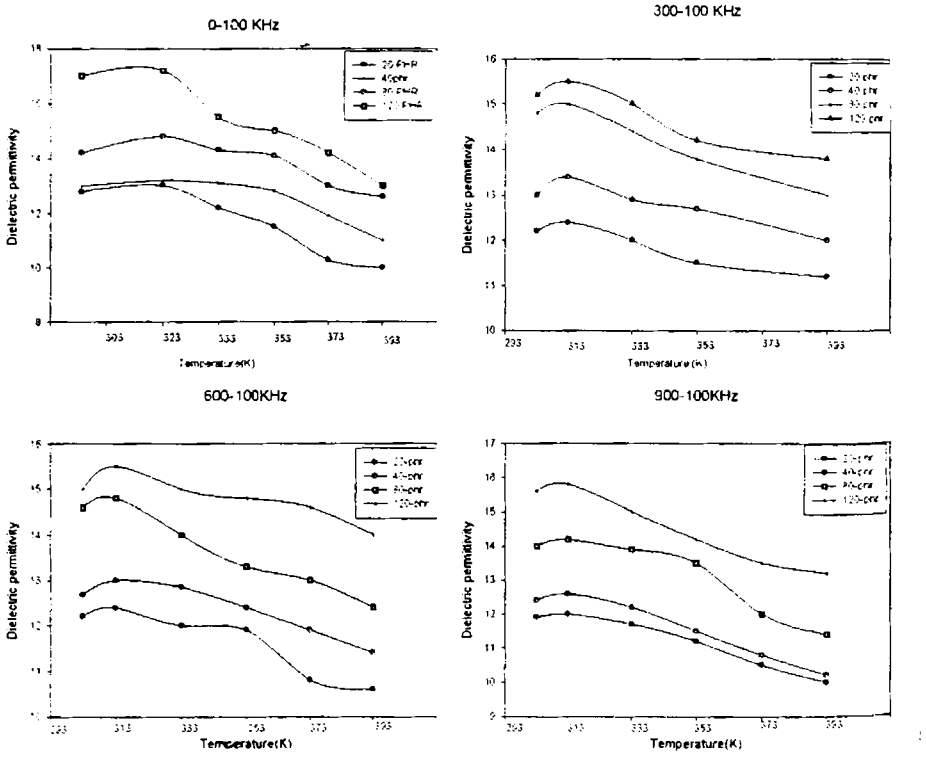

Fig.4.6. Variation of dielectric permittivity with temperature for RFCs.

The dielectric permittivity increases slightly with increase in temperature initially and then decreased. This result is different from that of natural rubber based RFCs(41).Soloman et al also got similar result in the case of NBR based RFCs(42).

4.5.3.Loading dependence

Variations of dielectric permittivity with the loading of magnetic filler were also studied. Fig.4.7. shows the variation in dielectric permittivity with loading. The dielectric permittivity was found to increase with increase in weight fraction of the ferrite material. Maximum value of dielectric permittivity is observed for loading corresponding to 120phr for all the fillers at different frequencies.

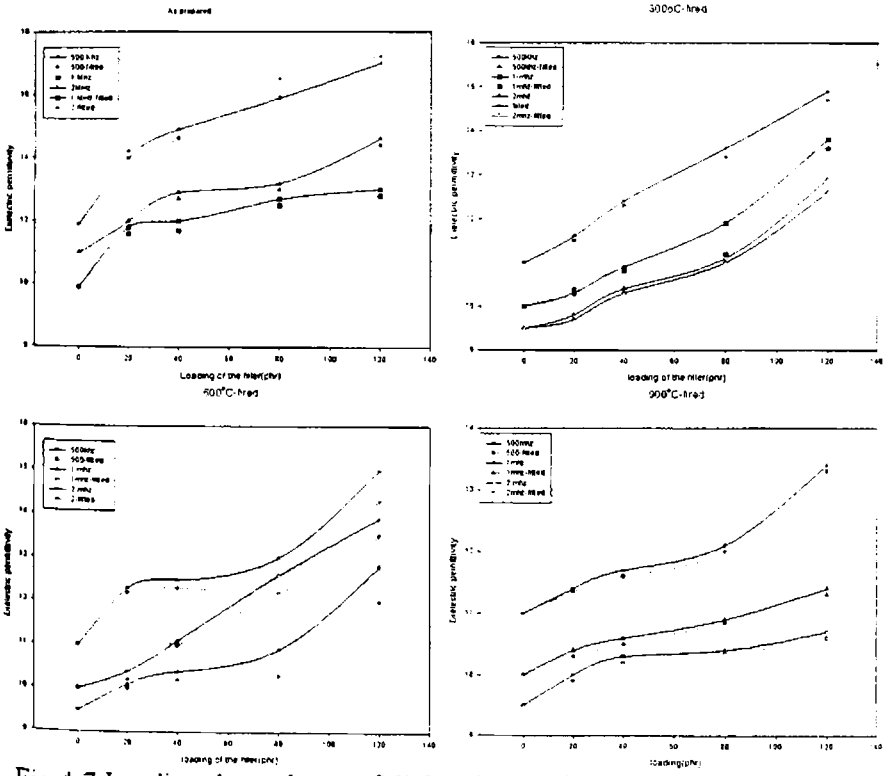

Fig.4.7.Loading dependence of dielectric permittivity of RFCs

Efforts were also made to correlate the dielectric permittivity of the composite samples with those of the ceramic filler and the blank matrix NBR. Several mixture equations exists and can be employed to predetermine the dielectric constant of the composites correctly[42,43]. For this, the composite dielectric has to be considered as a mixture of several components.

For example, for a mixture of m component the dielectric permittivity ε^* is connected by a relation,

$$\log \varepsilon^* = \sum_{i=1}^{m} y_i \log \varepsilon_i \qquad 4.4$$

Where ε^* is the dielectric permittivity of the mixture and y is the weight fraction of the component. For a two-component system the relationship can be written as

$$\log \varepsilon^* = y_1 \log \varepsilon_1 + y_2 \log \varepsilon_2 \qquad 4.5$$

where ε^* is the dielectric constant of the composite, ε_1 ,y_1 and ε_2 ,y_2 are the dielectric constant and weight fractions of the matrix and the filler component respectively.

Another mixture equation of the form

$$\varepsilon^* = \frac{\varepsilon_1 \varepsilon_2}{\varepsilon_1 y_2 + \varepsilon_2 y_1} \qquad 4.6$$

is also found to be useful in predicting the loading dependence of dielectric permittivity of the RFC. Fig.4.7 shows the observed and calculated values of permittivity

4.6.AC Conductivity Studies on Rubber Ferrite Composites

The theory and experimental details involved in the evaluation of ac conductivity from dielectric constant is discussed in detail in Chapter 2. From the dielectric loss and dielectric constant ac conductivity of these samples can be evaluated using the relation

$$\sigma_{ac} = 2\pi f \tan\delta \ \varepsilon_0 \varepsilon_r \qquad 4.7$$

f is the frequency of the applied field ε_0 is the absolute permittivity of air , ε_r is the relative permittivity of the samples and tanδ is the loss factor.

σ_{ac} is temperature and frequency dependent[49]and it is attributed to the dielectric relaxation caused by localized electric charge carriers and obeys the power law[45,47]

$$\sigma_{ac}(\omega,T)=B\,\omega^{n} \qquad 4.8$$

where Band n are composition and temperature dependent parameters.

AC conductivity for all the samples were evaluated in the frequency range from 100kHz to 8MHz. The measurements were carried out at different temperatures of 300K, 313K, 333K, 353K, 373K and 393K.

4.7.$NiFe_2O_4$-Powder samples

4.7.1.Frequency dependence of ac conductivity

The variation of ac conductivity with frequency at room temperature for the powder samples of $NiFe_2O_4$ is given in Fig. (4.8). The ac conductivity shows an increasing trend with increase in frequency for all samples. But at high frequencies the ac conductivity values show a decreasing trend.

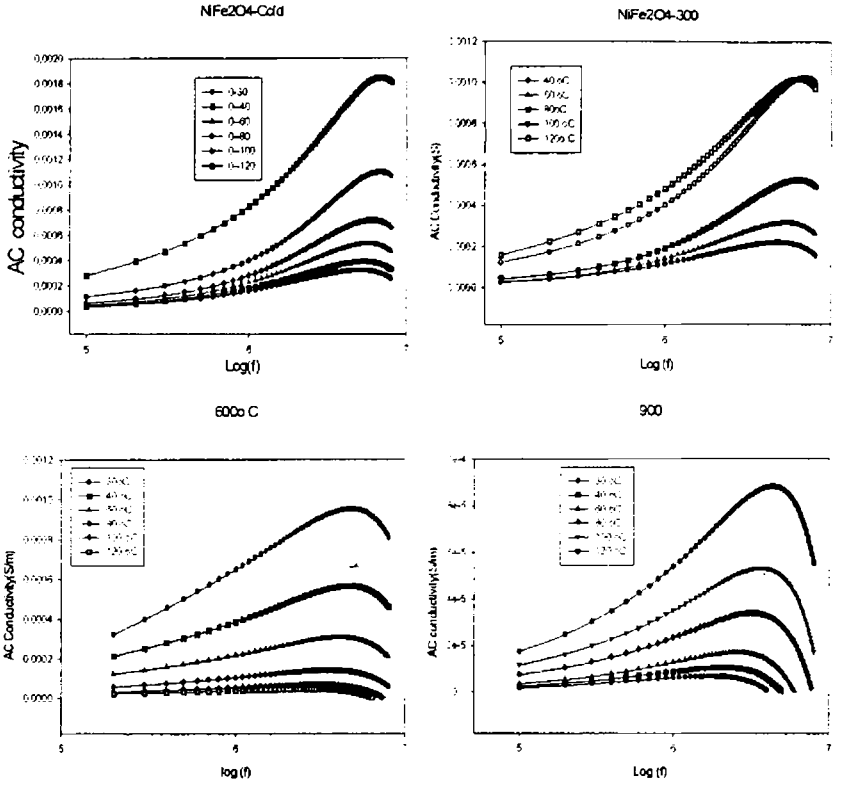

Fig.4.8.Variation of ac conductivity with logarithmic frequency of the applied field.

The small values of ac conductivity at low frequencies and their increase as the frequency increases can be explained on the basis of Koops Phenomenological theory and Maxell-Wagner theory [29,30], which is explained in section4.3. At lower frequencies these grain boundaries are more active and hence hopping of Fe^{2+} and Fe^{3+} ion is less at lower frequencies [46]. As the frequency of the applied field increases, the conductive grains become more active by promoting the hopping between Fe^{2+} and Fe^{3+} ions, there by increasing the hopping conduction. Thus we

observe a gradual increase in conductivity with frequency. But at higher frequencies the frequency of the hopping ions could not follow the applied field frequency and it lags behind it. This causes a dip in conductivity at higher frequencies.

According to the power law, the logarithmic relation between the ac conductivity and the angular frequency represents straight lines with slopes equal to the exponent n and intercept equal to log ω on the vertical axis at log ω=0. A.M.Abdeen conducted [47]an extensive study in nickel-zinc system and found that above the Curie point the ac conductivity is independent of frequency. This behaviour was also observed by another system of ferrites [11,48]

4.7.2.Temperature dependence

The effect of temperature on the ac electrical conductivity of nickel ferrites studied in the range 303K to 393K. It was observed that the conductivity increases with increase of temperature for all ceramic nickel samples. At low frequencies the variation is very minimal but at higher frequencies the variation is more rapid. The variation pattern of conductivity with temperature for different compositions are shown in Fig.4.9. The increase of ac conductivity with increase in temperature indicates the semiconductor nature of the samples.

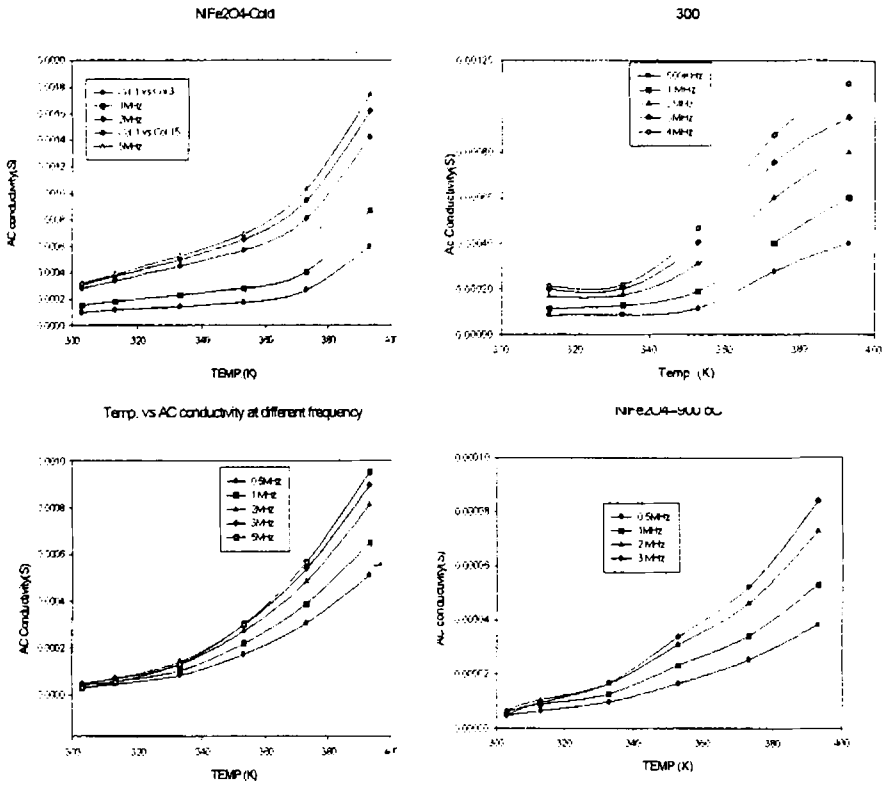

Fig.4.9Temperature dependence of ac conductivity

This behaviour was observed earlier for many mixed ferrites [48-52]. The increase in the electrical conductivity with increase in temperature attributed to increase in drift mobility of the thermally activated charge carriers according to hopping conduction mechanism. Increasing temperature thermally activates the electron exchange between Fe^{2+} and Fe^{3+} ions on the octahedral sites. This electron causes local displacements in the direction of the applied electric field; this includes the dielectric polarisation in ferrites,and thus ac conductivity is increased.

The parameters n and B for σ_{ac} $(\omega,T)=B\omega^{n}$ is calculated by A.M.Abdeen and found that as temperature increases n decreases while B increases. Above Curie temperature n becomes equal to zero because the power law becomes invalid and the conductivity is frequency independent or the dc conductivity. Therefore, n decreases on increasing temperature. So the electrical conduction becomes frequency dependent for $0 < n<1$.On increasing the temperature, the electrical conductivity$\sigma_{ac}(\omega,T)$ increases. Therefore the parameter increases too while the exponent n which determine the degree of frequency dependence of $\sigma_{ac}(\omega,T)$ decreases on increases the temperature.

4.7.3.Grain size dependence

The dependence of ac conductivity on size of the particles is shown in fig. 4.10.ac conductivity increases as the firing temperature of the samples or the size of the grains increased. The variation of ac conductivity with grain size reveals that both the dielectric permittivity and ac conductivity are basically electrical transport properties and their variation with temperature and grain sizes are similar and hence the same mechanism is responsible for both phenomena [21].

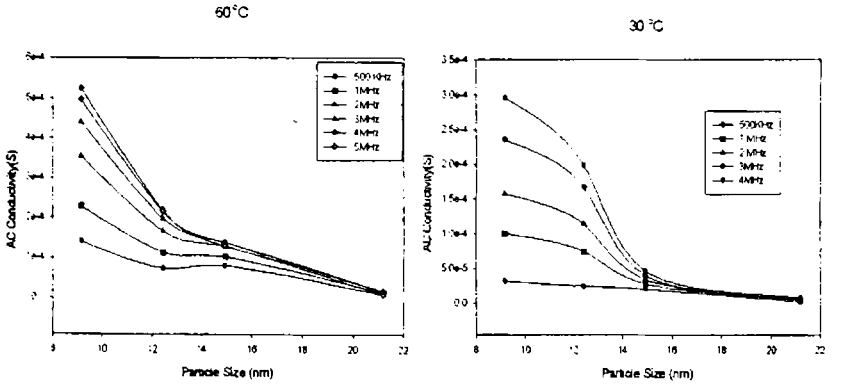

Fig.4.10.Variation of ac conductivity with grain size of $NiFe_2O_4$

Decrease in conductivity with firing temperature is due to the decrease in dielectric constant and this can be explained in terms of crystal order. Increased sintering temperature results more uniform crystal structure with reduced imperfections there by increasing the sample resistivity.

4.8.Blank Nitrile Rubber

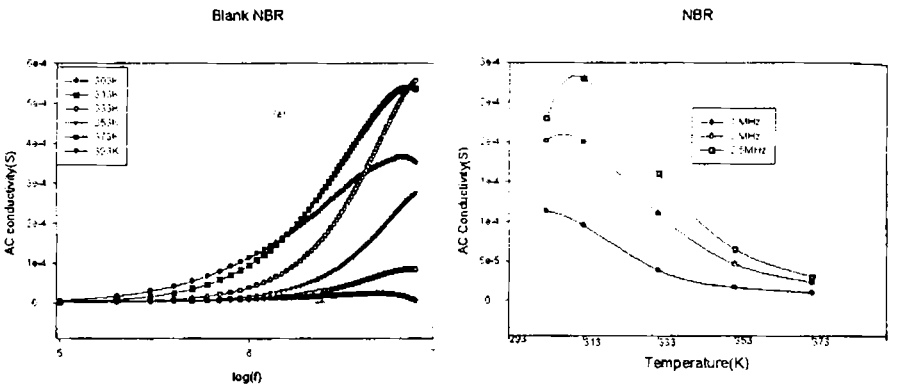

Fig.4.11.Variation of ac conductivity with (a) log(f) and (b) Temperature

Unvulcanised nitrile rubber is nonconducting and the vulcanised rubber contains different compounding ingredients which may act as carriers for conduction. Also polymers are known to be semi crystalline and nitrile rubber can be thought of as a continuous matrix of an amorphous polymer in which properties are modified by the crystalline regions which act as the reinforcing centers. As far as the electrical properties are considered the effect of crystalline centers is to lower the conductivity. If the conduction is ionic, ion mobility through the crystalline region will be low and in the case of electronic conduction the crystalline amorphous interface may act as a trapping region. Thus it can be considered similar to Maxwell-Wagner two layer model.[53-55]

The variation of ac conductivity with frequency for blank NBR is given in fig 4.10. (a) It can be noted that the ac conductivity increases with increase in frequency and drops after reaching a maximum at higher frequencies. At lower frequencies the crystalline- non crystalline interface may be more active and as the frequency increases the ions are able to move across this interface, which in turn will increase the conductivity. High frequency limit is reached when applied frequency is greater than maximum hopping rate.

Similar to dielectric permittivity the ac conductivity of nitrile rubber decreases as the temperature increases. The variation is shown in fig. 4.10(b). This may be due to the thermal expansion of the polymer and at higher temperature the polymer density is reduced by thermal expansion and thus reduce the conductivity

4.9.Composite samples

4.9.1.Frequency dependence

Frequency dependence of ac electrical conductivity in rubber ferrite composites was studied at different frequencies from 100KHz to 8 MHz and the variation shown in Fig.4.12.

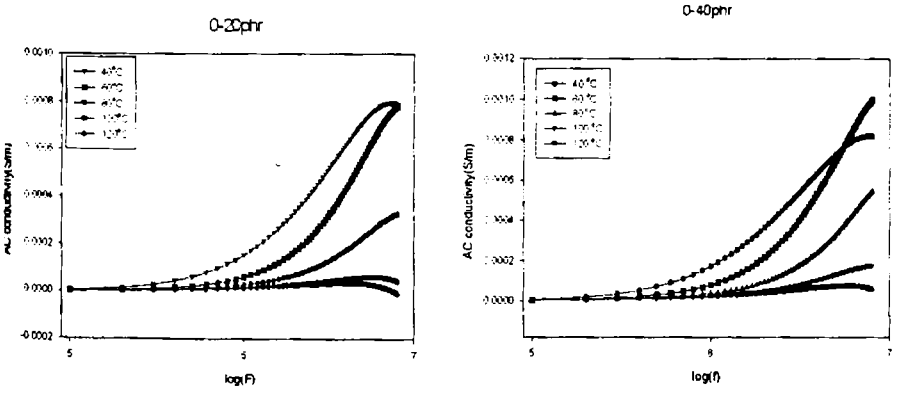

0-80phr

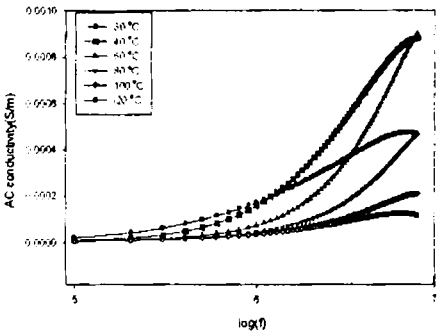

0-120phr

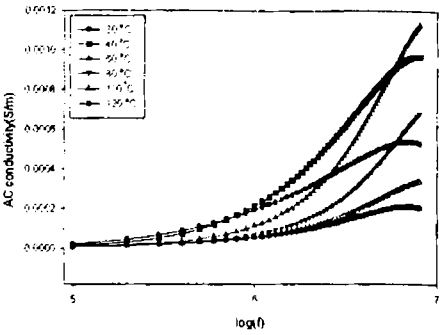

300-20phr

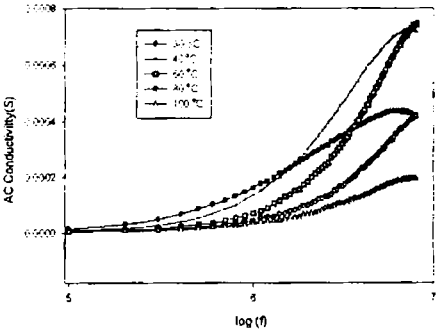

300-40

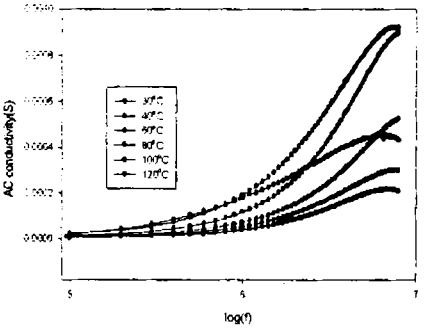

300-80 phr

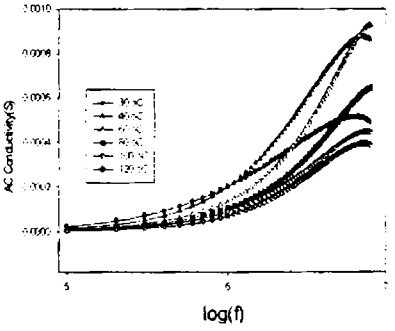

300-120phr

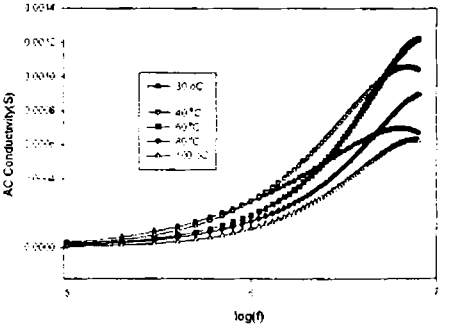

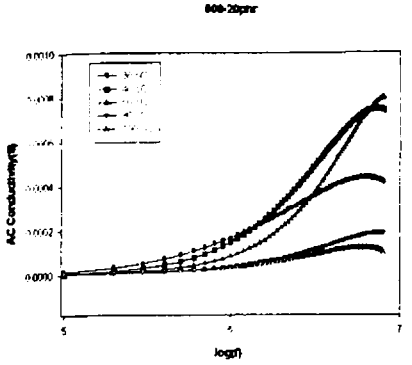
600-20phr
log(f)

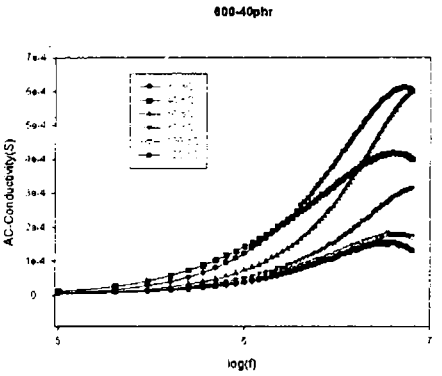
600-40phr
AC-Conductivity(S)
log(f)

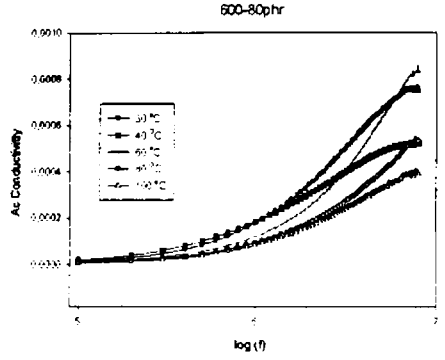
600-80phr
Ac Conductivity
log (f)

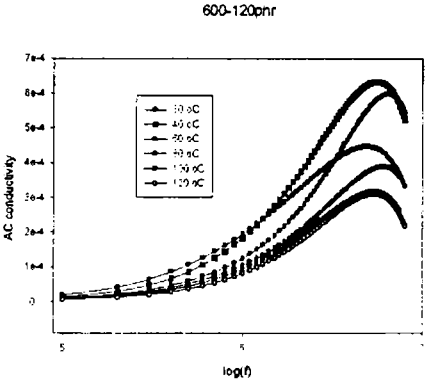
600-120phr
AC conductivity
log(f)

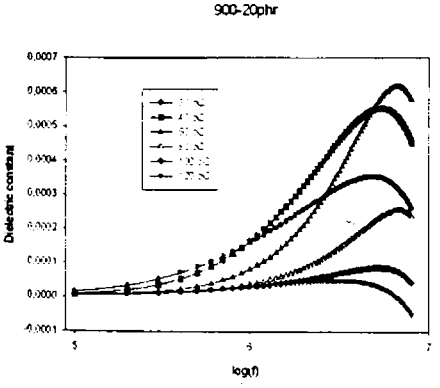
900-20phr
Dielectric constant
log(f)

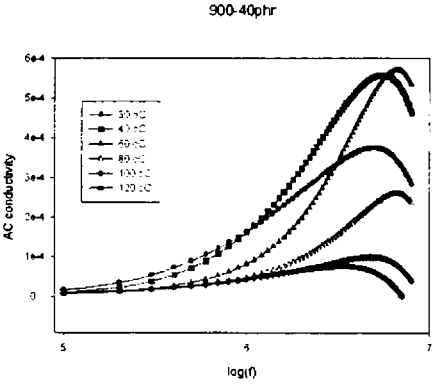
900-40phr
AC conductivity
log(f)

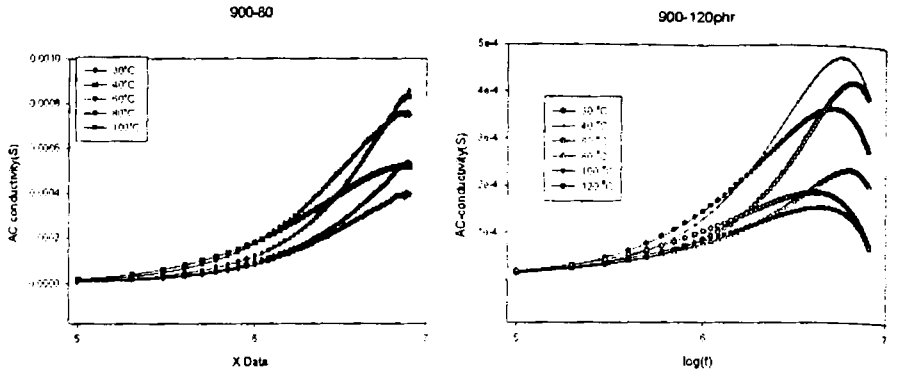

Fig.4.12.Variation of ac conductivity with log(f) for the composite samples of various loadings.

It is found that the variation is almost the same as that of the powder samples and this can also be explained on the basis of the interfacial polarisation.

4.9.2 Temperature dependence.

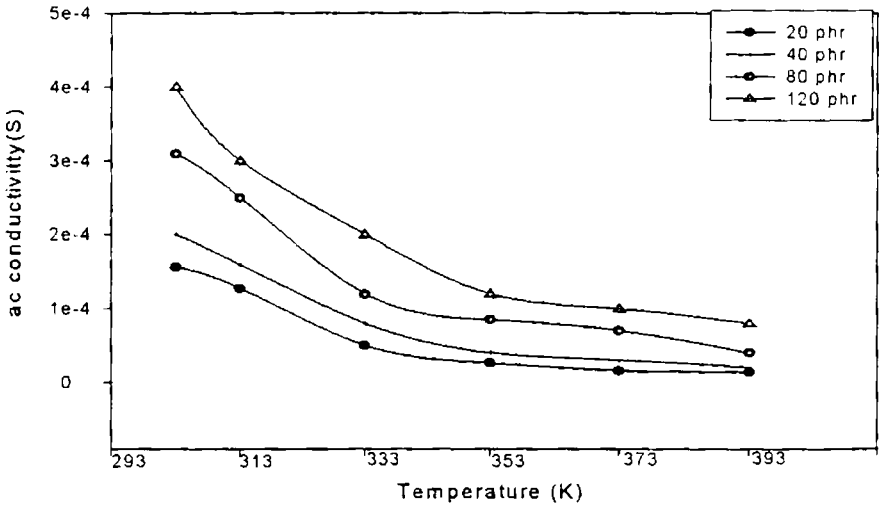

Fig.4.13 Variation of ac conductivity of the composite samples with temperature.

The variation of ac conductivity of the composite samples with temperature is shown in fig. (4.13). The ac conductivity of the composite samples was found to decrease as the temperature is decreases. This result is different from that of natural rubber based RFCs [41].

4.9.3.Loading dependence

In RFCs containing nickel ferrite, an increase in conductivity was observed with increase of the volume fraction of the filler. A maximum conductivity is observed for a maximum volume fraction of 120 phr. This is same for all samples. Graphs showing the variation pattern is depicted in Fig 4.14. At lower loadings the conductivity of the composites differs slightly from that of the host polymer. At percolation threshold conductive paths are formed and the conductivity increases sharply. Above percolation threshold it increases slowly.

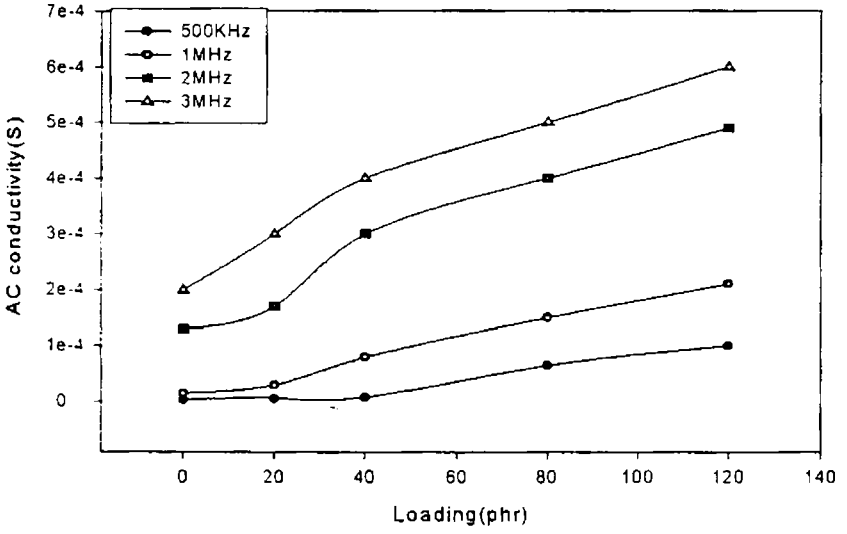

Fig.4.14.Dependence of ac conductivity of the RFCs with loadings of the filler.

Here no such sudden change in conductivity is observed by adding higher volume fraction of the filler and it was found that the percolation threshold was not yet reached even for a loading of 120phr. From the graphs it is obvious that the conductivity increases with increase of loading of the filler. This means that the filler modifies conductivity of the matrix. It may also be noted that the parameters like particle size, structure, aggregation, surface contamination and matrix filler interaction can have remarkable influence in the conductivity of the composites.

4.10.Conclusion

Nickel ferrite has been prepared by sol-gel method. By subsequent heat treating at different temperatures, particles of different grain sizes were prepared These samples are incorporated in to nitrile rubber matrix at various loadings. The electrical characterisation of both powder samples and RFCs were conducted .The dependence of both dielectric permittivity and the ac conductivity on frequency is in good agreement with Koops phenomenological theory of dielectrical dispersion. Both ac conductivity and dielectric permittivity shows an increasing trend as the temperature increases. Dependence of ac conductivity and dielectric permittivity with grain size of the nickel ferrite was conducted and both are found to increase as the grain size is decreased. Also the electrical properties of the RFCs get enhanced as the volume fraction of the ferrite increased. The modification of the electric properties of the RFCs will aid in the design of composite materials for possible applications particularly for electromagnetic wave absorbers.

References

1. Kulikowski, J. of Mag.and Magnetic materials **41** (1984) 56.
2. H.Igrash, K.Okazaki, J. American ceramic society **60** (1975) 51.
3. P.Raveendranathan, K.C.Patil, J. Mat. Sci. **22** (1987) 32.
4. E.J.W.Verwey, P.W.Haaigman, F.C.Romeyn, G.W.Van, Oosterhout, Philips Res. REP **5** (1950) 173.
5. M.Guyot, J. of Magnetism and Magnetic materials **18** (1980) 925.
6. C.G.Coops, Physical review **83** (1951) 121.
7. S.Jankowski, Journal of American ceramic society, (1988) c –176.
8. F.C.Brockman, R.T.White, J.of American ceramic society **54** (1971) 109.
9. P.V.Reddy, R.Sathyanarayana, T.S.Rao. Phys. Stat. Sol (a) **78** (1983) 109.
10. A.Verma, T.C.Goyal, R.G.Mindiretta, R.G.Gupta, Journal of Magnetism and Magnetic materials **192** (1999) 271.
11. M.A.El Hiti, J. of Magnetism and Magnetic materials **164** (1996) 187.
12. D.Y.Kim,Y.C.Chang,T.W.Kang,H.C,Kim .IEEE Transactions On Magnetics, **32**, No.2, March 1996
13. Y. Naito and K. Suetaki, " Application of ferrite to electromagnetic wave absorber and its charecoristics ," IEEE transactions, Microwave Theory, Tech, volume MTT- 19(1971) 65.
14. H M Musal. Jr. and HT Hahn. IEEE Transactions On Magnetics, **25** no 5, (1989) 3851.
15. H M Musal. Jr. and DC Smith. IEEE Transactions On Magnetics, **26** no 5 ,(September 1990) 1462.
16. C A Grimes and D M Grimes - journal of applied physics vol 69, no. 8. (April 1990) 6186.
17. C A Grimes and D M Grimes- Physical Review.B. **43**.no.13, 10780.
18. Anderg, Znidarsie and Miha Drofenik J. of American Ceramic society **82** (1999) 359.
19. Yootarou, Yamazaka, and Minuru Satou Jap. J. of Applied Physics **12** No. 7 (1973) 998.
20. Ahamed M.A and Elhiti Journal de Physique III **5** (1995) 775.

21. Shaikh.A.M, Bellard S.S and Chougule B.K. Journal of Magnetism and Magnetic Materials **195** (1999) 384.
22. Ahamed M.A and Elhiti, E.I.Nimar and Amar M.A Journal of Magnetism and Magnetic materials **152** (1996) 391.
23. Pal M, Brahma P and Chakravarthy D, Journal of Physical Society Jap. **63** No.9 (1994) 3356.
24. SA Mazen,F Metawe and S F Mansour J Phys D Appl. Phys.**30** (1997) 1799.
25. M.A.El Hiti, J. of Magnetism and Magnetic Materials **164** (1996) 187.
26. M.Guyot,J.Magn.Magn,Mater.**18** (1980)925.
27. Ramasastry C and Syamasundra Rao, J.Phys.E.Sci.Instrum.12 (1979) 1023.
28. I.C.Maxvell, Electricity and Magnetism, vol.1,Oxford univ .Press, Newyork,(1973)828.
29. K.W.Wagner, Amer,Phys.**40** (1973) 317.
30. C.G.Koops, Phys. Rev **83** (1951) 121.
31. L.T.Rabinkin, Z.I.Novikora.Ferrites.146 Izv. Acad. Nauk,USSR. Minsk 1960.
32. K.Kunar, G.S.Srivastava,J.Appl.Phys.**70** (1994) 6115.
33. E.M. Mohammed, K.A. Malini, P. Kurian, M.R. Anantharaman, Materials Research Bulletin **37** (2002) 753
34. A.M.Shaikh,S.S.Bellad,B.K.Chougule,J. Magnetic Materials **195** (1999)384.
35. K.J.Standley, Oxide Magnetic Materials, Clarendon Press, Oxford,(1962).323
36. O.S. Josyulu, J.Sobhanadri ,Phys.Stat.Sol.A **59**(1980) 323.
37. W.D. Kingery, H.K.Bowen, D.R. Uhlmann, Introduction to Ceramics, Wiley, NiwYork, (1975)904 .
38. G.C.Kuezynski,N.A.Hooton, C.F.Gibbon.Sintering and Related Phenomenon, Gordon and Breach, NewYork, (1967) 65.
39. L.G.VanUitert, J.Chim.Phys.**23** (10)(1955)1883.
40. K.A.Malini, E.M.Mohammed, S.Sindhu, P.Kurianand M.R.Anantharaman, Plastics,Rubber and Composites 31 No.10 (2002) 449.
41. PhD thesis, MA Solomon Department of Polymer Science, Cochin University of Science and Technology, Cochin.
42. Tareev B Physics of Dielectric Materials (Mir Publishers) Moscow (1979)
43. Ki Chulhan, Hyung Do Choi, Tak Jin Moon, Wang Sup Kim and Kyung yong Kim,J.Master.Sci.**30** (1995) 3567.

44. A.K. Jonscher, Dielectric Relaxation in Solids, Chelsea Dielectric, London,1983.
45. Y. Yamazaki, M.Satou, Jpn.J.Appl.Phys.**12** (1973) 998.
46. P.V. Reddy, T.S .Rao, J.Less-Common Met, **86** (1982) 255.
47. A.M.Abdeen, J. of Magnetism and Magnetic Materials **185**(1998) 199.
48. M.A.El Hiti, J.Phys.D: Appl.Phys.**29** (1996) 501.
49. P.V.Reddy ,R.Sathyanarayana,T.S.Rao,Phys.Stat.Sol.(a)**78**(1983)109.
50. M.A. El Hiti, Phase Trans.**54**(1995)117.
51. M.A..El Hiti, M.K.El Nimr, M.A.Ahmed,Phase Trans.(1995)137.
52. M.M.Mosaad,M.A.Ahamed,J.Magn.Mater.**150**(1995)51.
53. D.A.Seanor(edt) Electrical properties of Polymers, Academic press New York,1989.
54. James M. Margolis, (edt), Conductive Polymers and Plastics, Chapman and Hall,New York,1989.
55. Ya.Mpaushkin, T.P.Vishnyakova, A.F.Lumin, S.A.Nizova, Organic Polymeric Semiconductors, Ketr Publishing House Jerusalem Ltd, 1974.

Chapter V

Cure Characteristics and Mechanical Properties of Rubber Ferrite Composites

5.1. Introduction

Ferrites can be incorporated in various elastomer matrixes to produce flexible magnets or rubber ferrite composites (RFCs) [1-8]. The incorporation of these ferrite powders can be carried out in various matrixes to produce RFCs, both in natural and synthetic rubber. RFCs have the unique advantage of mouldability into complex shapes, which is not easily possible by conventional ceramic magnets. The addition of magnetic fillers in an elastomer matrix modifies the physical properties of the matrix considerably, in that they modify the dielectric properties and impart magnetic properties to the matrix [9,10]. In applications involving ferrites at high frequencies it is essential that the material posses an appropriate dielectric permittivity and suitable magnetic permeability [11-15]. When preparing RFCs, the choice of compounding ingredients, compounding conditions and their processability are important. Also factors like percolation limit and nature of the matrix like saturated /unsaturated/ polar/non polar rubber, all influence the final properties of the composites.

It has also been reported that the incorporation of ferrites in polymer matrix can lead to the development of magnetic nanocomposites with excellent performance characteristics [16-19]. The preparation of RFCs and evaluation of various properties such as magnetic, dielectric and mechanical assumes significance not only in tailor making compounds but also in understanding the fundamental aspects that govern these properties.

Chapter 5

Knowledge of cure characteristics throws light on the processability and mechanical properties of composites [20-22]. Information regarding particle size, surface area and porosity are also valuable tools in explaining the properties .By selecting appropriate matrix, magnetic fillers can be incorporated to form a composite of required mechanical, magnetic and dielectric properties. Nitrile- rubber is selected as the elastomer for mixing the magnetic filler. Nitrile rubber, otherwise known by the generic name Buna-N or NBR, is a special purpose synthetic rubber. NBR shows no self-reinforcing effect, as there is no stress-induced crystallisation [23]. Since it does not crystallise, reinforcing fillers are necessary to obtain optimum tensile strength, tear strength and abrasion resistance. Here the choice of compounding ingredients, compounding conditions and their processability are significant as far as the properties of RFCs are considered.

The mechanical properties like tensile strength, elongation at break and the modulus are important properties of plastic materials because all applications involve some degree of mechanical loading [24-28]. A tensile test is a measurement of the ability of a material to withstand the forces that tend to pull it apart and to determine to what extent the material stretches before breaking. Different types of polymeric materials are often compared on the basis of their tensile strength, elongation at break and modulus. Hence the evaluation of these properties also assumes significance in making devices based on RFCs. The mechanical properties namely tensile strength, elongation at break 100% modulus and 200% modulus of the prepared RFCs are evaluated and they are studied as a function of loadings and size of the fillers. The size of the filler is an important parameter, which determines the mechanical properties of the RFCs.

The parameters namely particle size, porosity and surface area of the ceramic filler are very important in determining the mechanical properties of the composite. Since, after incorporation of fillers, RFCs are to be moulded /cured, their effects on the cure parameters are also to be determined. The mechanical properties of the cured compound is also dependent on the amount of filler in the matrix and their porosity/particle size/surface area. Hence the evaluation of their cure characteristics and estimation of their mechanical properties is a prerequisite for further applications.

After incorporation of ferrite fillers in to nitrile rubber for various loadings, their cure parameters are evaluated. Further after curing and moulding, their mechanical properties are investigated. Factors like tensile strength, modulus and elongations are determined by standard ASTM procedure. The results are correlated with loadings of the filler, particle size and porosity. The details of these findings are presented here in this chapter.

5.2. Cure Characteristics of RFC

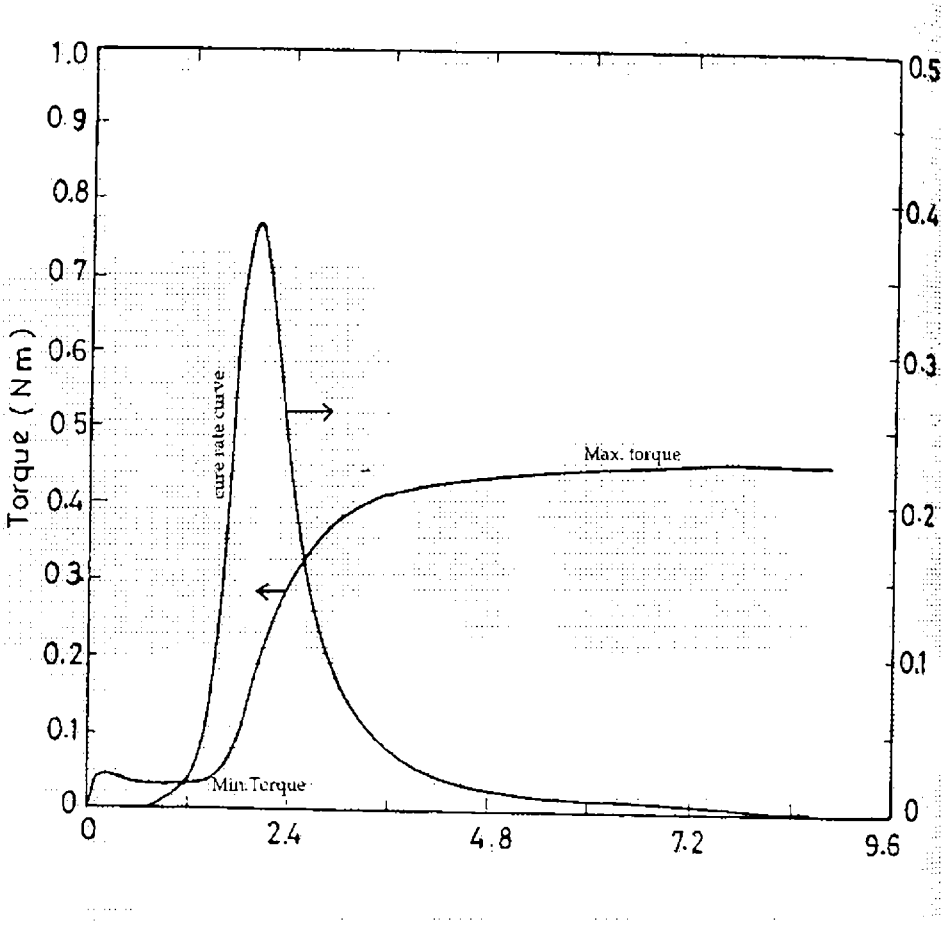

Fig. 5.1. Representative Cure Characteristic curve for RFC.

Pre-characterized nickel ferrites heat-treated at various temperatures were incorporated into nitrile rubber matrix according to a specific recipe. The mixing was done in a Brabender plasticorder and the cure characteristics of the prepared composites were determined by using the Gottfert elastograph as explained in Chapter II. Cure characteristics

were plotted for all composites. A representative cure characteristic curve is shown in fig. 5.1.

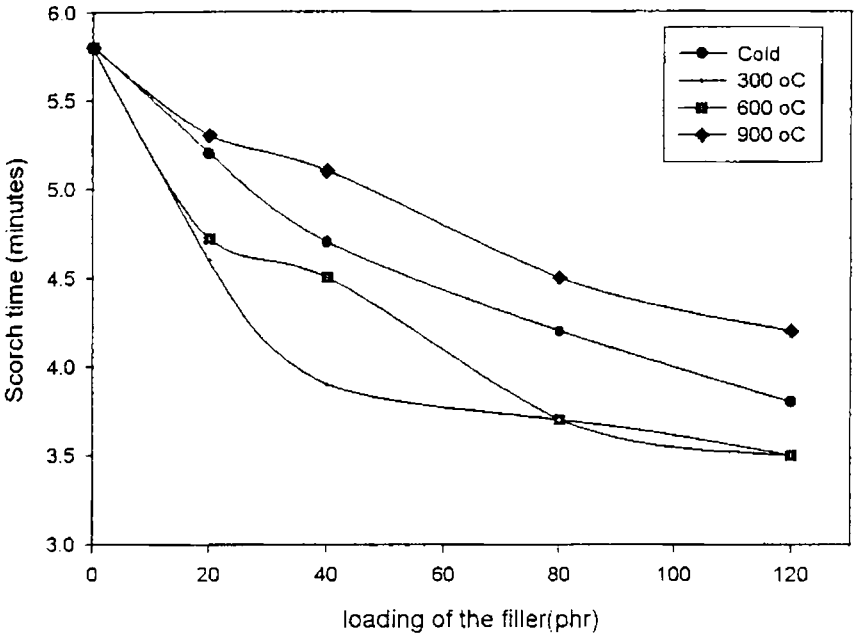

Fig.5.2.Variation of scorch time with loading of the filler.

Fig.5.2 shows the variation of scorch time with loadings of nickel ferrite with varying particle sizes. The scorch time (t_{10}) decreases with the loadings of the fillers. All the samples show the same variation. The decrease in scorch time with increase in filler loading is due to the increase in the heat of mixing, with increase in filler loading

Cure time is defined as the time required for optimum vulcanization of the samples. From fig.5.3 it is seen that cure time sharply decreases for initial filler loadings (20 phr) and then increases for higher

loadings. The high cure times at higher filler loading is due to the adsorption of curatives by the filler particles.

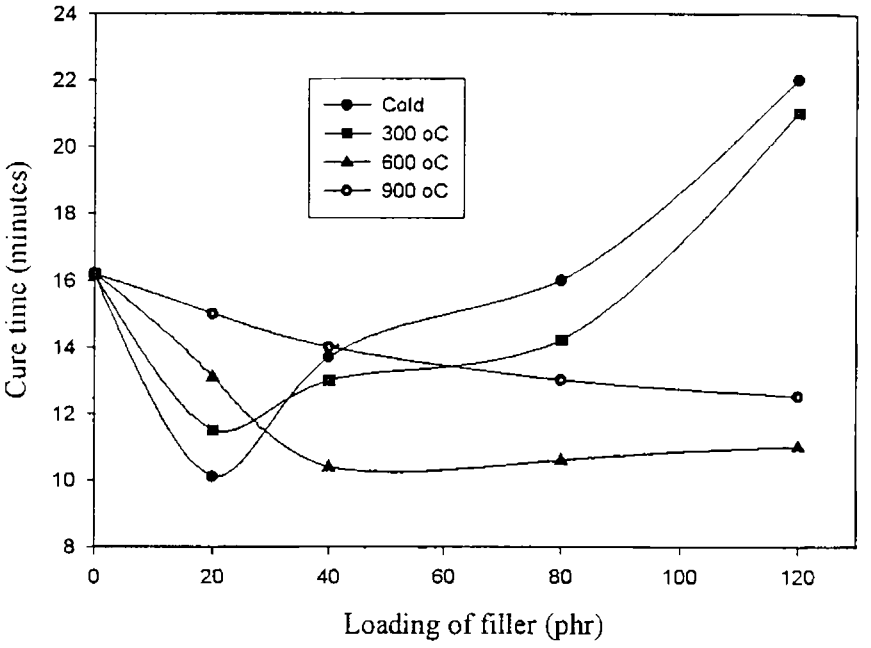

Fig.5.3 Variation of cure time with loading of filler

RFCs based on nickel ferrites fired at low temperatures and having low grain sizes, the cure time increases for higher loadings of fillers. But the change in cure time is only marginal for additional loadings of fillers for higher grain sizes. These observations confirm that fillers of low grain sizes affect the processability of the composite into a certain extent while that of larger grains do not affect the processability of the composites.

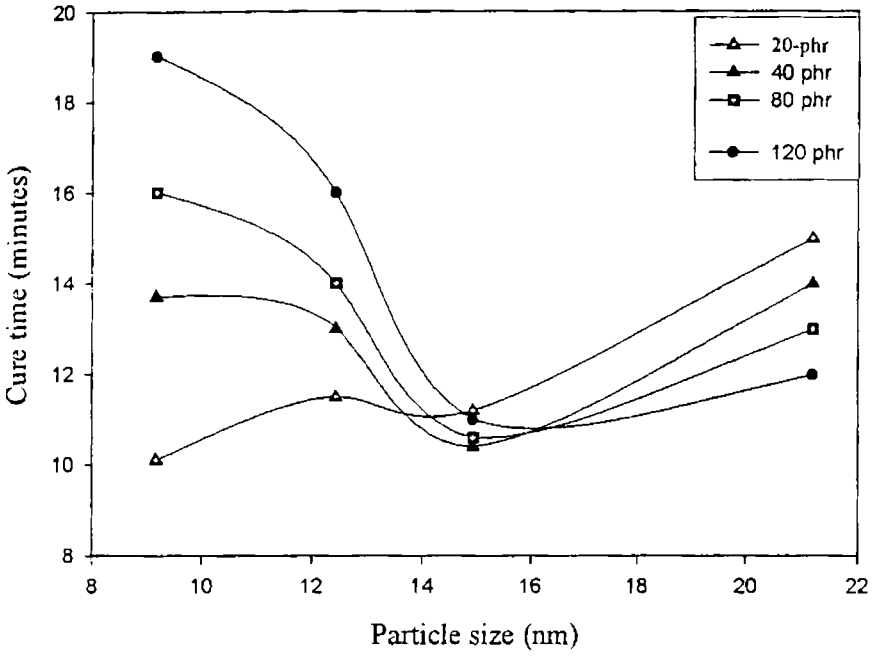

Fig.5.4 Variation of cure time with grain size of the filler

Cure time is studied as a function of grain size of nickel ferrite filler and their variation is shown in fig.5.4. From the curve it is evident that for fillers having less than 14 nm; the cure time decreases with particle sizes Also for fillers of small grains and for higher loadings, there will be an increasing tendency for agglomeration and this will retard the action of the accelerator and hence the cure time increases.

Fig.5.5 shows the variation of maximum torque with loadings of the fillers fired at various temperatures. It is observed that the maximum torque increases with loading for almost all composites. Maximum torque gives an indication about the modulus of the compound. It shows an

increasing trend with loading. Solomon et al [22] obtained the same variation in case of hexagonal ferrites incorporated in nitrile rubber. From the fig 5.5 it is clear that, for nickel ferrite filler fired at low temperatures, the maximum torque shows an increasing trend.

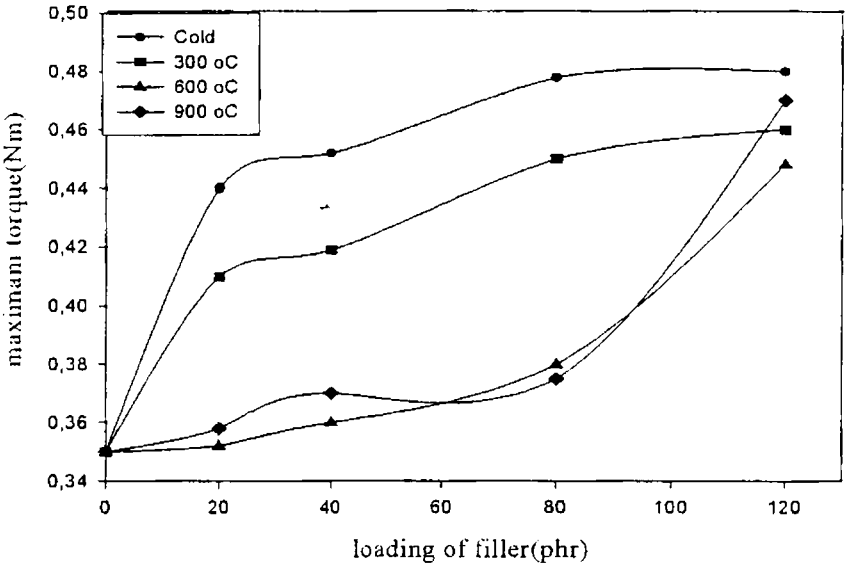

Fig.5.5 Variation of maximum torque with loading

Minimum torque is an indirect measure of the viscosity of the compound, or it can be generally treated as the measure of the stiffness of the unvulcanised rubber compound at the lowest point of the curve. Variation of minimum torque with loadings of the fillers with varying particle sizes are shown in fig. 5.6. Minimum torque increases with loadings of the filler.

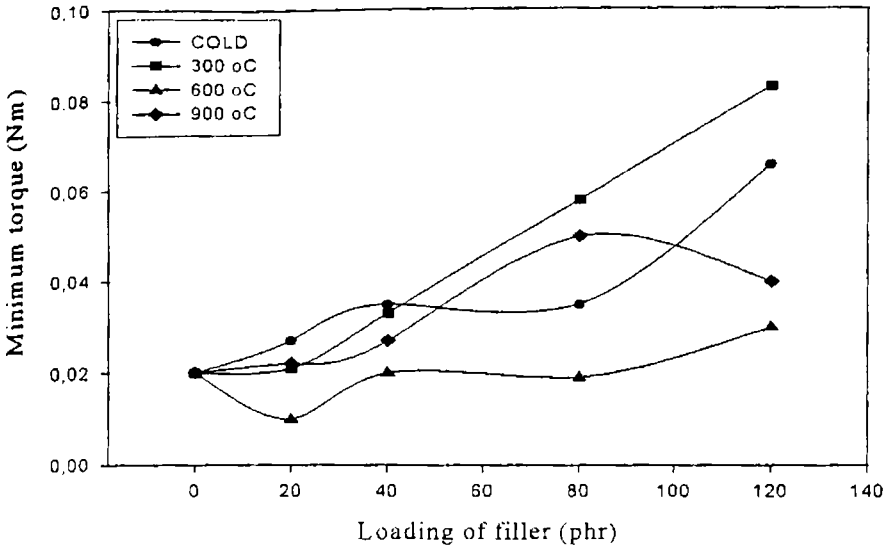

Fg.5.6. Variation of minimum torque with loading of filler

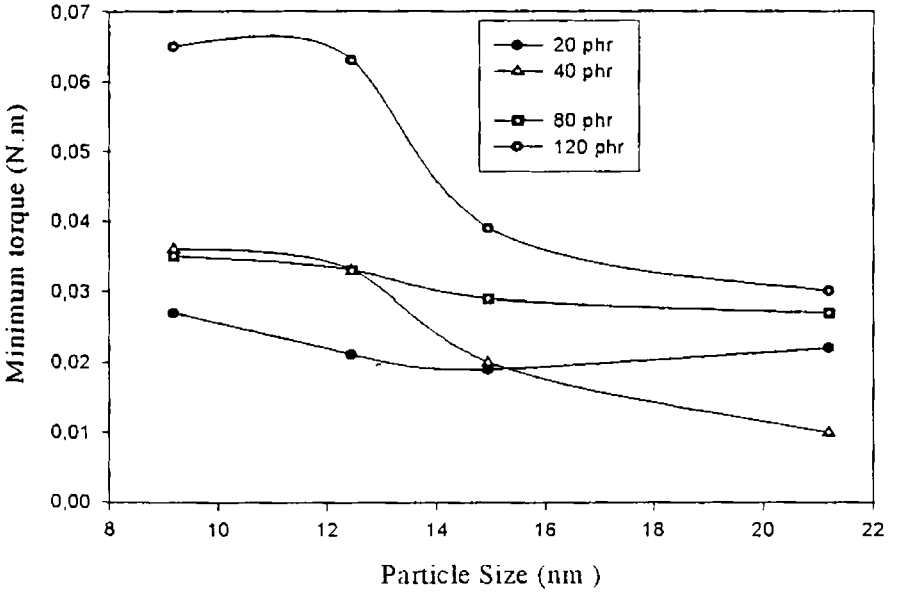

Fig.5.7 Variation of minimum torque with grain size of the filler

Variation of minimum torque with grain size of the nickel ferrite is shown in fig.5.7. These observations confirm that the addition of nano ferrite in nitrile rubber affect the processability of the composite and thus nano ferrite act as a reinforcement agent for the matrix

5.3.Mechanical Properties

The mechanical properties of the RFCs were determined using an Instron Universal Testing Machine, Model 4500 Test System. Dumbbell shaped specimens where cut from the prepared RFCs containing nickel ferrites of different particle sizes, at loadings of 20, 40, 80 and 120 phr as per ASTM procedure. Parameters namely tensile strength, modulus at different percentages, and elongations at break, which are some of the most important indications of the strength of the material [22,29,30] were determined and their variation with loading and with grain size were studied.

Variation of tensile strength with loading of nickel ferrite is shown in fig.5.8. The tensile strength increases with the loading of Nickel ferrite. The addition of nickel ferrite filler greatly reinforces the nitrile rubber matrixes and showed a maximum reinforcement for the nickel ferrites of small grain size. NBR gum vulcanisate has relatively low tensile strength due to lack of stress induced crystallization, which increases with increasing filler loading. The addition of ferrite filler reinforces the NBR matrix and showed maximum reinforcement for samples fired at low temperature or samples with low grain size. For higher loadings of nickel ferrite (120 phr) the change in tensile strength is only marginal, which is due to the diminishing volume fraction of the polymer available for wetting the filler particles

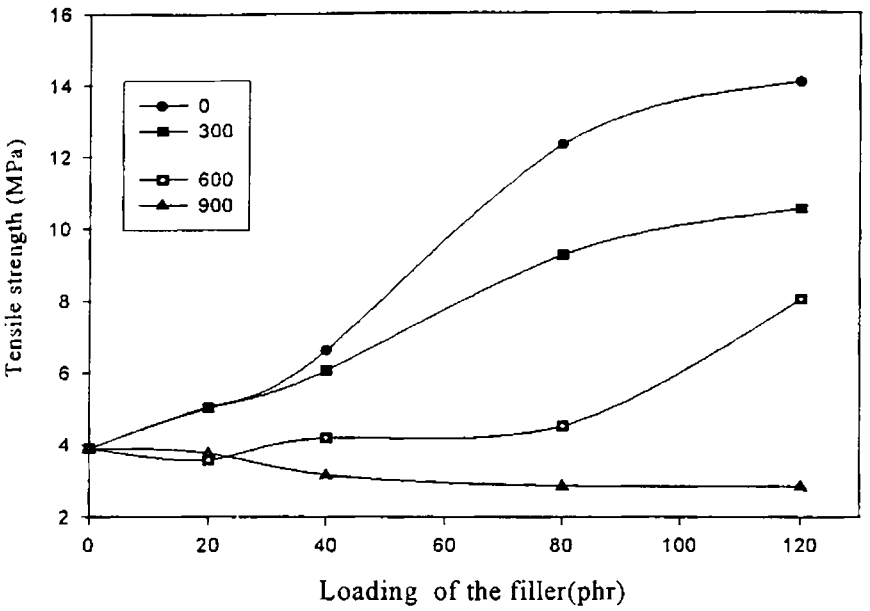

Fig.5.8 Variation of tensile strength with loading of the filler.

The tensile strength of the RFCs, were studied as a function of grain size of the ferrite filler and their variation is given in fig.5.9. Tensile strength of the RFCs, were found to increase with decreasing particle size. As the grain size of the filler decreases, the specific surface area available for wetting with rubber molecules increases; and as a result the reinforcement increases.

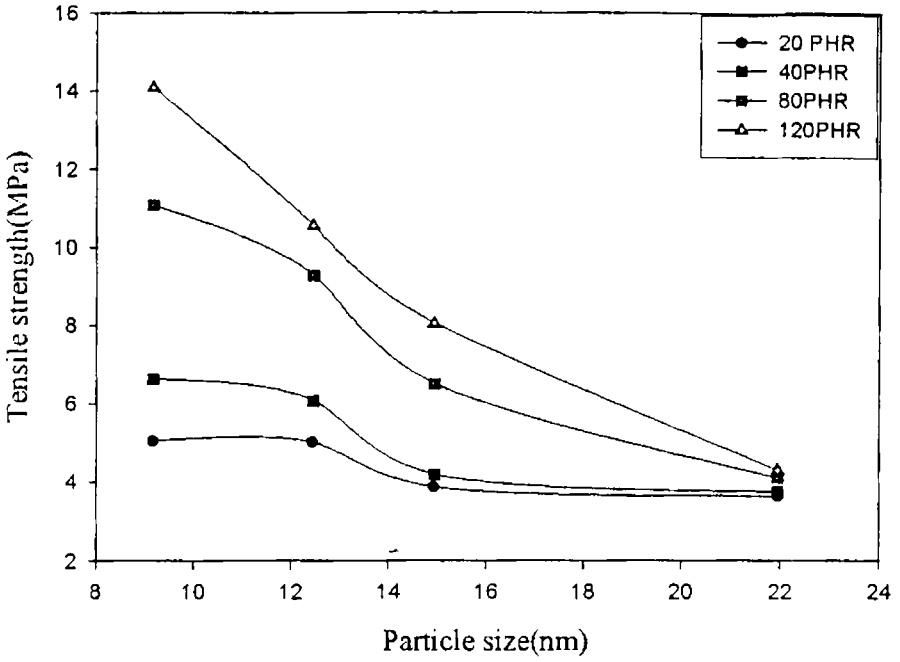

Fig.5.9 Variation of tensile strength with grain size of the filler.

As the firing temperature increases, the grain size of the particles increases and the porosity decreases. For samples prepared at low temperatures the porosity is maximum. As the porosity increases the chance of bound rubber formation increases due to the flow of the macro molecules (rubber molecules), and as a result the tensile strength increases.

The modulus of the composites increases with increase in the loading of the filler, which is characteristic of reinforcing filler. Figures 5.11and5.12 depict the variation of 100% and 200% modulus with loading of the filler.

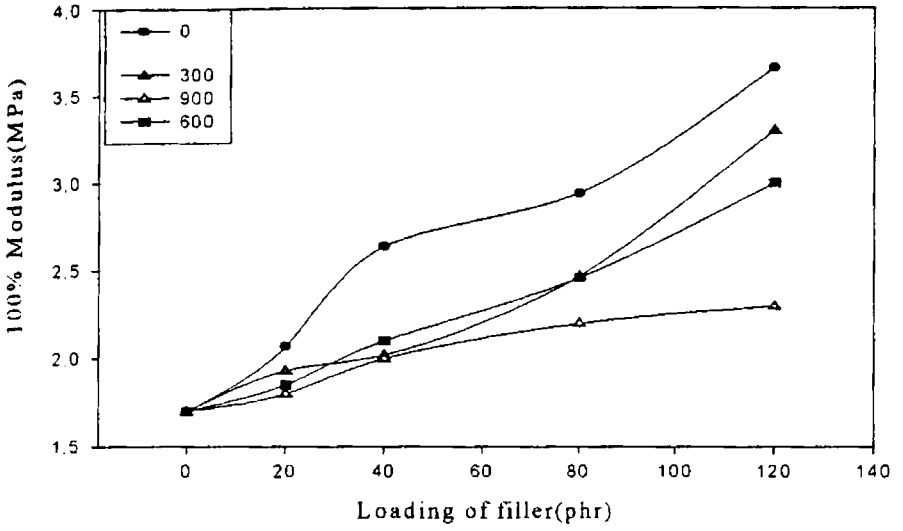

Fig.5.10.Variation of 100% modulus with loadings of the filler

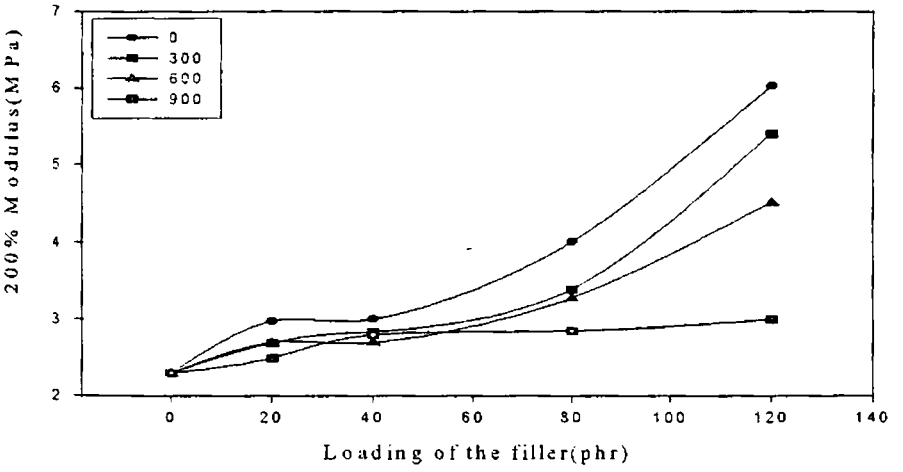

Fig.5.11.variation of 200% modulus with loading of the filler

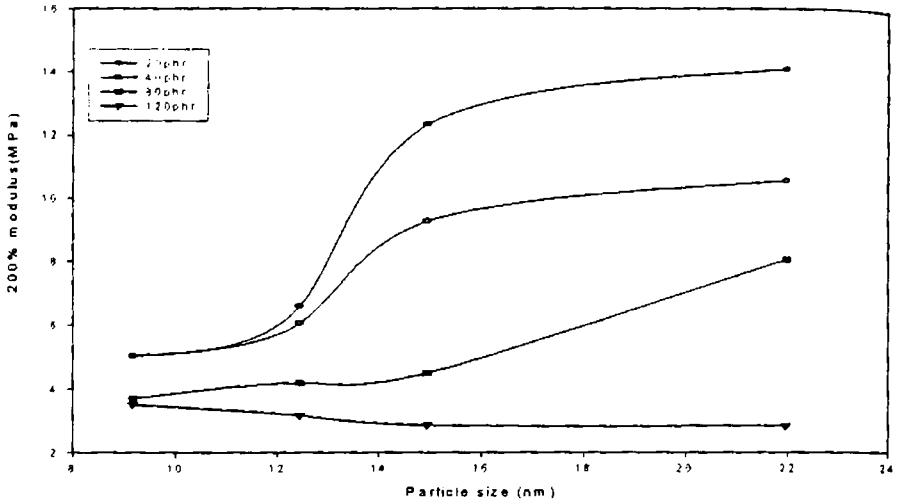

Fig.5.12.Variation of 200%modulus with grain size of the filler

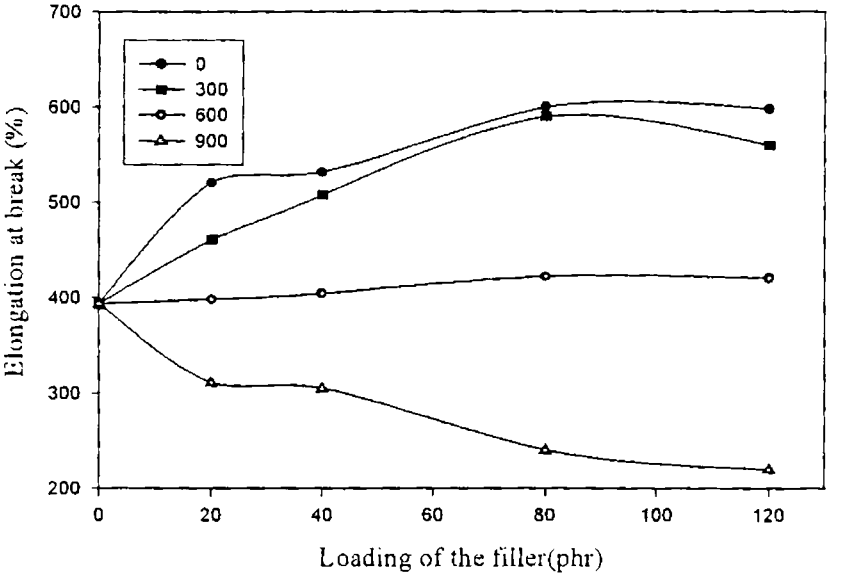

Fig.5.13. Variation of elongation at break with loading of the filler.

For fillers fired at low temperatures the elongation at break increases with loadings. But for samples fired at 900°C, the elongation at break decreases with loadings. The variation is given in fig.5.13. The coarser particles generally decrease the elongation at break.

Elongation at break increases with loadings of the fillers in case of ferrite samples fired at low temperature or fillers having lower particle sizes. For smaller particles, the polymer filler interface will be stress bearing and this will lead to the increase in elongation at break

The variation of elongation at break with the size of the filler is shown in fig.5.14.

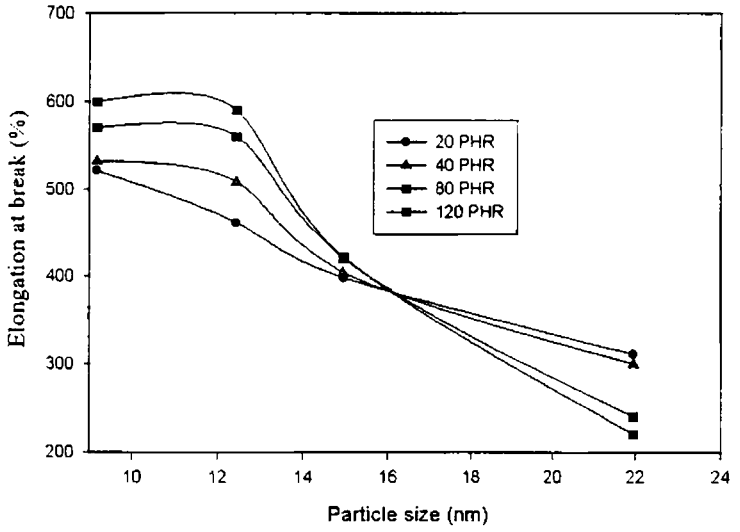

Fig.5.14. Variation of elongation at break with particle size.

5.4.Conclusion

Rubber ferrite composites containing nickel ferrites heat treated at different temperatures in nitrile rubber have been prepared. The cure characteristics reveal that if the particle size of the filler is below 15 nm, the loading of the filler affects the processability of the matrix. The minimum and maximum torque values increases with increase in loading of the filler. If the grain size of the filler is in the nanoregiome. grain size has a strong bearing on the cure parameter.

The addition of ferrite fillers can enhance the mechanical properties of the nitrile rubber-matrix. The tensile strength, 100% modulus, 200% modulus and elongation at break are found to increase with increase in the loading of the filler. Thus the nanoparticles of nickel ferrite act as a reinforcing agent for nitrile rubber matrix. The grain size and the porosity of the filler plays a vital role in determining the mechanical properties. The increase in porosity of the filler enhances the mechanical properties. As the porosity increases, the chance for bound rubber formation increases due to the flow of the macromolecules (rubber molecules), and as a result the tensile strength increases.

Reference:

1. Safari Ardi M, Dick W and McQueen D.H, Plastic Rubber and Composites Processing Applications, **24,** (1995), 157.
2. M.R Anantharaman, S.Jagatheesan, S.Sindhu, K.A. Malini, C.N .Chinnasamy, A. Narayansamy, P.Kurian and Vasudevan, Plastic Rubber and Composites Processing Applications,**27**, No.2, (1998), 77.
3. Anantharaman M.R, S.Sindhu, S. Jagatheesan K.A.Malini and Philip Kurian, Journal of Physics D Applied Physics **32,** (1999), 1801.
4. E.M. Mohammed, K.A. Malini, P. Kurian, M.R. Anantharaman, Materials Research Bulletin **37,** (2002), 753
5. Katz H.S and J.V.Milweski, 'Handbook of Reinforcement of Plastics,Vannostrand Reinhold, New York ,(1978),
6. Praveen Singh & T.C. Goel, Indian J. Pure and Appl Phys., **38,** (2000), 213.
7. Anantharaman M.R, P.Kurian, B.Banerjee, E.M.Mohammed, and M.George, Kautschuk Gummi Kunstsoffe, (Germany), **49**, No.6,(1996),424
8. Anantharaman M.R, K.A.Malini, S.Sindhu, E.M.Mohammed, S.K Date, S.D.Kulkarni,P.A.Joy, and Philip Kkurian, Bull.Mater.Sci., **24**, 6,(2001), 623.
9. Jozef Slama, Anna Gruskova, Ludovit Keszesh, Mojmir Kollar,IEEE Trans. Mag, **30,** No.2, (1994)
10. Z.Osawa, K.Kawaguchi, M.Iwata, H.Harada, J.Mater. Sci. **23,** (1988), 2637.
11. D.Y.Kim, Y.C.Chang, T.W.Kang, H.C,Kim. IEEE Transactions On Magnetics, **32**, No.2, (1996)
12. Y. Naito and K. Suetaki IEEE transactions, Microwave Theory, Tech, **MTT-19,** (Jan 1971), 65.
13. H M Musal. Jr. and HT Hahn. IEEET Transactions on Magnetics, **25,** No 5 (Sept 1989), 3851.
14. H M Musal. Jr. and DC Smith. IEEE Transactions on Magnetics, **26,** No 5, (Sept 1990), 1462.
15. C A Grimes and D M Grimes - journal of applied physics **69**, No.8. (April 1990),6186.
16. K.A.Gscheindner, Jr.and V.K.Pechkary, J.Appl.Phys., **85**, No.8, (1999), 5365.
17. R.D.Shull, J.J.Ritter and L.J.Swartzendruder, J.Appl.Phys., **69,** (1991), 5414
18. R.D Shull and L.H Bennet, Nanostructured Materials, **1**, No 9,(1992), 83.
19. A.gravin and C.L.Chein, J.Appl.Phys.**67,** (1990), 938.

20. K.A.Malini, P.Kurian, M.R.Anantharaman., Mater. Letters, **57,** (2003), 3381.
21. E.M.Mohammed, K.A.Malini, Philip Kurian, M.R.Anantharaman, Materials Research Bulletin, **37,** (2002), 753.
22. M.A.Soloman, Philip Kurian, M.R.Anantharaman, Progress in Rubber Plastics and Recycling Technology, **18**, No.4, 2002
23. S.Blow, Handbook of Rubber Technology, Galgotia Publishing, 1998.
24. George G Winspear (Edt), The Vanderbilt Rubber Handbook R.T.Vanderbilt Company Inc.New York, 1958.
25. Vishu Shah, Hand Book of Plastic Testing Technology, John Wiley and Sons Inc, USA ,1998.
26. A.W. Allen, Natural Rubber and the Synthetics, Granda, Publishing Ltd.1972.
27. ASTM D2084-95.
28. Charles A Harper, Handbook of Plastic, Elastomers and Composites ,(Second Edition) McGraw Hill Inc.,1992.
29. Ph.D Thesis, K.A.Malini, Cochin University of Science and Technology, Cochin, India, 2001.
30. Roberts.A.D, Natural Science and Technology, Oxford University Press, New York, (1998), 556.

Chapter VI

Dielectric Permittivity Studies of Rubber-Ferrite Composites in X-band

6.1.Introduction

It is known that microwaves are detrimental to human kind as well as electronic circuits employed in their day-to-day life. In the former, microwaves affect living tissues while in the latter they can interfere and produce noise in the electronic circuit [1-5]. So it is essential that they be prevented from leaking out of a microwave based device as well as to stop them from getting in to it.

Electromagnetic interference (EMI)–a specific kind of environmental pollution, is drawing more attention recently, due to the explosive growth in the utilisation of electrical and electronic devices in industrial, commercial and military applications. To provide adequate solutions for the EMI problem, the shielding and / or absorbing of the electromagnetic field is considered. There has been considerable interest in recent years in the applications of magnetic materials to the problem of microwave absorber design [6-9]. This is because, if a material with lossy dielectric is imparted a magnetic permeability by appropriate means, the absorbing characteristics of the material can be greatly modified. The modulation of the absorbing characteristics is based on the electromagnetic theory. The cardinal principle based on which absorbers are designed is the surface impedance.

Surface impedance can be written as [10]

$$Z = \sqrt{\frac{\mu_r}{\varepsilon_r}} \tanh [\, j \frac{2\pi}{\lambda} \sqrt{\mu_r \varepsilon_r}\, t], \qquad 6.1$$

where μ_r and ε_r are the complex permittivity and permeability of the composites of thickness t. The reflection coefficient is expressed as

$$R\,(dB) = 20 \log \frac{Z-1}{Z+1}. \qquad 6.2$$

Ferrites are materials, which can satisfy the above criteria; because the composition in a particular ferrite material can be altered to tailor the magnetic permeability and dielectric permittivity. There has been considerable efforts by microwave engineers to model an absorber for optimum performance.

For a lossy material the minimum thickness required for the absorber is 0.4 λ_L where λ_L is the lowest wavelength of the electromagnetic wave band [11].

For microwave absorber based on a ferrite material, the minimum matching thickness is governed by [11]

$$t = \lambda/2\pi\mu'' \qquad 6.3$$

Where λ is the wavelength of radiation and μ'' is the magnetic loss factor. The matching thickness of the ferrite absorber has been evaluated and found to be 2mm and 8mm. This augurs well as far as economy and compactness of the absorber is concerned [12-14]. For stealth applications, it is also necessary that a coating of minimum thickness of the absorber be provided on the body surface. In other applications involving microwave absorbers, gadgets of complex shapes are often required. This necessitates flexibility, mouldability and appropriate strength. All the above criterion can be easily met by preparing a composite based on rubber and ferrites.

Ferrites are already known for their microwave absorption in UHF and VHF band. Combining the properties of a lossy dielectric and that of a ferrite, RFC's can be synthesised. RFC's can be prepared by incorporating ferrite filler in NBR matrix according to specific recipe. Chapter II gives a detailed description of the preparation of composites.

As evident from 6.1, the most important property that governs electromagnetic absorption is the dielectric permittivity and magnetic permeability at the desired bandwidth operation [15,16]. The dielectric permittivity depends on the size, microstructure and loading of the ferrite filler in the matrix [17-19]. Hence the evaluation of both real and imaginary part of the permittivity is significant. In this chapter, the results of such studies are presented. The data generated in the X-band (8GHz to 12GHz) are analysed and correlated with the loading and particle size of the filler.

6.2. Permittivity Measurements

Pre-characterized nickel ferrites heat-treated at various temperatures were incorporated into nitrile rubber matrix at loadings of 20phr, 40 phr, 80phr and 120phr so as to prepare the RFCs The real and imaginary parts of the complex permittivities of the RFCs in the frequency range 8-12GHz were measured by cavity perturbation technique. The complete theory and the experimental details are described in chapter II.

6.3.Frequency dependence of permittivity

The real permittivity spectra RFCs at ferrite loadings of 20phr, 40phr, 80phr and 120phr of different particle sizes are shown in fig.6.1. The real permittivity increases as the loadings or the volume fraction of ferrites increases. The permittivity is maximum for the loading of 120phr. The dielectric properties of RFCs arise mainly due to the interfacial polarisation

along with some contribution from ionic polarisation and intrinsic electric dipole polarisation. As the frequency increases upto about 10GHz, the real permittivity increases slightly. This may be due to a possible polarisation transition in the composite material [20]. Above 10.5GHz the permittivity shows a decreasing trend. This is because at very high frequencies, only the effects of electronic polarisation is prominent and effects of interfacial polarisation decreases.

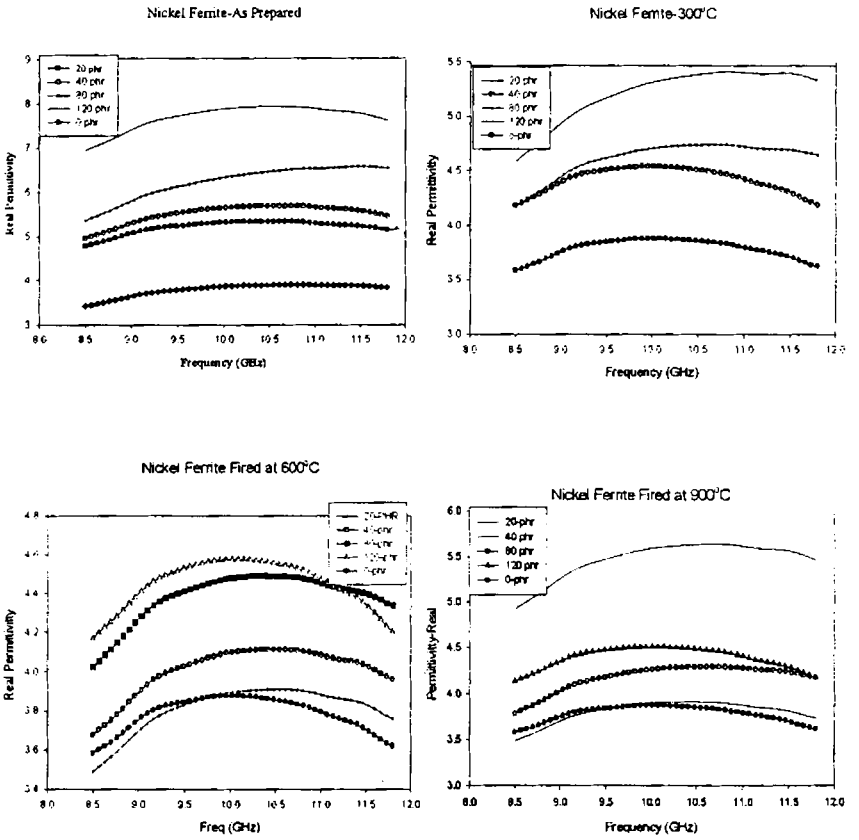

Fig.6.1.Dependence of real permittivity of the RFCs heat-treated at various temperatures with frequency

Fig.6.2. Represents the dependence of imaginary permittivity with frequency in the range 8GHz to 12GHz. The permittivity initially increases with frequency and then there is a dip at 11.5GHz. Permittivity increases as the volume fraction of the ferrites increases and shows the maximum for the ferrite loading of 120phr.

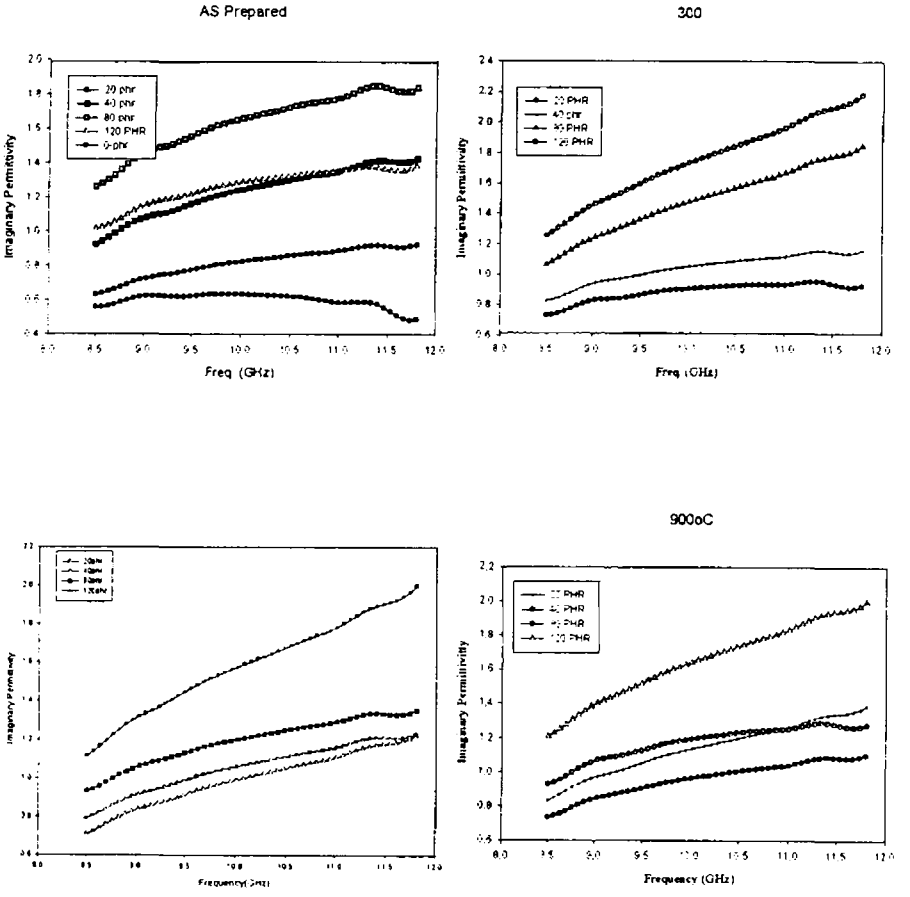

Fig.6.2.Permittivity (Imaginary) spectra for RFCs

6.4.Effect of loading of the fillers on permittivity

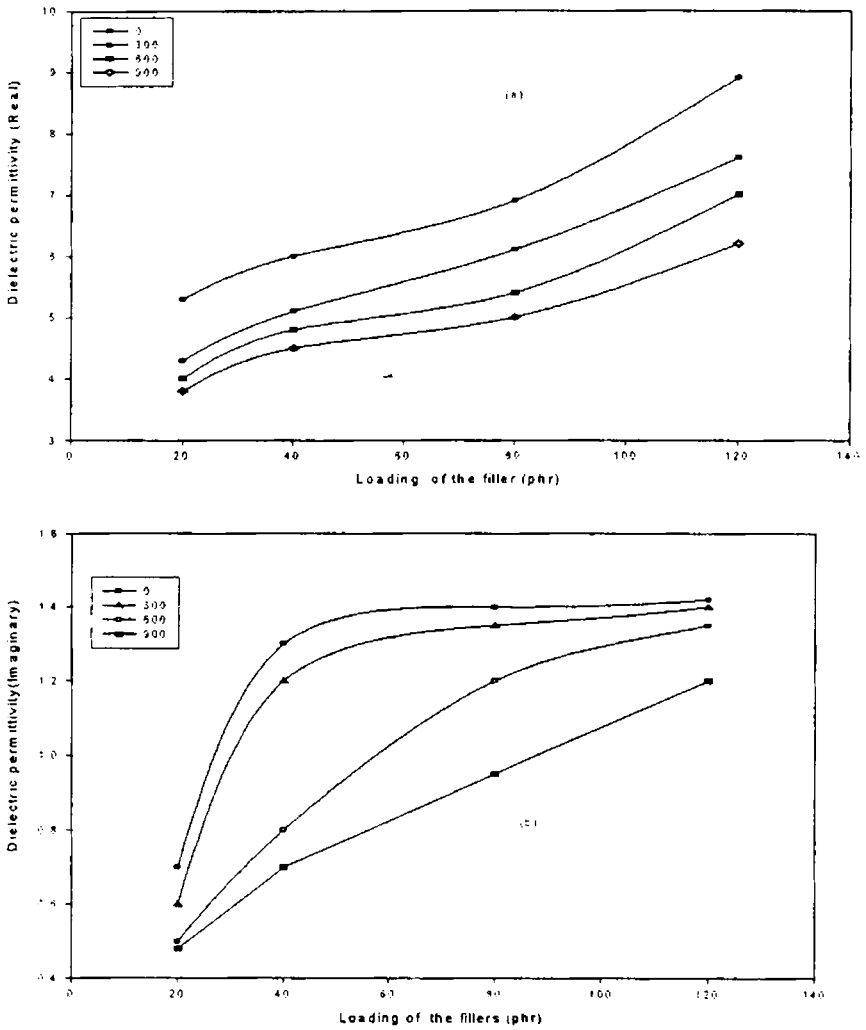

Fig.6.3 Variation of (a) real permittivity and (b) imaginary permittivity with loading of the filler at 9GHz

Variation of the permittivity with loading of the filler in is shown in fig. 6.3.

The permittivity increases with increase in loading of the fillers. A general rule of mixture is applied to the permittivity of the RFCs at GHz frequency range can be written as

$$\varepsilon_c = V_f \varepsilon_f + V_m \varepsilon_m , \ (V_f + V_m = 1), \qquad 6.3$$

Where ε_c, ε_f and ε_m represent the permittivity of composite, ferrite, and polymer, V_f, V_m represent volume fractions of ferrite and polymer respectively.

Maxwell, discussed the problem of the effective conductivity of a binary system consisting of spheres of one conductivity distributed uniformly in a continuum of a different conductivity. Wagner [21] adapted Maxwell's expression to the dielectric case. It can be expressed as

$$\varepsilon_c = \frac{\varepsilon_m \{1 - 2V_f \frac{(\varepsilon_m - \varepsilon_f)}{(2\varepsilon_m + \varepsilon_f)}\}}{\{1 + V_f \frac{(\varepsilon_m - \varepsilon_f)}{(2\varepsilon_m + \varepsilon_f)}\}} \qquad 6.4$$

The Nelson and You equation [22] is

$$\varepsilon_c = ((1-V_f).\varepsilon_m^{1/2} + V_f.\varepsilon_f^{1/2}))^2 \qquad 6.5$$

The Bruggman effective medium theory is also applicable to find the effective permittivity of the composite. The effective permittivity is given as [1]

$$V_f \frac{\varepsilon_f - \varepsilon_c}{\varepsilon_a - 2\varepsilon_c} + (1 - V_a) \frac{\varepsilon_m - \varepsilon_c}{\varepsilon_m - 2\varepsilon_c} = 0 \qquad 6.6$$

Lee and Kim applied Bruggeman effective medium theory to calculate the effective permittivity of MnZn ferrite silicone rubber composites [23].

Effective permittivity is calculated using equation 6.6 and the fitted curve is shown in fig.6.4. Experimental and calculated values are in good agreement as evident from the graph (fig.6.4).

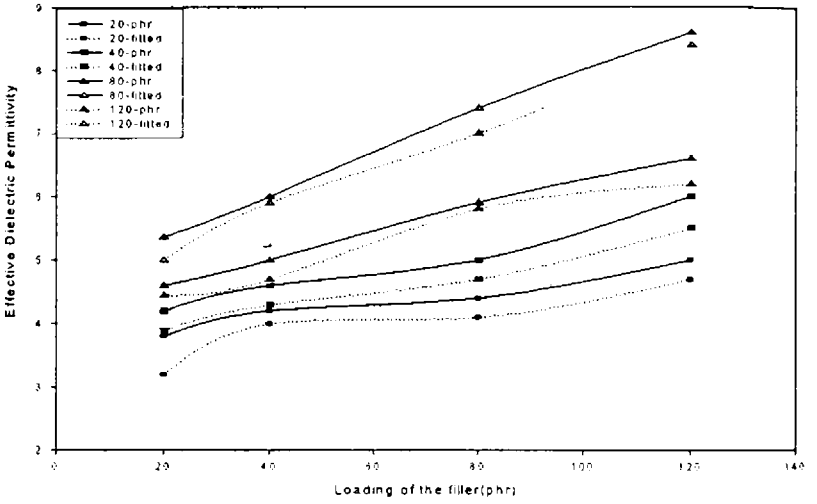

Fig.6.4. Fitted curves for the effective permittivity

Fig. 6.5 represents the dependence of permittivity of the RFCs with grain size of the ferrite fillers. The composites based on the as prepared nickel ferrite shows maximum permittivity. The permittivity decreases with increase in size of the filler. The higher value of permittivity in samples sintered at lower temperatures is due to the presence of localised stage in the forbidden energy gap, which arises due to lattice imperfections. The presence of this states effectively lowers the energy barriers to the flow of electrons.

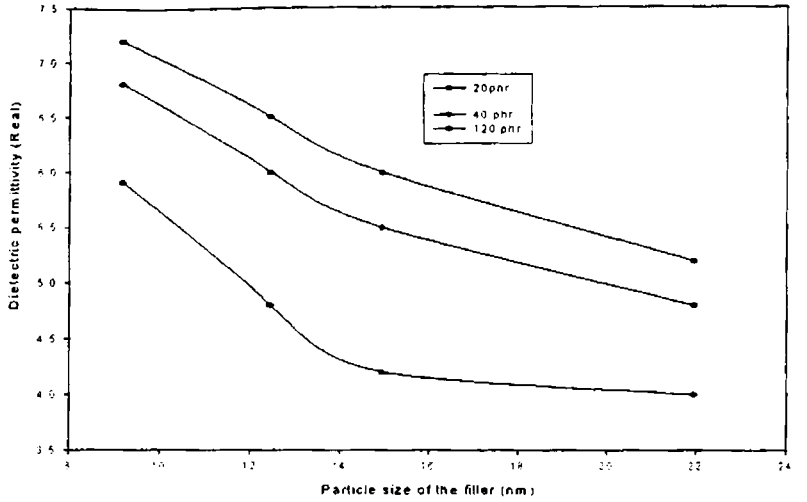

Fig.6.4. (a). Variation of permittivity (real) with grain size of the filler.

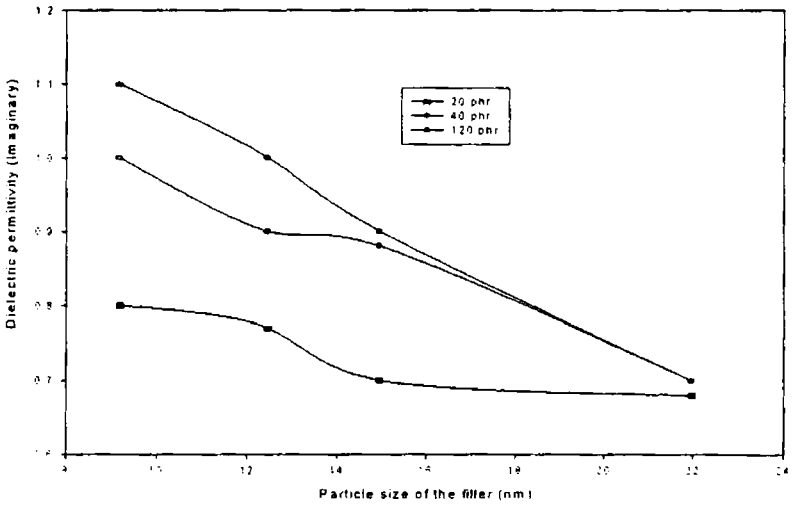

Fig.6.4. (b) Variation of permittivity (imaginary) with particle size of the ferrite filler.

The reduction in permittivity of the composites with increase in firing of the fillers or the increase in grain size of the fillers is due to the reduction in conductivity of the fillers. The conductivity of the ferrite fillers as (24)

$$\sigma(\omega)=\frac{\pi^3}{24} N^2 \varepsilon \; R_\omega{}^6 \omega \qquad 6.7$$

Where, N is the concentration of defect sites contributing to the hopping mechanism. ε the dielectric permittivity and R_ω the hopping distance. Increase in sintering temperature can increase the structural improvement there by decrease the value of N, which reduces the value of conductivity. Also increase in firing temperature increases the grain size of the ferrite fillers. Since the dielectric permittivity is directly proportional with square root of conductivity, the permittivity decreases as the grain size of the filler increases. It must be noted here that composite containing the fine particles of nickel ferrite exhibited a maximum permittivity of around 7.5 at 9GHz for a maximum loading of 120phr This result is in agreement with the variation of permittivity of nickel ferrites (chapter 4).

6.5. Effects of dielectric loss on frequency

The variation of dielectric loss with frequency in the range 8GHz-12GHz are studied and their variations are given in fig.6.5.The loss factor increases with increase in frequency, but there is a dip at two frequencies. This is an indication of maximum absorption of radiations at these frequencies. Also this is a typical result for ferrite based absorbers which possess two matching frequency.

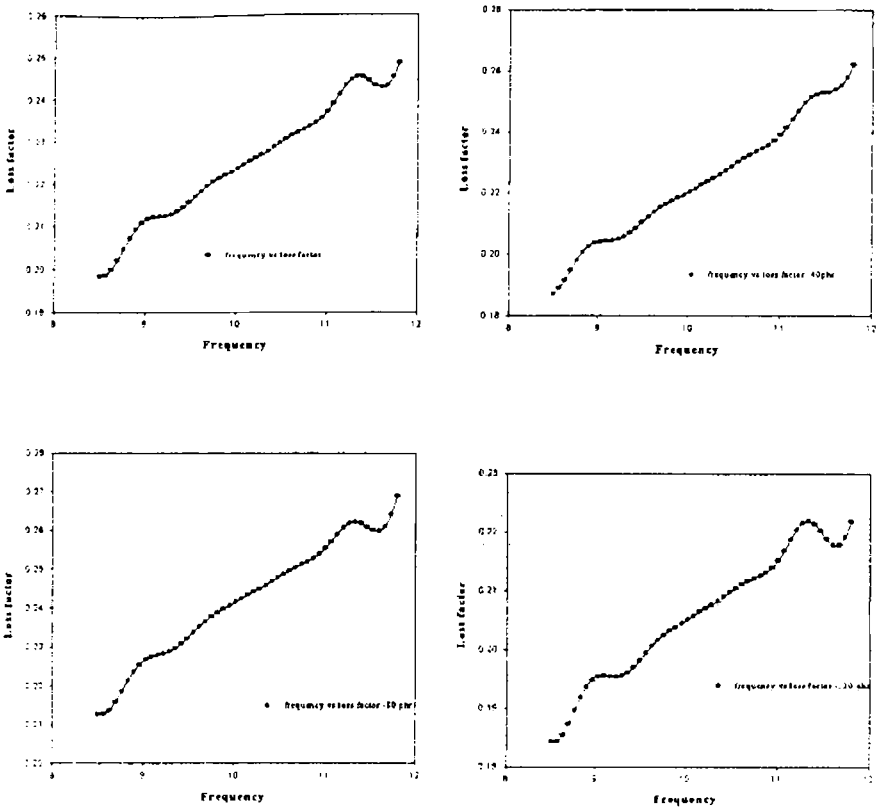

Fig.6.5.Variations of dielectric loss with frequency

The variation of dielectric loss with frequency actually is an indication of absorption. However, magnetic permeability is also required for designing an absorber with minimum thickness as per equations 6.1 and 6.2. Incorporation of other additives like carbon black also improves the performance of the composite absorber [25].

Chapter 6

6.6. Conclusion

The complex permittivity of the composites based on nickel ferrite and nitrile rubber was measured in the frequency range 8GHz to 12GHz by perturbation method. Both the real and imaginary permittivity of the composites increases with the volume fraction of ferrite. The effective permittivity of the composite can be determined by a general mixture rule, which depend the volume fraction of the ferrite fillers. The calculated values are in good agreement with that of the experimental values. The permittivity of the composites was found to depend on the grain size of the filler. The electromagnetic wave absorbing characteristics can be determined by measuring the complex permittivity and permeability of the composite.

Reference

1. D.Y.Kim, Y.C.Chung, T.W.Kang and H.C.Kim, IEEE Transactions on Magnetics, **32**. No.2 (1996)
2. Mingzhong Wu,Huahul He,Zhensheng Zhao and Xi Yao J.Phy. D.Appl.Phys.**33** (2000)2398.
3. Hyung Do Choi,Hwan Woo Shim, Kwang Yun Cho, Hyuk Jae Lee, Journal of Applied Polymer Science, **72**, (1999) 75.
4. John L. Wallace, IEE Transactions on Magnetics, **29** No.6 (1993)
5. Morihiko Matsumoto and Yoshimori Miyata, IEEE Transactions on Magnetics, **33** No.6 (Nov 1997)
6. Renachao Che, Yongqing Li, Zhaohui Chen, Hongji Lin, J. Materials Science Letters **18** (1999) 1963.
7. Praveen Sing, T C Goel, Indian Journal of Pure and Applied Physics **3** (March 2000)213.
8. Yoshimori Miyata and Morihiko Matsumoto IEEE Transactions on Magnetics, **33**. No.5, (Sept.1997).
9. J.Y. Shin and J.H.Oh, IEEE Transactions on Magnetics, **29**, No.5, (Sept.1993)
10. K.A Malini, E.M. Mohammed, S.Sindhu, P. Kurian, M.R. Anantharaman, Plastics, Rubber and Composites **31** No.10 (2002) 449.
11. Y. Naito and K. Suetaki, IEEE Transactions, Microwave theory. Tech, **MTT- 19**. (Jan 1971) 65.
12. Choi,H.D. Kim,W.S.Joon,T.H.Polymer(Korea) **21**(1997), 112.
13. Nedkov, I.Petkov A and Karpov V, IEEE Transactions on Magnetics **26** (1990)1483.
14. C A Grimes and D M Grimes - journal of applied physics **69**, no. 8. (April 1990) 6186.

Cobalt ferrite ($CoFe_2O_4$) is a spinel and is usually assume to have a collinear ferrimagnetic structure [19]. This spinel was observed to be partially inverse with formula $(Co_xFe_{1-x})[Co_{1-x}Fe_{1+x}O_4]$, where the round and square bracket indicates A and B sites, respectively. The ratio Fe(A)/Fe(B), has been found to vary from 0.61±0.04 to 0.87±0.04 for two extremes [20-21]. Several authors using, large applied fields, have found that the saturation magnetisation of $CoFe_2O_4$ nano particles diminishes rapidly with decreasing particle size [16,19]. Such a phenomenon has been interpreted consistently with the help of Mossbauer spectroscopy conducted on small $CoFe_2O_4$ particles [16,19] and it has been found that a non collinear arrangement possibly at or near the surface of $CoFe_2O_4$ particles. A non collinear structure has been found near the surface for various materials in the fine particles such as $NiFe_2O_4$, γ-Fe_2O_3 and CrO_2 [17-18].

Coercivity of magnetic particles also has a striking dependence on their size. As the particle size decreases, the coercivity increases and reaches a maximum and then decreases This change in coercivity is attributed to the change from multidomain structure to singledomain structure [22].

Nano particles of cobalt ferrites and cobalt containing iron oxides are potential materials for isotropic permanent magnets, magnetic recording and magnetic fluids [23-24]. Cobalt ferrite thin films are of great interest for magneto- optical recording because of their large faraday rotation in the spectral range of 700-800 nano meter and their good chemical stabilities [25-27]

The electrical properties of cobalt ferrites were studied in plenty [28-30]. Ferrites which have many applications ranging from microwave frequencies to radio frequencies are very good dielectrical materials. The electrical properties of ferrites are dependent upon several factors namely

method of preparation, grain size, chemical composition etc [31-33]. The conduction mechanism in ferrites is quite different from that in semiconductors. In ferrites the temperature dependence of mobility affects the conductivity and the carrier concentration is almost unaffected by temperature variation [34,35] The ferrites behave as inhomogeneous dielectric materials in which individual high conducting grains are separated by low conducting layers [36-38]. For microwave applications, materials with high resistivity with low dielectric losses are favoured [39-41]. The study of electric properties of ferrites produces valuable information regarding the behaviour of localized electric charge carriers leading to a grater understanding of the mechanism of dielectric polarisation of the ferrites [42-43]. In this chapter, $CoFe_2O_4$ is prepared in the nanoregime with varying particle dimensions. The magnetic and dielectric properties are evaluated and correlated.

7.2. Structural Studies of Cobalt Ferrites

Cobalt ferrites of varying grain sizes were prepared and structural characterisation of all the samples were carried out by the X-ray diffraction (XRD) technique. The details of the preparation and the characterisation were described in chapter-II.

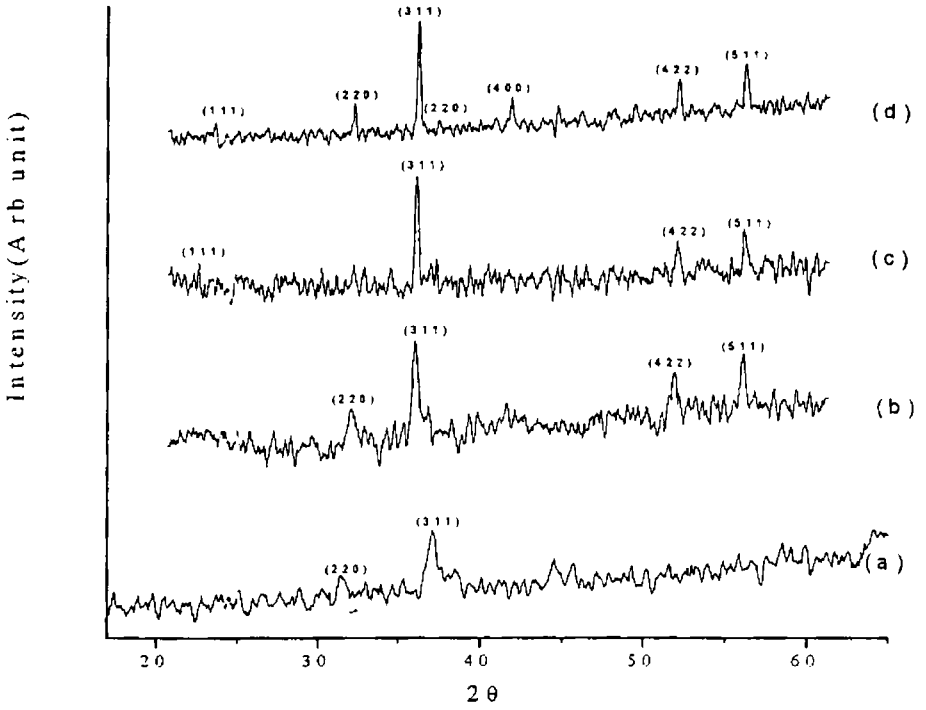

Fig.7.1: X-ray diffraction pattern of the (a) prepared $CoFe_2O_4$ powder, (b) the $CoFe_2O_4$ powder heated at 300°C, (c) at 600°C and (d) at 900°C

Fig7.1. shows the X-Ray diffraction pattern of the four samples of $CoFe_2O_4$ powders synthesized by the sol-gel technique The X-ray pattern of the samples shown in fig.7.1 can be ascribed to spinel $CoFe_2O_4$. A sharp increase in the crystalline nature of the cobalt ferrite powders was observed as the firing temperature was increased which is recorded as a decrease in the broadening of the peaks in the diffraction pattern. This clearly shows that the grain size has increased with increase in firing temperature. The grain size of the four samples, heated at different temperatures was evaluated by employing Debye-Scherer formula and as shown in table. 7.1.

Table.7. 1

Structural parameters of $CoFe_2O_4$

Firing Temperature (°C)	Particle Size (nm)	Specific surface area (m^2/gm)	Theoretical Density (gm/cc)	Experimental Density (gm/cc)	Porosity (%)
As prepared powder	19.2	72.3	5.19	4.32	16.76
300	27.6	49.4	5.20	4.44	14.6
600	38.4	31.81	5.24	4.91	6.2
900	59.4	19.8	5.28	5.08	3.9

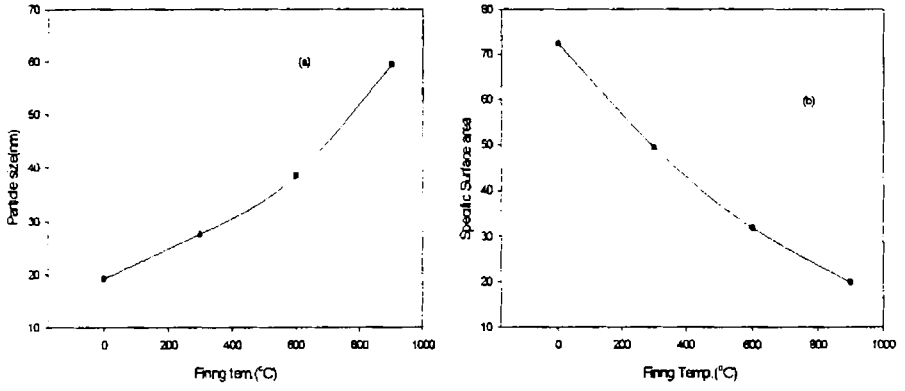

Fig.7.2 (a) Dependence of particle size

(b) specific surface area with firing temperature.

Fig.7.2 (a) shows the variation of particle size with firing temperature for all the four samples. From the figure it is clear that the grain size increases with increase of firing temperature. From fig.7.2.b, it is revealed that the specific surface area of the particle decreases with increase in firing temperature of the samples indicating the increase of the size of the grains.

Fig.7.3 represents the variation of porosity of the samples with firing temperature. Similar to nickel ferrite samples, the porosity decreases with increase in firing temperature.

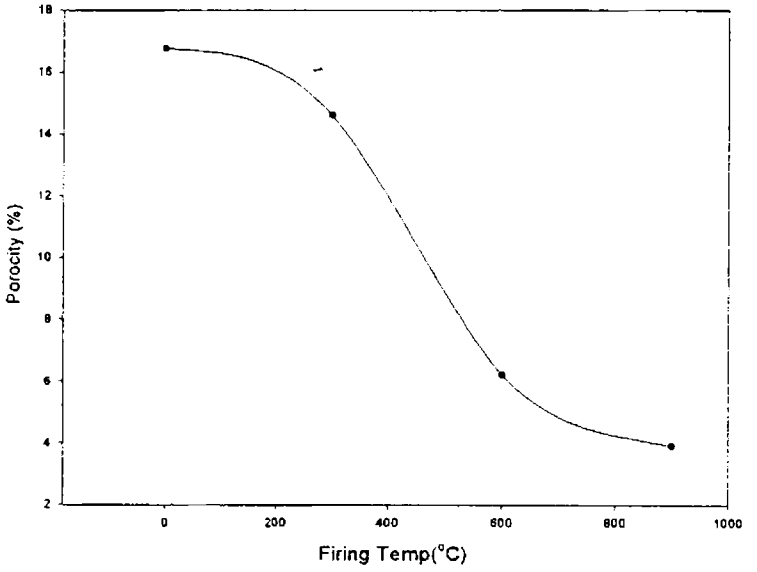

Figure7.3: Variation of porosity with firing temperature for the sol-gel synthesized $CoFe_2O_4$ powders

The sample fired at 900°C posses more than 96% of the theoretical density of the samples.

7.3.Magnetic Properties of Cobalt Ferrites

Magnetic measurements were carried out using a Vibrating Sample Magnetometer (EG & G PAR 4500) for all the four samples at room temperature. The magnetic properties like saturation magnetization and coercivity were elucidated from the hysteresis curve. Fig.7.4. shows the hysteresis curve for the $CoFe_2O_4$ nanoparticles measured at room temperature.

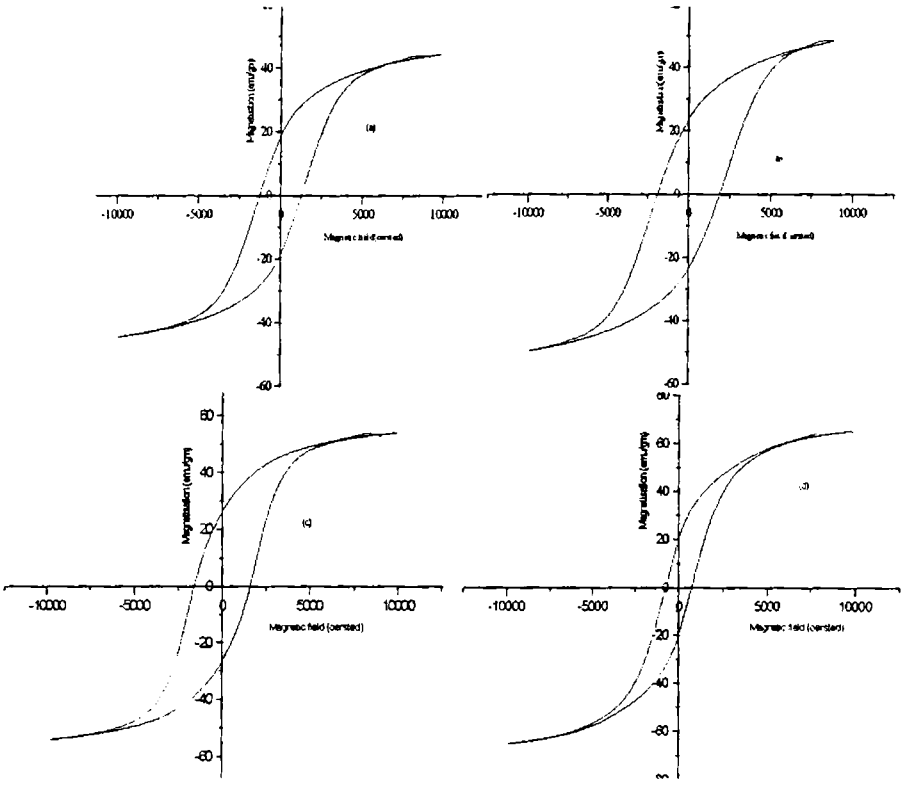

Fig.7.4. Hysteresis curve for the sol-gel synthesized (a) as prepared $CoFe_2O_4$ powder (b) $CoFe_2O_4$ powder heat treated at 300°C (c) 600°C and (d) 900°C

Fig.7.5 (a) gives the variation of saturation magnetisation with particle size of the cobalt ferrites. Similar to nanoparticles of nickel ferrite (chapter 3), the saturation magnetisation of fine particles of cobalt ferrite decreases as the grain size of the particles decreases. The linear decrease in saturation magnetization was accompanied by an increase in specific surface area as shown in fig.7.5 (b)

Table7. 2 Magnetic parameters of $CoFe_2O_4$ samples

Firing Temp.°C	Particle Size (nm)	Saturation Magnetisation (emu/g)	Coercivity (Oersted)
0	19.2	44.3	1289
300	27.6	49.5	1915
600	38.4	54.1	1588
900	59.4	65.1	730

This reduction in magnetisation can be thought to be due to the presence of a nonmagnetic dead layer of thickness 6Å [44]. But Haneda and Morrish [12,18] had shown by Mössbauer experiments that there is no dead layer on the surface of the fine particles of cobalt ferrite, which is known to have a relatively a high magneto crystalline anisotropy, but have noncollinear spins and high field effective anisotropy fields in the surface [7,18,45].

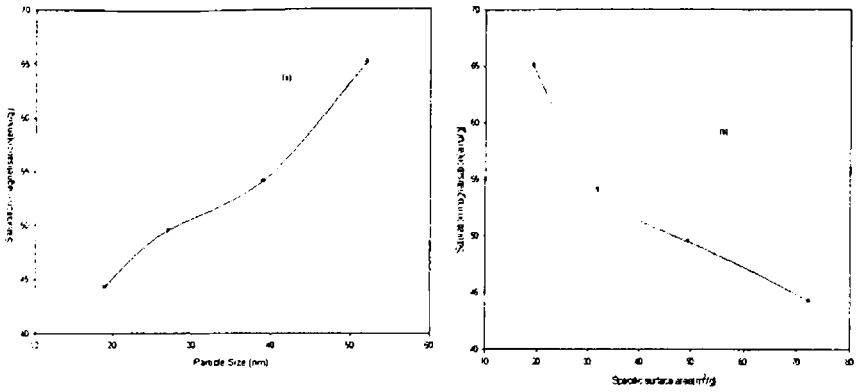

Fig.7.5. Variation of saturation magnetisation with (a) particle size (b) specific surface area of cobalt ferrite samples.

Cobalt ferrite is usually assumed to have a collinear ferrimagnetic structure. In the usual structural model, the magnetization of tetrahedral (A) sublattice is antiparallel to that of octahedral (B) sublattice and the structure is collinear. However ultrafine cobalt ferrite have non-collinear magnetic structure in the surface layer [18]. The fine particles of cobalt ferrite consists of a core with the collinear spin arrangement and the surface layer with magnetic moment inclined to the direction of magnetisation [45]. As increasing this specific surface area owing to the decreasing particle size, causes an increase in the proportion of non-collinear magnetic structure, in which magnetic moments are not aligned with the direction of external magnetic field. $CoFe_2O_4$ particles heat treated at 900^0C exhibited an M_s of 65 emu/gm. Applying Neels theory it has been estimated that $CoFe_2O_4$ exhibits an M_s of 60 emu/gm and the reported value is 74 emu/gm.

Fig.7.6. shows the variation of coercivity with average grain size of the cobalt ferrite at room temperature. It is evident from the graph that as the particle size increases, the value of coercivity increases, reaches a maximum value and then decreases. This variation of H_c with particle size can be explained on the basis of domain structure, critical diameter and the anisotropy of the crystal [38-40].

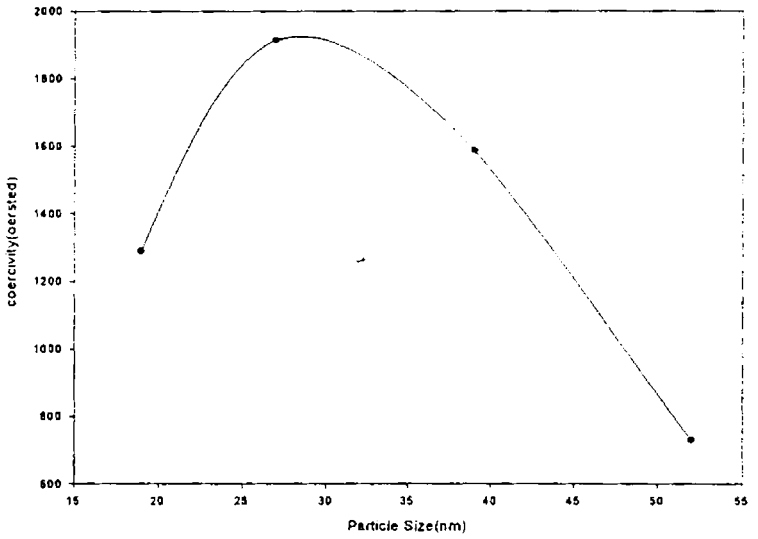

Fig.7.6. Variation of coercivity with particle size of cobalt ferrite.

Coercivity of magnetic samples has a striking dependence on their size. As the particle size decreases, the coercivity increases and reaches a maximum and then decreases. The change in coercivity is attributed to its change from the multi domain nature to the single domain. In the multi domain region the variation of coercivity with particle size is expressed as [22],

$$H_c = a + \frac{b}{D} \qquad 7.1$$

where 'a' and 'b' are constants and 'D' is the diameter of the particle. Hence in the multi domain region the coercivity decreases as the particle diameter increases. Below the critical diameter D_s, the coercivity decreases, because of thermal effects. As the particle size decreases H_c decreases below a critical particle size as governed by the equation

$$H_{ci} = g - \frac{h}{D^{3/2}} \qquad 7.2$$

where 'g' and 'h' are constants A crystal will spontaneously break up into a number of domains in order to reduce the large magnetization energy it would have if it is a single domain. The ratio of the energies before and after division into domains varied as $\sqrt{d}$, where d is the particle diameter. Thus as d, becomes smaller, the reduction in energy becomes smaller and this suggests that for very small d the crystal prefers to remain in the single domain. For cobalt ferrites there is only one magnetic easy axis, which is directed along the hexagonal 'c' axis [46]. So nano particles of cobalt ferrite possess high value of coercivity compared to nano particles of other soft ferrites.

7.4. Electrical Properties of Cobalt Ferrites

The electrical properties of cobalt ferrite samples were carried out by using a homemade cell and an LCR meter HP 4285A. Pellet shaped samples were employed for the evaluation of the electrical properties. The dielectric permittivity (ε_r) of the samples were calculated using the relation

$$\varepsilon_r = \frac{Cd}{\varepsilon_0 A} \qquad 7.3$$

Where 'C' is the measured value of capacitance of the sample, 'd' is the thickness, 'A' is the surface area, and 'ε_0' is the dielectric permittivity of air. From the dielectric loss and dielectric permittivity, ac conductivity of ferrite samples can be evaluated using the relation

$$\sigma_{ac} = 2\pi \varepsilon_0 \varepsilon_r f \tan\delta \qquad 7.4$$

where, f is the frequency of the applied field ε_0 is the absolute permittivity of air , ε_r is the relative permittivity of the samples and tanδ is the loss factor. σ_{ac} is temperature and frequency dependent [46], and it is attributed to the dielectric relaxation caused by localized electric charge carriers which obeys the power law [47].

$$\sigma_{ac}(\omega,T)=B\,\omega^{n} \qquad 7.5$$

where B and n are composition and temperature dependent parameters. The theory and details of the dielectric measurements are explained in ChapterII.

7.5. Frequency dependence of electrical properties

7.5.1. Dielectric permittivity

Fig.7.6. shows the variation of dielectric permittivity with frequency in the range 100kHz to 8MHz.The variation of dielectric constant with frequency reveals that the dispersion is due to Maxwell-Wagner type [37,38] interfacial polarisation in agreement with Koops' phenomenological theory of dielectric dispersion. Koops interpreted the result by considering the dielectric as an inhomogeneous medium of a Maxwell- Wagner type. The high values of ε could be explained on the basis of Maxwell- Wagner theory, which is a result of the inhomogeneous nature of dielectric structure. This dielectric structure is supposed to be composed of two layers [37]. The first layer is the large ferrite grains of fairly well conducting materials, which is separated by the second thin layer (grain boundaries) of relatively poor conducting grains.

The grain boundaries are found to be effective at lower frequencies, while the ferrite grains are more effective at higher frequencies [48,49]. This model thus explains the decrease of permittivity as the frequency increases.

The frequency dispersion relation given by Habery and Wijn as [50,51]

$$\varepsilon(\omega, T) = \left[(1 + x) \frac{\left(\varepsilon_{hf}\, x (x \sigma_{lf}^{2} + \sigma_{hf}^{2}) + \omega^{2} \varepsilon_{0}^{2} \varepsilon_{hf}^{3} (1 + x) \right)}{\left(x^{2} (\sigma_{lf} + \sigma_{hf})^{2} + \omega^{2} \varepsilon_{0}^{2} \varepsilon_{hf}^{2} (1 + x)^{2} \right)} \right] \quad 7.6$$

where $x=d_l/d$. d_l and d are the thickness of the surrounding layer and bulk ferrite grain respectively is also applicable to cobalt ferrite.

The dielectric permittivity decreases with increasing frequency reaching a constant value for all the samples. Similar behaviour was observed earlier for other systems of ferrites.

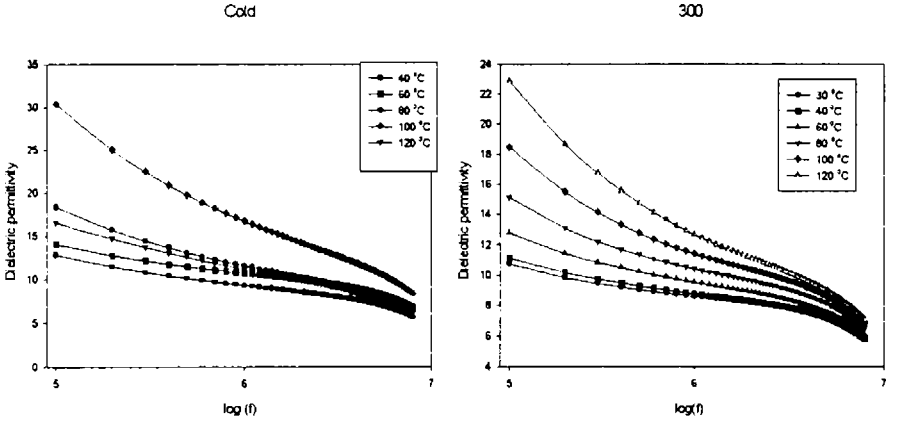

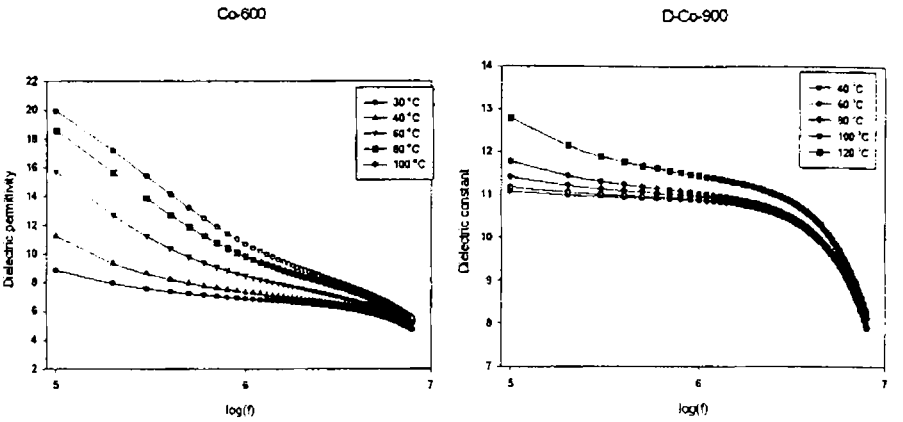

Fig.7.6.Variation of dielectric permittivity with logarithmic frequency

The conduction is due to the exchange between $Fe^{2+} \leftrightarrow Fe^{3+}$ and due to this exchange displacement of electrons is produced in the direction of the applied field. These electrons determine the polarisation in ferrites [48]. The polarisation decreases with increase in frequency and then reaches a constant value due to the fact that, beyond a certain frequency of external field the electronic exchange $Fe^{2+} \leftrightarrow Fe^{3+}$ cannot follow the alternating field.

7.5.2.Ac Conductivity

Fig.7.7. represents the variation of ac conductivity with logarithmic frequency in the frequency range 100kHz to 8MHz.,which is the normal behaviour of ferrites. The ac conductivity shows an increasing trend with increase in frequency for all samples. But at high frequencies the ac conductivity values shows a decreasing trend.

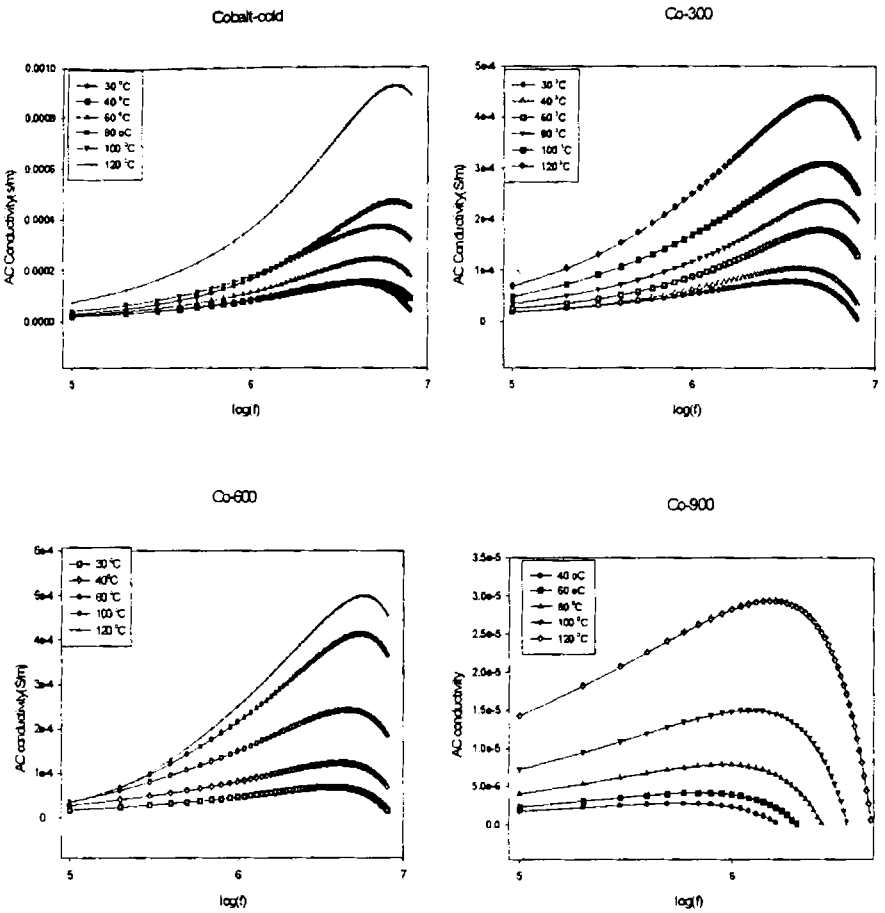

fig.7.7. Variation of ac conductivity with logarithmic frequency

The variation of ac conductivity with frequency also reveals the dispersion due to Maxwell-Wagner type [37,38] interfacial polarisation. As the frequency of the applied filed increases the conductive grains become more active by promoting the hopping between Fe^{2+} and Fe^{3+} ions on octahedral sites, there by increasing the hopping conduction. Thus we observe a gradual increase in conductivity with frequency. But at higher frequencies the frequency of the hopping ions could not follow the applied

field frequency and it lags behind it. This causes a dip in conductivity at higher frequencies.

Jonker [35] studied the electrical conduction of a series of ferrites $Co_{1-x}Fe_{2+x}O_4$ and observed two regions of conductivity. One region was of low conductivity containing Co^{2+} and Co^{3+} ions and other type was of high conductivity containing Fe^{2+} and Fe^{3+} ions. The presence of cobalt on the octahedral site of the spinel favours a conduction mechanism

$$Co^{2+} + Fe^{3+} \leftrightarrow Co^{3+} + Fe^{2+}$$

which explains the predominant conduction mechanism in cobalt ferrite. The presence of impurities can also influence the conductivity of the ferrite [52] Parker studied the electrical conductivity of $NiFe_2O_4$ with a small Co substitution and confirmed the idea of cobalt existing in the ferrite in two valance states [53].

A general relation of the following form explains the variation of conductivity with frequency is

$$(r-r') = \varepsilon''/(\varepsilon' \times \omega) \qquad 7.7$$

Where ε' and ε'' are the real and imaginary parts of the dielectric constant and r and r' are the ac and dc conductivity respectively and ω is the frequency.

7.6. Temperature Dependence of Electrical Properties

7.6.1. Dielectric permittivity

Fig 7.8.shows the variation of dielectric permittivity with temperature. From these figures it can be seen that the dielectric permittivity increases slowly with temperature in the beginning up to about 373K and above this temperature permittivity increases rapidly for all samples. The high dielectric permittivity values at low frequencies found at high temperature

may be explained as due to the presence of permanent dipole moments indicating a small effective charge separation [43]. Such a small separation must be due to asymmetry in the fields experienced by either oxygen or metallic ions. The temperature dependence of permittivity is due to the polarisation effect.

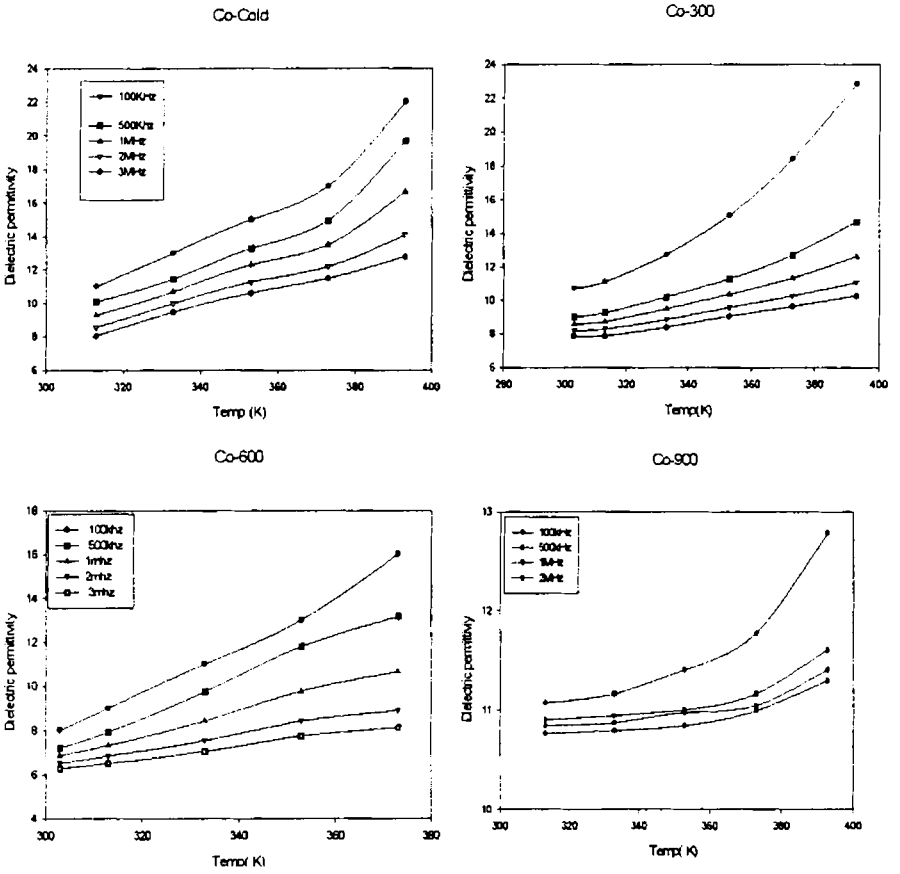

Fig.7.8. Temperature dependence of dielectric permittivity

The space-charge polarisation is governed by the number of space charge carriers. With rise in temperature, the number of carriers increases,

resulting in an enhanced build-up of space charge polarisation and hence an increase in dielectric properties [53]. For the lower frequencies the polarisation is increased by the electric field and also by the increase in the number of charge carriers with increase in temperature. Both effects tend to increase the dielectric permittivity. For the higher frequencies, the electric field will have more effect than temperature. In section 7.4, it is found that conductivity saturates at high frequencies. This means that saturation in the generation of charge carriers was reached at high temperature and at high frequency. Therefore the electronic exchange cannot follow the field variation and hence the dielectric permittivity decreases accordingly. When temperature rises, the orientation of these dipoles is facilitated and this increases the dielectric polarization. But at very high temperature the chaotic thermal oscillations of molecules are intensified and the degree of orderliness of their orientation is diminished and thus the permittivity passes through a maximum value.

7.6.2 Ac Conductivity

The dielectric permittivity and electrical conductivity are basically electrical transport properties and their variation with temperature is similar. It may be assumed that the same mechanism is responsible for both the phenomena. Hence the mechanism of dielectric polarisation is similar to that of conduction process.

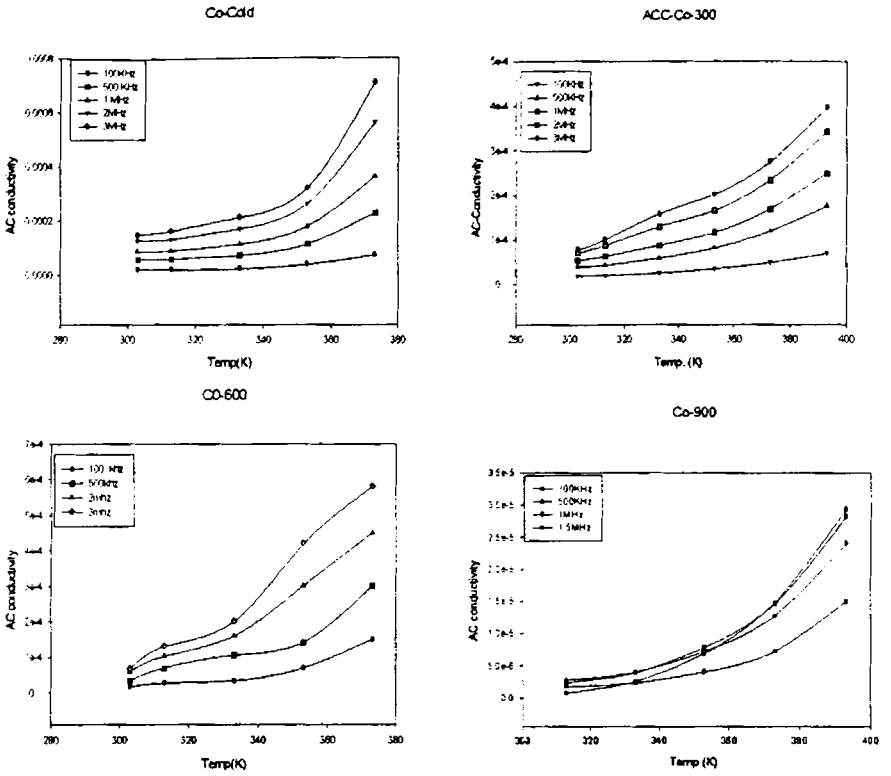

Fig.7.9.Temperature dependence of ac conductivity

The increase in the electrical conductivity with increase in temperature attributed to increase in drift mobility of the thermally activated charge carriers according to hopping conduction mechanism. Increasing temperature thermally activates the electron exchange between Fe^{2+} and Fe^{3+} ions on the octahedral sites. This electron causes local displacements in the direction of the applied electric field; this includes the dielectric polarisation in ferrites. As the increase in temperature the ac conductivity increases due to the increase in the drift mobility of the thermally activated electrons [47,48]. Similar results were observed for other system of ferrites.

7.7.Grain size dependence of electrical properties

The grain size, grain boundaries, porosity and stochiometry are imported factors influences the conductivity and permittivity. It has been reported [60,61] that the resistivity of a polycrystalline material in general increases with decreasing grain size. Smaller grains imply larger number of insulating grain boundaries which acts as a barriers to the flow of electrons. Smaller grains also imply smaller grain- grain surface contact area and therefore a reduced electron flow. As expected, the increase grain size with increase in temperature. Based on the above arguments the resistivity of the ferrites is expected to decrease with increase in sintering temperature or the increase in grain size. However, a reverse trend is observed the present work for sintering the samples upto 900^{0}C. The comparatively lower value of resistivity or higher value of permittivity in samples sintered at lower temperatures are possibly due to the presence of localised stage in the forbidden energy gap which arises due to lattice imperfections. The presence of this states effectively lowers the energy barriers to the flow of electrons.

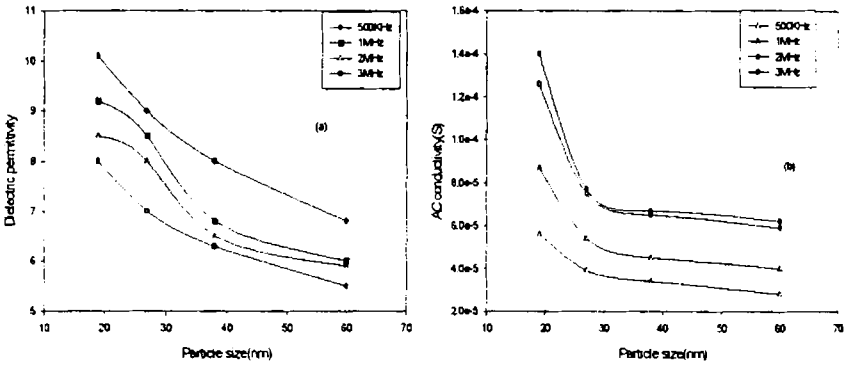

Fig.7.10.Grain size dependence of (a) dielectric permittivity (b) ac conductivity

According to the correlated barrier hopping model [62] predicts an ac conductivity as

$$\sigma(\omega)=\frac{\pi^3}{24} N^2 \varepsilon \; R_\omega^6 \omega \qquad 7.8$$

where, N is the concentration of defect sites contributing to the hopping mechanism, ε, the dielectric permittivity and R_ω the hopping distance. Increase in sintering temperature can increase the structural improvement. Increasing sintering temperature results in more uniform crystal structures with reduced imperfections there by decrease the value of N, which ultimately reduced the value of ac conductivity. Hence samples fired at high temperature or samples with greater grain size possesses low value of conductivity. The above discussion suggests that the effect of structure has an influence, which is more significant than that of the anticipated effect of grain size. A similar trend in conductivity was reported by Van Uitert [39], who also explain it in terms of increased homogeneity and structural perfection with increase in sintering temperature. Since the dielectric permittivity is directly proportional with square root of conductivity, the variation of permittivity with grain size is similar.

7.8.Conclusion

Nanoparticles of cobalt ferrite were prepared by sol-gel method. By heating the sample at subsequent temperatures, cobalt ferrites of various grain sizes were obtained. The structural characterisation of the samples were conducted by the X-ray diffraction technique. The XRD studies showed that the $CoFe_2O_4$ prepared exists in the inverse spinel structure and the X-ray data agrees well with the reported data. The magnetic studies carried out using Vibration Sample Magnetometer showed that the specific saturation magnetization (σ_s) of the nanosized $CoFe_2O_4$ decreased with

decrease in particle size. This reduction in magnetisation was explained in terms of noncollinear spins and high field effective anisotropy fields on the surface of the fine particles of cobalt ferrite. As the particle size of cobalt ferrite decreases, the coercivity is found to increase, attain a maximum value and then decreases. This change in coercivity is attributed to its transition from the multi domain nature to the single domain. The electrical parameters namely dielectric permittivity and ac conductivity were evaluated for all the samples and studied as a function of frequency, temperature and size of the particles. The dependence of both dielectric permittivity and the ac conductivity on frequency is in good agreement with Koops phenomenological theory of dielectrical dispersion. Both ac conductivity and dielectric permittivity shows an increasing trend with increasing temperature. The high dielectric permittivitiy at high temperature was explained as due to the presence of permanent dipole moments indicating a small effective charge separation. The enhancement of electric properties with decreasing particle size was explained on the basics of the correlated barrier-hopping model.

Reference

1. Magnetic properties of fine particles, edited by J.Ldorman and D.fiorani (North Holland, Amsterdam 1992)
2. C.Kittel, Phys.Rev.70, 965(1946).
3. .L.S.Jacobs and C.P.Bean, in Magnetism, edited by, G.T.Rado and H.Suhl(academic press, New york, 1963), Vol.III, Chapter 6.
4. E.M.Chundnovsky and L.Gunther, Phys. Rev. Lett.**60**, 661 (1988).
5. L.Gunther, Physics World, December 1990, 28-346.
6. R.G.L Aurdran and A.P.Huguenard, U.S Patent 4 302523, (1981).
7. R.F.Ziolo, U.S. Patent 4 474866 (1984).
8. R.E.Rosenweig, ferrohydrdynamics (MIT Press, Cambridge, 1985)
9. .R.D.McMichael, R.D.Shull,, L.J.Swartzendruder,L.H. Bennett and R.E.Watso, J, Magnetism and Magnetic materials, III, 29 (1992)
10. A.E.Berkowitz, W.J.Shuele, and P.J.Flanders, J. Appl Phys, **39**, (1968) 1261
11. J.MD.Coey, Phys.Rev.Lett.**27**, (1971) 1140
12. A.H.Morrish, K.Hanada, and P.J.Schurer J.Phys.C **37**, (1976) 6
13. T.Okada, H.Sekizawa, F.Ambe and T.Yamada, J.Magnetism and Magnetic materials **105** (1983) 31
14. F.T.Parker, M.W.Foster D.T.margulies, and A.E Berkowitz, Phy. Rev. B **47**, (1993) 78
15. S.Linderoth, P.V.Hendriksen, F.Bodker, S.Wells,K.Davis,S.W.Charles and S.Morup, J.applied Physics, 75, (1994) 6583
16. D.Lin, A.C.Numes, C.F. Majkrzak, and A.E.Berkowitz, J Magnetism and Magnetic materials **145**, (1995) 343
17. A.H.Morrish and K.Hanida. J. applied Physics **52**, (1981) 2496
18. R.H.Kodama, A.E.Berkowitz, E.J.McNiff. Jr. and S.Foner, Phys. Rev. Lett.77, (1996)394.
19. K.Haneda A.H.Morrish ,J.Appl.Phys.63(8).(1988).
20. G.A.Sawatzky,F.vander Woude and A.H.Morrish J.Appl.Phys.**39**, (1968) 1204
21. G.A.Sawatzky F.vander Woude and A.H.Morrish Phys.Rev.**187** (1969) 747

22. B.D.Cullity,*Introduction to Magnetic Materials* Addison-Weiseley Publishing Company,Inc(1972).
23. A Trestman-Matts, S.E.Dorris, S.Kumarakrishman, T.O.Mason, J. American Ceramic Society. **66** (1983) 829.
24. H.Mohan, L.A.Saikh, R.G.Kulkarni, Solid state communication **82** (1992) 907.
25. R.K.Ahrenkiel, T.J.Coburl, I.E.E.E. Trans. Mag.**11** (1975) 110
26. J.W.D.Martens, W.L.Peters, H.M.Van Noort, M.Errman J. Physics Chem. Solids **46** (1985) 411.
27. K.Suzuki. T.Namikava. T.Yamazaki, J. Applied physics **27** (1988) 361
28. A.D.D.Broemme, IEEE Transactions Elect. Insulation **26** (1991) 49.
29. C.Constantin, M.Rosenberg, Solid state communications **9** (1971) 675.
30. B.AGriffiths, D.Elwell, R.Parker, Phisos. Mag.**22** (1970) 163.
31. P.V.Reddy, R.Sathyanarayana, T.S.Rao, Phys. Stat. Sol (a) **78** (1983) 109.
32. .A.Verma, T.C.Goyal, R.G.Mindiretta, R.G.Gupta, Journal of Magnetism and Magnetic materials **192** (1999) 271.
33. M.A.El Hiti, Journal of Magnetism and Magnetic materials **164** (1996) 187.
34. Ferrite Materials, Science and Technology, Narosa Publishing House. New Delhi
35. G.H.Jonker;J.Phys.Chem.Solids **9** (1959) 165
36. I.C.Maxvell,ElectricityandMagnetism,.**1**,Oxford. Univ Press, Newyork. (1973)
37. K.W.Wagner,Amer.Phis.**40**(1973)317.
38. C.G.Koops.Phys. Rev **83**(1951)121.
39. Y. Naito and K. Suetaki. " Application of ferrite to electromagnetic wave absorber and its charecoristics , " *IEEE transactions, Microwave Theory*, Tech, volume **MTT- 19**. (Jan 197)165
40. H M Musal. Jr. and HT Hahn, *IEEE Transactions On Magnetics*, **25** no 5 , (Sept 1989) 3851
41. C A Grimes and D M Grimes - *journal of applied physics* **69**, no. 8 (April 1990) 6186.
42. Ahamed M.A and Elhiti (1995) Journal de Physique III **5** 775.
43. Shaikh.A.M, Bellard S.S and Chougule B.K. Journal of Magnetism and

Magnetic Materials **195** (1999) 384

44. M.Zheng, X.C. Wu, B.S. Zou and Y.J. Wang, *J. Magn.& Magn. Mater.*, , **183**, (1998)152.
45. R.H.Kodama, A.E.Berkowitz, Phys. Rev .B volume **59**. (1999) 6321
46. P.V.Reddy,R.Sathyanarayana,T.S.Rao,Phys.Stat.Sol.(a) **78** (1983)109
47. A.M.Abdeen,J. of Magnetism and Magneticm aterials **185**(1998)199
48. L.T.Rabinkin,Z.I.Novikora.Ferrites, Izv.Acad.Nauk,USSR,Minsk (1960)146
49. A.M.Shaikh,S.S.Bellad,B.K.Chougule,Journal of Magnitic Materials **195** (1999)384
50. F.Haberey and H.P.J.wus,phys.stat.sol. **26**. (1968) 231
51. .N.Saxena,B.K.Kunar Z.H.Zaidi and G.P.Srivastava,phys.stat.sol.(a) **127**, (1991) 231
52. O.S.Josyulu and J.Sobhanadri,phys.stat.sol(a) **59**, (1980) 323
53. Parker.D.Elewell,J.appl.Phys. **17** (1966) 1269
54. .S A Mazen,F Metawe and S F Mansouur, J.Phys.D:Appl.Phys. **30**(1997) 1799.
55. .M.A.El Hiti, J.Phys.D: Appl.Phys. **29** (1996) 501.
56. M.A.El Hiti,Phase Trans. **54**(1995)117.
57. M.A..El Hiti,M.K.El Nimr,M.A.Ahmed.Phase Trans.(1995)137.
58. M.M.Mosaad,M.A.Ahamed,J.Magn.Mater.**150**(1995)51.
59. W.D. Kingery, H.K.Bowen, D.R. Uhlmann, Introduction to Ceramics, Wiley, NiwYork, (1975).904.
60. G.C.Kuezynski,N.A.Hooton, C.F.Gibbon,Sintering and Related Phenomenon,Gordon and Breach,NewYork,(1967).65.
61. L.G.VanUitert,J.Chim.Phys. **23**(10)(1955)1883
62. M.Pal, P.Brahma and D.Chakravorthy, Journal of Physical Society of Japan, **63**,Nov.9,(Sept,1994).3356.

Chapter-VIII

Structural, Magnetic and Electrical Properties of $Li_{0.5}Fe_{2.5}O_4$

8.1.Introduction

Magnetic nanoparticles continue to be a fascinating of subject of interest both from the fundamental and application point of view[1]. Their properties at the nanolevel are quite different from their coarser sized cousins and they exhibit altogether different magnetic and electrical properties [2-9].

Lithium ferrites ($Li_{0.5}Fe_{2.5}O_4$) are useful materials for microwave device and memory core applications [10-13]. Lithium ferrite crystallise in the inverse spinel structure. Though lithium ferrites have been a thoroughly investigated ferrite system [13,14], because of their excellent square sloop characteristics, these system is being revisited to investigate the finite size effects as well as to device new materials based on lithium ferrite for microwave and other applications. Synthesis of structurally stabilised lithium ferrite with and with out flux are still a hot topic of research in the area of magnetic materials.

Magnetic saturation, coercivity, magnetization and loss, change drastically as the size of the particles move down into the nanometre range [15-26]. As the particle size of $Li_{0.5}Fe_{2.5}O_4$ decreases the coercivity increases and reaches a maximum and then decreases. This change in coercivity is attributed to the transition from multidomain to single domain structure. Reduction in saturation magnetisation has been observed in magnetic nano particles especially in ferrites and has been related, alternatively, to surface anisotropy, surface spin disorder, or finite size effects. But the fine particles of $Li_{0.5}Fe_{2.5}O_4$ show an anomalous variation of magnetisation.

Chapter 8

Lithium ferrite is a high resistivity, low mobility semiconductor that has low eddy-current losses [27,28]. The electrical properties of ferrites are dependent upon several factors namely method of preparation, grain size, chemical composition, sintering temperature and atmosphere [29-32]. The wider use of lithium ferrites particularly in microwave devices was restricted due to the difficulties experienced in sintering the material at the high temperatures employed to achieve high densities in stoichiometric form. The irreversible loss of lithium and oxygen during sintering was the main cause that made lithium ferrites technologically difficult to prepare. Sol-gel method provides an easy method for the preparation of nano $Li_{0.5}Fe_{2.5}O_4$ at low temperature. Lithium ferrite has been prepared by sol-gel method and it heat treated to change the particle dimensions. Their magnetic and electrical properties have been studied wit ha view to correlate the properties. So the details of the findings are enlisted in this chapter.

8.2.Structural Studies of Lithium Ferrites

Lithium ferrites of varying grain sizes were prepared and structural characterisation of all these samples were carried out by the X-ray diffraction (XRD) technique. The details of the preparation and the characterisation are discussed in chapter II.

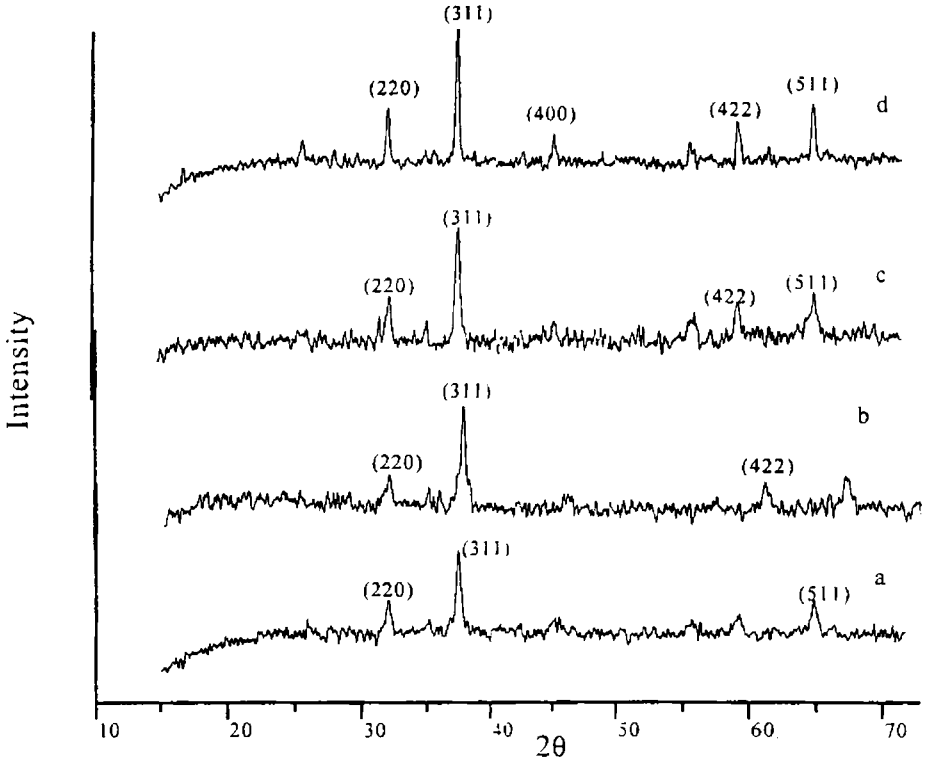

Fig.8.1: X-ray diffraction pattern of the (a) as prepared $Li_{0.5}Fe_{2.5}O_4$ powder, (b) the $Li_{0.5}Fe_{2.5}O_4$ powder heated at 300°C, (c) at 600°C and (d) 900°C

Fig.8.1.shows the X-ray diffractogram of lithium ferrites sintered at various temperatures. As the sintering temperature increases the width of the central maxima decreases and the intensity of the peaks increases. This is due to the increase of grain size of the ferrite particles as the firing temperature increases .The grain sizes of the samples were evaluated by measuring the FWHM. The specific surface area was calculated from the relation $S = 6000/d_g\rho$ and the porosity was calculated from the observed and

theoretical density for all the four samples. The results are shown in table 8.1.

Table.8.1

Structural parameters of sol-gel synthesized $Li_{0.5}Fe_{2.5}O_4$

Firing Temperature (^oC)	Particle Size (nm)	Specific surface area (m^2/gm)	Theoretical Density (gm/cc)	Experi-mental Density (gm/cc)	Porosity (%)
As prepared powder	11.8	162.83	4.68	3.12	33.7
300	14.2	111.94	4.70	3.8	18.8
600	21.6	66.13	4.73	4.2	11.2
900	32.3	42.02	4.74	4.42	6.5

Fig 8.2a.represents the variation of grain size with firing temperature. From the graph it can be noticed that grain size is increased upon firing. The change is more prominent at high temperature. The specific surface area of the particles increases as the particle size decreases. The variation pattern shown in Fig.8.2.b.

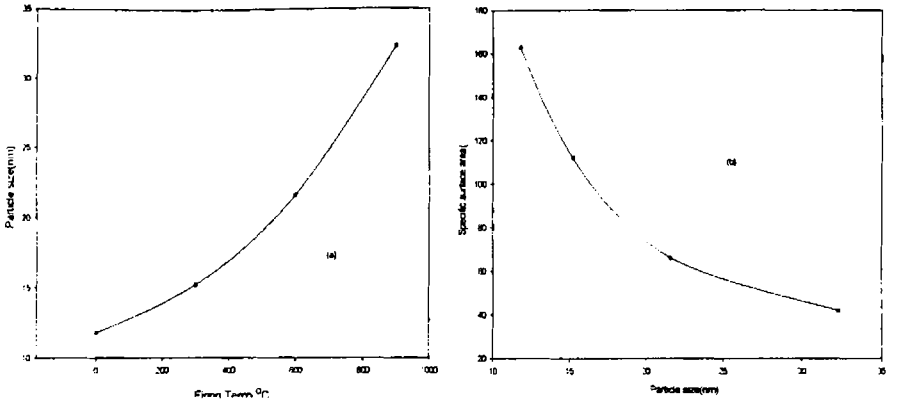

Fig.8.2 Variation of particle size with. (a) firing Temp.
(b) specific surface area for $Li_{0.5}Fe_{2.5}O_4$

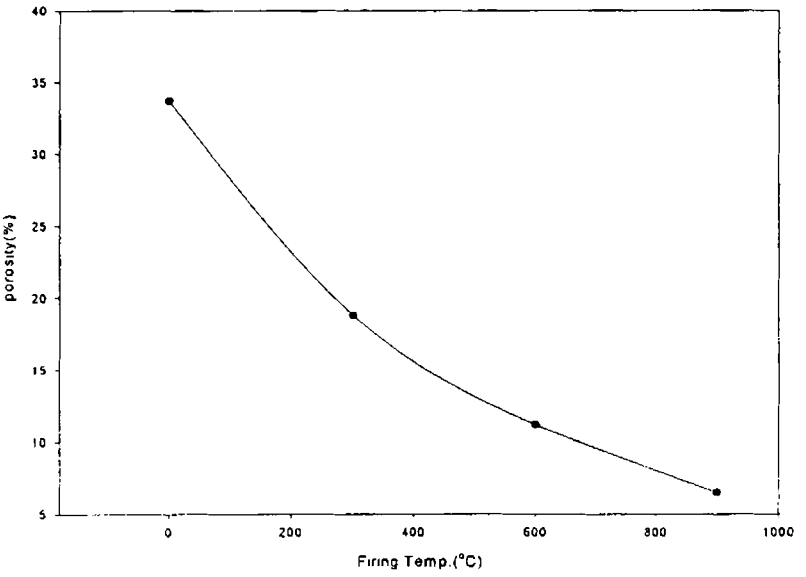

Fig.8.3.Variation of porosity with firing temperature. for $Li_{0.5}Fe_{2.5}O_4$

The variation of porosity of the samples with firing temperature is shown in fig.8.3.The as prepared sol-gel samples is 34% porous and the

samples sintered at 900°C exhibited a porosity of 6.5%. This indicates that high temperature sintering is necessary to achieve maximum density for lithium ferrite.

8.3.Magnetic Properties of Lithium Ferrites

Magnetic measurements were carried out using a Vibrating Sample Magnetometer (EG & G PAR 4500) for lithium ferrite powder at room temperature. The details of measurements are cited in chapter II. Fig.8.4. shows the hysteresis curve for the $Li_{0.5}Fe_{2.5}O_4$ particles measured at room temperature.

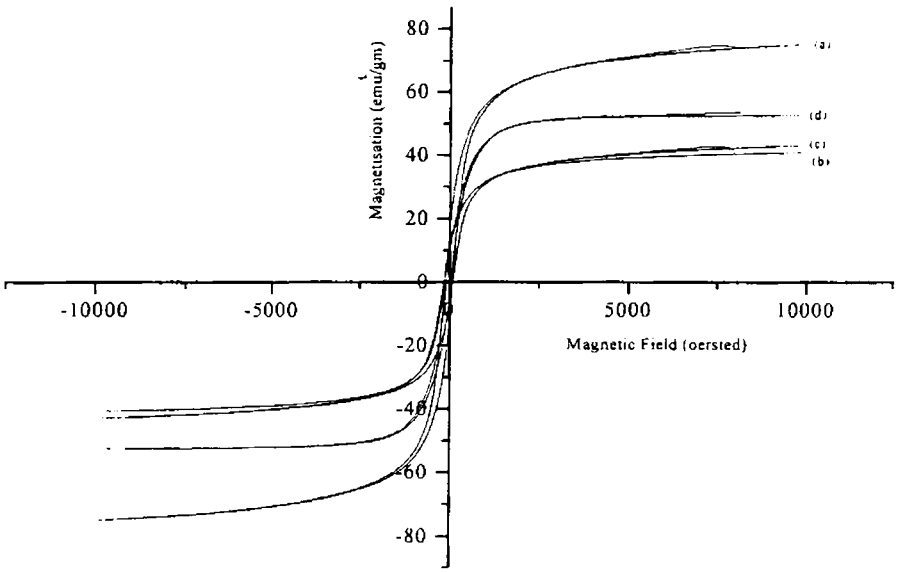

Fig.8.4 Hysteresis curve for the sol-gel synthesized (a) as prepared $Li_{0.5}Fe_{2.5}O_4$ powder (b) $Li_{0.5}Fe_{2.5}O_4$ powder heat treated at 300°C (c) 600°C and (d) 900°C

Parameters like saturation magnetisation and coercivity were elucidated from the hysteresis graph and are tabulated in table 8.2.

Table8. 2 Magnetic parameters of $Li_{0.5}Fe_{2.5}O_4$ samples

Firing Temp.°C	Particle Size (nm)	Saturation Magnetisation (emu/g)	Coercivity (oersted)
0	11.8	75	90
300	15.2	42.8	114.5
600	21.6	40.8	163
900	32.3	52.5	56.6

Fig.8.5. and 8.6 represents the variation of saturation magnetisation with firing temperature and grain size of the lithium ferrite samples sintered at various temperatures.

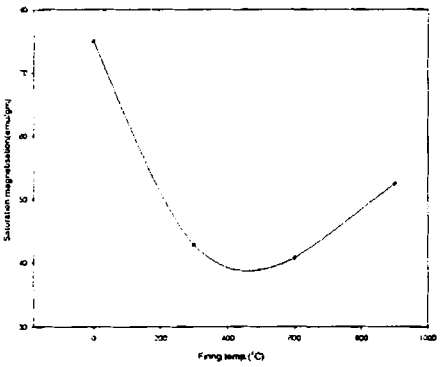

Fig.8.5.

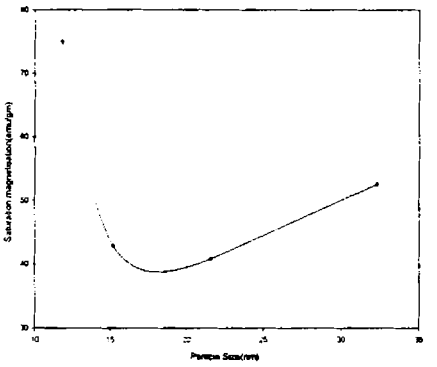

Fig.8.6.

The as prepared sample of lithium ferrite shows a maximum saturation magnetisation of 75 emu/g. The magnetisation of the sample sintered at 300°C drops to 42.8emu/gm and sample sintered at 600°C has a saturation magnetisation of 40.8 emu/g. Further firing at 900°C increases the magnetisation. This is due to the volatization of lithium and oxygen .The

loss of Li_2O results in the formation of α-Fe_2O_3 and their by reducing the saturation magnetisation. From the XRD, it seems that the peak of α-Fe_2O_3 is enhanced in 300°C and much prominent for the sample fired at 600°C.Furtaer firing, diminishes the peak of α-Fe_2O_3.This confirms the volatization and the formation of α-Fe_2O_3. α-Fe_2O_3 being antiferromagnetic, the its presence reduces the value of saturation magnetisation.

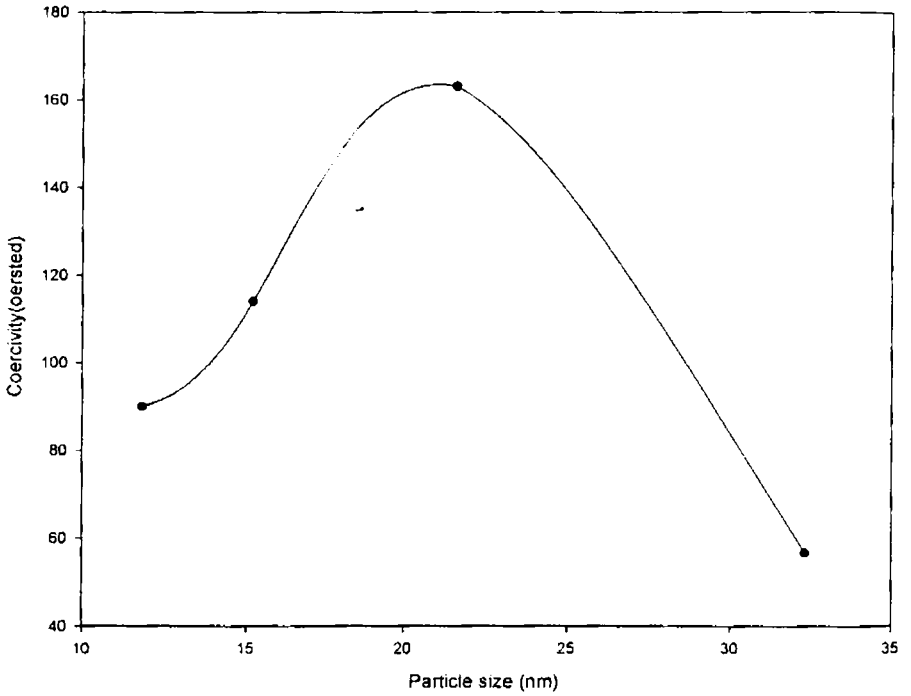

Fig.8.7.Variation of coercivity with particle size of $Li_{0.5}Fe_{2.5}O_4$

Fig.8.7.represents the dependence of coercivity on grain size of the particles. To reduce the magnetisation energy, small grains will prefer single domain structure and large grains prefer multi domain nature. As the particle

size decreases the coercivity increases, reaches a maximum and then decreases. This change in coercivity is attributed to its change from the multi domain to the single domain nature. In the multi domain region the variation of coercivity with particle size is expressed as $H_c = a + b/D$ [15], where 'a' and 'b' are constants and 'D' is the diameter of the particle. Hence in the multi domain region the coercivity decreases as the particle diameter increases. In the single domain region the coercivity decreases, because of thermal effects. As the particle size decreases H_c decreases below a critical particle size as governed by the equation $H_{ci} = g - h/D^{3/2}$

8.4.Electrical Properties of Lithium Ferrites

The theory and experimental details employed for the evaluation of parameters namely, dielectric permittivity and ac conductivity are dealt in detail in chapter II. The dielectric permittivity (ε_r) of the pellet shaped samples were calculated using the relation

$$\varepsilon_r = \frac{Cd}{\varepsilon_0 A}, \qquad 8.1$$

Where 'C' is the measured value of capacitance of the sample, 'd' is the thickness, 'A' is the surface area, and 'ε_o' is the dielectric permittivity of air. From the dielectric loss and dielectric permittivity, ac conductivity of ferrite samples was evaluated using the relation

$$\sigma_{ac} = 2\pi f \tan\delta \ \varepsilon_0 \varepsilon_r \qquad 8.2$$

f is the frequency of the applied field ε_0 is the absolute permittivity of air , ε_r is the relative permittivity of the samples and tanδ is the loss factor. σ_{ac} is temperature and frequency dependent [33]and it is attributed to the dielectric relaxation caused by localized electric charge carriers which obeys the power law [34]

$$\sigma_{ac}(\omega,T)=B\,\omega^{n} \qquad 8.3$$

where B and n are composition and temperature dependent parameters respectively.

8.5.Frequency dependence of electrical properties

8.5.1.Dielectric permittivity

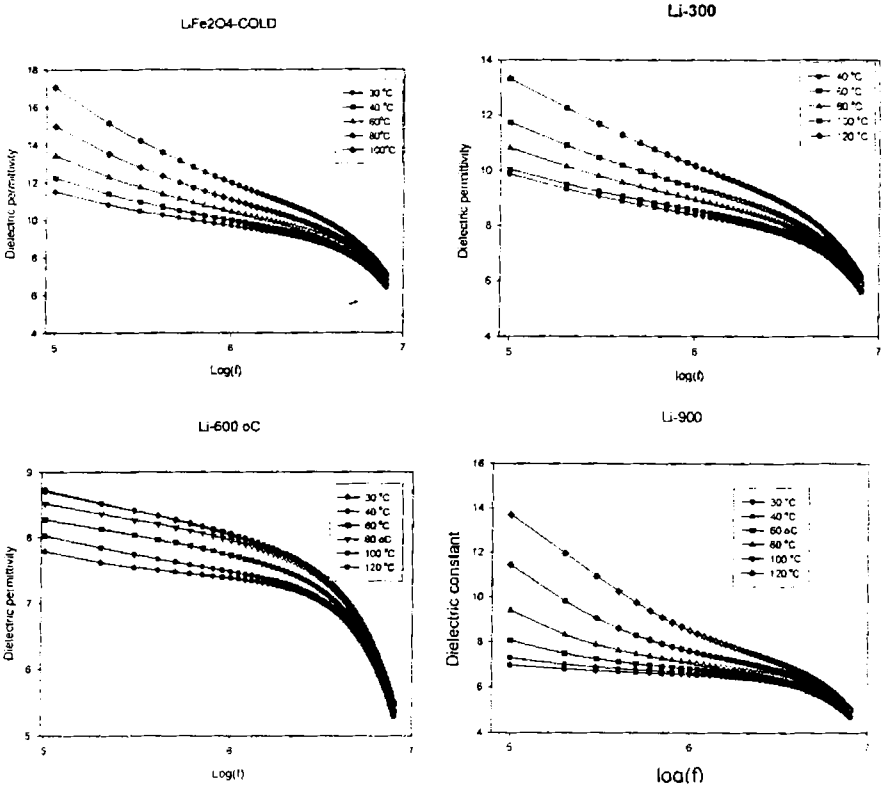

Fig.8.8.Variation of dielectric permittivity with logarithmic frequency

The frequency dependence of the dielectric permittivity for all the samples were studied at various temperatures.Fig.8.8.shows the variation of permittivity with frequency. Dielectric permittivity deceases as frequency

increases from 100KHz to 8MHz.The decrease is rapid at lower frequencies and slower at higher frequencies. Similar results were observed for other system of ferrites [35-39]. The decrease in permittivity with frequency can be explained on the basis of Koops theory [40],which considers the dielectric structure as an inhomogeneous medium of two layers of Maxwell-Wagner type [41].

In this model, the dielectric structure is imagined to consists of well-conducting grains which are separated by poorly conducting grain boundaries. It was found for ferrites that the permittivity is directly proportional to the square root of conductivity [38].Therefore the grains have higher values of conductivity and permittivity, while the grain boundaries have lower values. At lower frequencies the grain boundaries are more effective than grains in electrical conduction, therefore permittivity is high at lower frequencies and decreases as frequency increases. The decrease in permittivity takes place when the jumping frequency of electric charge carriers cannot follow the alternation of applied ac electric field beyond a certain critical frequency.

8.5.2.ac conductivity

Fig.8.9.represents the variation of ac conductivity with logarithmic frequency in the frequency range 100KHz to 8MHz. The ac conductivity shows an increasing trend with increase in frequency for all the samples. But at higher frequencies the ac conductivity tends to have a decreasing trend.

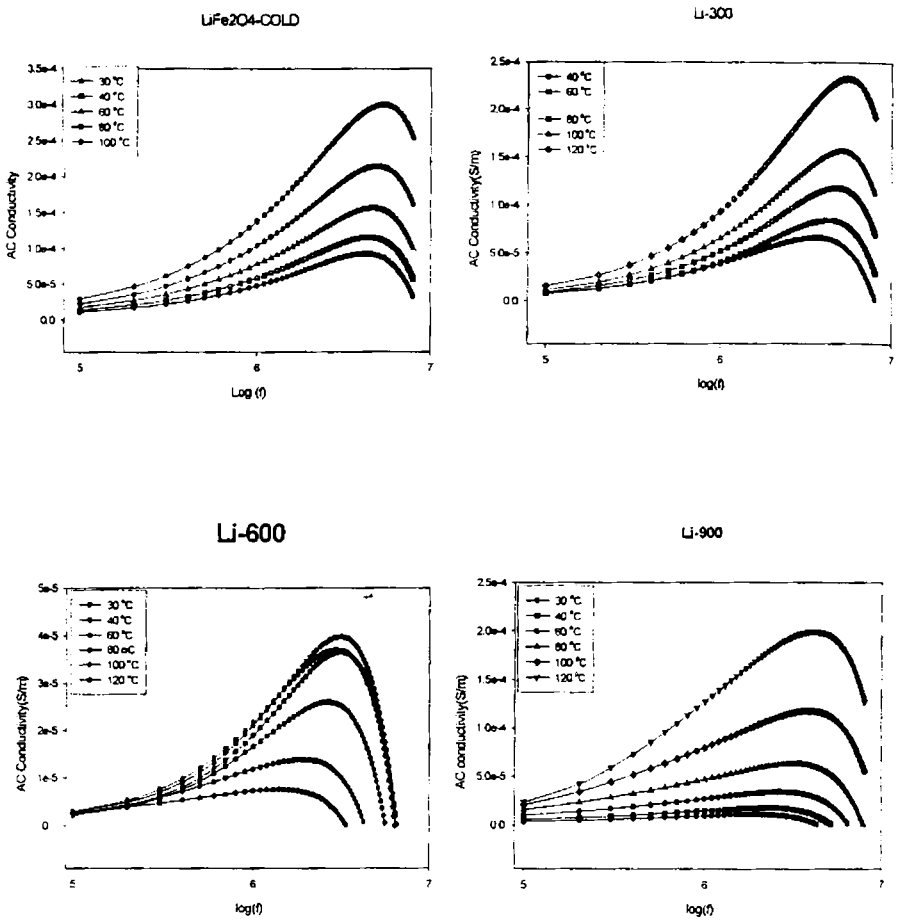

Fig.8.9.Variation of ac conductivity with logarithmic frequency

This behaviour can be akin to the Maxwell-Wagner type. The dielectric structure of ferrites is given by Koops Phenomenological theory and Maxell-Wagner theory. At lower frequencies the grain boundaries are more active and hence hopping of Fe^{2+} and Fe^{3+} ion is less at lower frequencies. As the frequency of the applied field increases, the conductive grains become more active by promoting the hopping between Fe^{2+} and Fe^{3+}

ions, there by increasing the hopping conduction. A gradual increase in conductivity was observed with frequency. But at higher frequencies the frequency of the hopping ions could not follow the applied field frequency and it lags behind it. This causes a dip in conductivity at higher frequencies. According to the power law the logarithmic relation between the ac conductivity and the angular frequency represents straight lines with slopes equal to the exponent n and intercept equal to log ω on the vertical axis at log ω=0. Various researchers [33,34] have found that at temperature $>T_c$ the conductivity is dependant on frequency. Here it must be noted that the templates employed here for studying the variation are much below T_c.

8.6.Temperature dependence of Electrical properties

8.6.1.Dielectric permittivity

Fig.8.10. shows the variation of permittivity with temperature. From these figures it is observed that the dielectric permittivity increases slowly with temperature in the low temperature region up to 373K and above this temperature, permittivity increases rapidly and sharply for all samples.

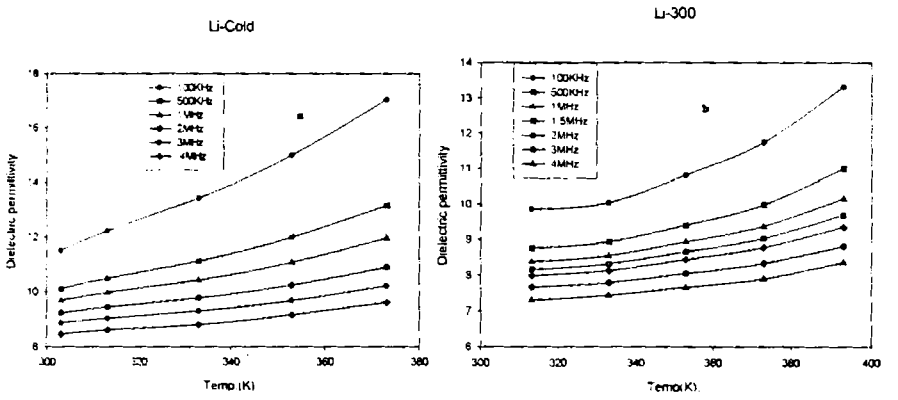

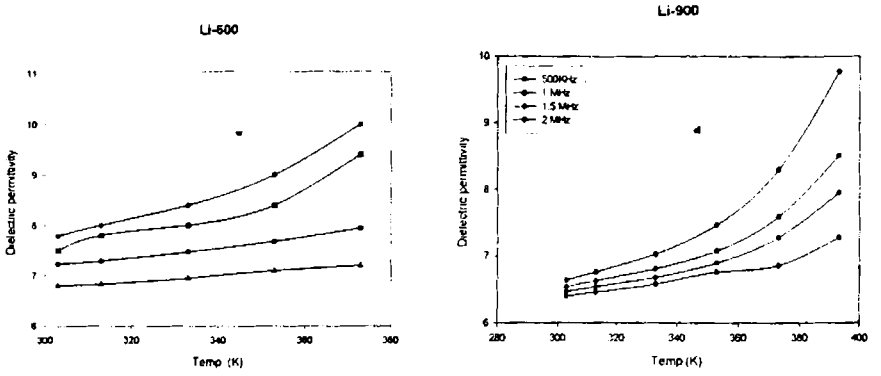

Fig.8.10 (a-d). Temperature dependence of dielectric permittivity

The resistivity of ferrites decreases with increase in temperature because ferrites were considered as magnetic semiconductors. According to Koops, the dielectric permittivity is inversely proportional to the square root of resistivity. Therefore increase in dielectric permittivity with temperature is expected. The high dielectric permittivity at low frequencies and high temperature is due to the presence of permanent dipole moments indicating a small effective charge separation [37,38]. This small separation must be due to asymmetry in the fields experienced by either oxygen or metallic ions. In most cases, the atoms or molecules in the samples cannot orient themselves at low temperature region. When temperature rises, the orientation of these dipoles is facilitated and this increases the dielectric polarization At very high temperatures the chaotic thermal oscillations of molecules are intensified and the permittivity passes through a maximum value.

At lower frequencies, an equation of the form $\varepsilon=\varepsilon_0+A \exp(BT)$ where ε and ε_0 are the dielectric permittivity at temperature T and 0K and A and B are constants . This relation holds good only at lower frequencies. For

higher frequencies, variation in ε is nominal since the dipoles are not free to orient at a higher frequency and hence the orientation polarization will be less at higher frequencies. Thus the total increase in polarisation will be less with the rise in temperature at higher frequencies. This explains the changes in dielectric constant with temperature at higher frequencies.

8.6.2.ac conductivity

The variation of ac conductivity with temperature of $Li_{0.5}Fe_{2.5}O_4$samples is shown in fig.8.11. It was observed that at higher temperature the conductivity is higher and as the temperature is decreased the conductivity also decreases but a marked difference is found in this variation at low and high frequencies. At low frequencies the ac conductivity increases with increase in temperature while at higher frequencies the conductivity increases sharply up to a certain temperature and thereafter the rate of change increases significantly with the increase in temperature. The conductivity increases with increase in frequency at all temperatures, but at lower temperatures this difference is not much prominent. The increase in the electrical conductivity with increase in temperature attributed to increase in drift mobility of the thermally activated charge carriers according to hopping conduction mechanism. Increasing temperature thermally activates the electron exchange between Fe^{2-} and Fe^{3+} ions on the octahedral sites. This electron causes local displacements in the direction of the applied electric field; this includes the dielectric polarisation in ferrites.

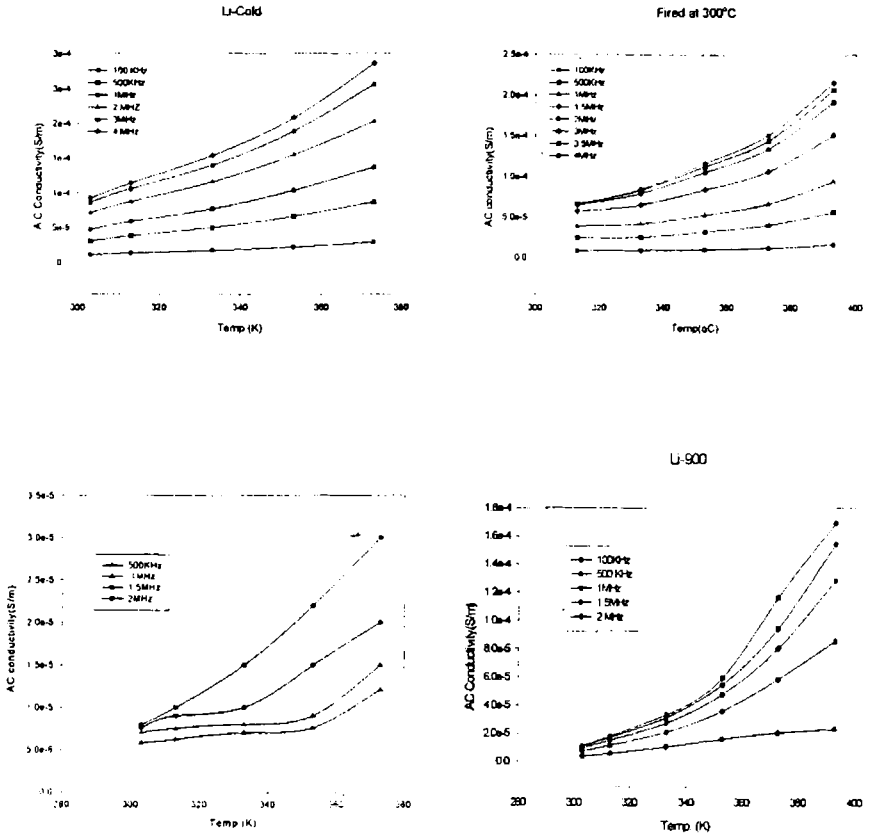

Fig.811.Variation of AC conductivity with temperature

As temperature increases, ac conductivity increases due to the increase in drift mobility of the thermally activated electrons [30,35]. Also the space charge polarisation is caused by the number of space charge carriers. With the rise in temperature the number of carriers increases resulting in an enhanced build-up of space charge polarization and hence increases the conductivity. Above Curie temperature the term n in power law becomes equal to zero because the power law becomes invalid and the

conductivity is frequency independent or dc conductivity. Therefore, n decreases as temperature increases. So the electrical conduction becomes frequency dependent for $0 < n < 1$.

8.7.Grain size dependence of electrical properties

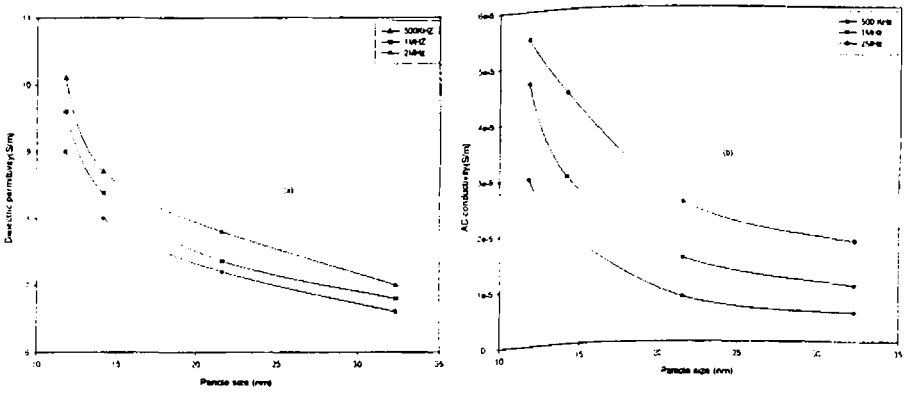

Fig.8.7. Particle size dependence of (a) Dielectric permittivity (b) Ac conductivity

The grain size, grain boundaries, porosity, and sintering temperature are important factors influencing the conductivity and permittivity. Both dielectric permittivity and ac conductivity decreases as the grain size of the ferrite particles increases. The comparatively lower value of resistivity or higher value of permittivity in samples sintered at lower temperatures are possibly due to the presence of localised stage in the forbidden energy gap which arises due to lattice imperfections. The presence of this states effectively lowers the energy barriers to the flow of electrons.

According to the correlated barrier hopping model [42,43] ac conductivity

$$\sigma(\omega)=\frac{\pi^3}{24} N^2 \varepsilon \; R_\omega{}^6 \omega \qquad 8.4$$

Where, N is the concentration of defect sites contributing to the hopping mechanism, ε, the dielectric permittivity and R_{ij} the hopping distance. Increasing sintering temperature results in more uniform crystal structures with reduced imperfections there by decreasing the value of N, which ultimately reduces the value of ac conductivity. Hence samples fired at high temperature or samples with greater grain size possess low value of conductivity. A similar trend in conductivity and permittivity was reported by Van Uitert [44], who also explained it in terms of increased homogenity and structural perfection with increase in sintering temperature.

Conclusion

Ultrafine particles of lithium ferrites were prepared by sol-gel method. The X Ray diffraction studies reveal that, even samples prepared at low temperature are almost in phase and sintering at higher temperature enhances the purity of the sample. Porosity of the samples decreases upon firing and the samples fired at 900^0C attains 95% of the theoretical density. Magnetisation measurements show that anomalous magnetic behaviour was shown by the ferrites. Unlike nickel ferrite and cobalt ferrite, magnetisation decreases initially with sintering and then increases. The coercivity increases with size of the grains, reaches a maximum and then decreases. This behaviour is similar to other system of ultrafine particles and which is due to the transition from single domain to multi domain structure. The electrical parameters namely dielectric permittivity and ac conductivity were evaluated for all the samples and studied as a function of frequency, temperature and size of the particles. The dependence of both dielectric permittivity and the ac conductivity with frequency is in good agreement with Koops phenomenological theory of dielectrical dispersion.

Reference

1. J.L.Dorman,D.Fiorani,Magnetic Properties of fine Particles, North Holland, Amsterdam, 1992.
2. F.Soffge, E.Schmidbauer, J.Magn.Magn.Mater.,**24,**(1981),54.
3. M.El-Hilo.R.W.Chantrell,K.O Grady,J.Appl.Phys., **84.**(1998),5114.
4. A.E.Berkowitz, R.H.Kodama, S.A.Makhlouf, F.T.Parker. J. Magn. Magn. Mater., **196,** (1999) 591.
5. F.Bentivegna, J.Ferre, M.Nyvlt, J.P.Jamet, D.Inhoff, M.Canava, A.Brun, P.Veillet, S.Visnovsky, J.Appl.Phys.**83,**(1998),7776.
6. I.Hrianaca, C.Caizer, S.Savil, M.Popovoci, J. Adv. Matr.,**2,**(2000),634.
7. I.Hrianaca,I.Malaescu, J.Magn.Magn.Mater.**150,** (1995),131
8. I.S.Jacobs, C.P.Bean, Magnetism III, Academic Press. New York, 1963, 271.
9. C.Caizer, Solid State Communications, **124**, (2002),53
10. Watanabe A. Yamamura H,Moriyoshi and Sharkskin. 1981, Ferrites: Proc. Int.Conf. TAP, (Sept-Oct1980) ,170.
11. Gill N Kand Puri R K, J.Mater.Sci.Lett.**4,** (1985), 396
12. Reddy PV,.Reddy M B, Muley V N and Ramana Y V. J.Mater. Sci. Lett.7 , (1988), 1243.
13. N.Saxena, B K Kunar, Z H Zaidi and G P Srivastva, Phys Stat. Sol A. **127** (1991) .231
14. G.O White and C.E Patton J.Magn.Magn.Mater.**9**, (1978), 299.
15. B.D.Cullity, Introduction to Magnetic Materials Addison-Weiseley Publishing Company, Inc (1972).
16. A.H.Morrish and K.Hanida. J. Applied Physics, **52,** (1981), 2496
17. R.H.Kodama, A.E.Berkowitz, E.J.McNiff. Jr. and S.Foner, Phys. Rev. Lett.77. (1996), 394
18. K.Haneda, A.H.Morrish, J.Appl.Phys.63, (1988), 8
19. I.M.L. Billas, A.Chatelain, W.A. de Heer. Science, **265.** (1994), 1682.
20. D.D. Awschalom. D.P.D. Vincenzo, Physics Today, April. **43,** (1995),.21.
21. J.Shi, S.Gider, K.Babcock, D.D.Awschalom, Science. (1996), **271**, 937
22. R.E.Rosenweig, Ferrohydrdynamics MIT Press, Cambridge, 1985
23. R.D.McMichael, R.D.Shull,, L.J.Swartzendruder,L.H. Bennett and R.E.Watso, J, Magnetism and Magnetic Materials, **29,** (1992),111

24. A.E.Berkowitz, W.J.Shuele and P.J.Flanders, J. App. Phys., **39**,1261 (1968)
25. J.MD.Coey, Phys.Rev.Lett.**27**, (1971), 1140
26. A.H.Morrish, K.Hanada, and P.J.Schurer J.Phys.C **37**, (1976). 6
27. D.H.Ridgley, H. Lensoff and H.D. Childress, Journal of . American .Ceramic .Soc.**53,** (1970),304.
28. S A Mazen, F Metawe ,S F Mansour, J. Phys.D.Appl.Phys.**30,** (1997) ,1799
29. P.V.Reddy, R.Sathyanarayana, T.S.Rao, Phys. Stat. Sol (A) , **78,** (1983),109.
30. A.Verma, T.C.Goyal, R.G.Mindiretta, R.G.Gupta, Journal of Magnetism and Magnetic Materials, **192,** (1999), 271.
31. M.A.El Hiti, J. of Magnetism and Magnetic Materials ,**164,** (1996) 187
32. G.Banopadhya and R.M.Fulrath, J. Am. Cer. Soc, **57**, (1974), 483,
33. M.A.El Hiti, J. Magnetism and Magnetic Materials, **164,** (1996), 187.
34. A.M.Abdeen, J. Magnetism and Magnetic Materials, **185**, (1998), 199
35. P.V.Reddy, R.Sathyanarayana, T.S.Rao, Phys.Stat.Sol.(A),**78,** (1983), 109
36. B.K.Kunar, G.S.Srivastava, J.Appl.Phys., **70,** (1994), 6115.
37. Ahamed M.A and Elhiti , Journal de Physique III, (1995) 5 775.
38. Shaikh.A.M, Bellard S.S and Chougule B.K. Journal. Magnetic . Magnetic . Mat. **195,** (1999) ,384.
39. Ahamed M.A and Elhiti, E.I.Nimar and Amar M.A . Journal of Magnetism and Magnetic Materials ,**152,** (1996) 391
40. C.G.Koops, Phys. Rev **83**,(1951), 121
41. K.W.Wagner, Amer, Phys. **40,** (1973),317.
42. W.D. Kingery, H.K.Bowen, D.R. Uhlmann, Introduction to Ceramics, Wiley, New York, 1975, 904.
43. Pals M, Brahma P and Chakravarthy D, Journal of Physical Society Jap. **63 No.9** (1994) 3356-3360.
44. L.G.VanUitert, J.Chim.Phys.**23,** (10), (1955), 1883.

Chapter IX

Summary and Conclusion

In the realm of magnetism and magnetic materials, ferrites and derivatives of ferrites continue to occupy a prominent position. Enormous, / vast and extensive investigations have been carried out beginning from the foundations laid by Smit and Wijn, Snoek and various other researchers. Ever since the propounding of the theory of super exchange interaction, ferrites have been a hot candidate for studying ferrimagnetism and other related phenomenon. The formulation of Neel's two sublattice theory made it easier for engineers/ chemists and physicists alike to synthesize various combination of these ferrites and thus tailor the properties for various applications led to many devices based on ferrites for various applications ranging from rudimentary devices like permanent magnets/magnetic separators to the present day sophisticated gadgets like spin valve transistors. Devices based on ferrites outsmarted various other devices based on iron, permalloy. This was possible because of the high resistivity and low eddy current losses exhibited by these materials aided by high permeability and excellent high frequency characteristics.

Earlier investigations on ferrites, especially, on the modification/ manipulation of properties, were based on the structure-property relation. That is, there exist a close relation between the composition and structure with the electric and magnetic properties of ferrites. Many factors like the cationic charge, size, the lattice energy, and cation distribution determine the overall properties of these materials.

Most of the bulk/microscopic/macroscopic properties were explained based on the grain boundaries, grain sizes, which were all in the micron regime. This was because, in earlier days the attempt to synthesize ferrites were all by ceramic techniques. Towards the fag end of the 20^{th} century, to be precise, in the earlier 90's, an explosive amount of investigations begun in the area of nanomaterials and this spread like wild fire. Thus a great deal of work on nanomagnetic materials have also been carried out by various researchers. Conventional ceramic technique was soon replaced by novel methods like sol-gel, reverse micelle methods, aerogel, gas based condensation etc.

Various phenomena like spin polarised tunnelling, quantum magnetisation, super Paramagnetism and, single domain characteristics have become common and day to day jargons. These phenomena gave rise to new theories and speculations in the area of condensed matter physics and gave birth to a new area called soft condensed matter physics. One of the important manifestations of these phenomena is the finite size effects on various properties of magnetic materials. Delving in depth into the finite size effect on the electrical and magnetic properties of spinel ferrites may provide answers to various unanswered questions. This is significant from the fundamental point of view to study the physics of interacting particles, noninteracting particles, surface spins, grain boundary effects, spin glass behaviour and superparamagnetism. A clear understanding of these phenomena will lead to the making of new devices, which will replace the old ones or remove obsolescence. The tasks undertaken in this particular investigation encompass only miniscule of the above problems and its related effects.

Three typical ferrites belonging to the inverse spinel category have been chosen in this study. They have been synthesized by sol-gel technique and further heat treated to produce various particle sizes. This was done with a view to studying the finite size effects of some inverse spinels and studies of composites based on nitrile rubber. Nickel ferrite was chosen because it crystallises in the inverse spinel structure unlike zinc ferrite, which crystallises in the normal spinel structure. Investigations conducted on these ferrites earlier in the Magnetics lab indicated that there is anomaly in the magnetic properties and needed a thorough investigation. Various controversies prevail especially with respect to various hypothesis put forwarded to explain the anomaly in the magnetic properties of normal and inverse spinels. It has been thought that a dead layer theory exists, which is thought to be responsible for the reduced magnetisation exhibited by ultrafine particles. Other hypothesis like cation redistribution, spin glass behaviour and core-shell model also exist and have been invoked at various places to explain the anomalous magnetisation. The present investigations carried out as a part of the thesis clearly indicate that in the case of nickel ferrites, in the ultrafine regime, anomaly cannot be because of the existence of dead layer, it could be only because of noncollinear structure existed at the surface. The observed decrease in magnetisation with decreasing particle size has been explained based on this.

In the case of nickel ferrites and cobalt ferrites, the magnetisation decreases with decreasing particle size. In the case of lithium ferrites, the magnetisation decreases initially with increasing particle size and then increases. This is an anomaly in 'anomaly'. It may be noted that lithium ferrite possessing a particle size of 10 nm exhibited a saturation magnetisation value of 75 emu/g while cobalt ferrite and nickel ferrite

possess 65 emu/g and 45 emu/g respectively. This anomaly could be because of the appearance of αFe_2O_3 and vitalisation of lithium ions. The variation of coercivity for all the three system were studied in order to determine the critical particle size at which the particle transform from multidomain to single domain. It has been found that for cobalt ferrite, the critical particle size is around 40 nm, for nickel ferrite, it is around 15 nm and for lithium ferrite, it is around 20 nm. Normally in the ultrafine regime the coercivity exhibited by fine particles are very low. However in applications involving nano dimensions, cobalt ferrite having a very large coercivity can be employed. Here in the present study, cobalt ferrite in the ultra fine regime possesses a coercivity of 1588 Oe, which is high enough for any application at high frequency.

The evaluation of permittivity at various temperatures throws light especially on spin polarised tunnelling with in grains and gives information about hopping between different ionic states of the cations in the ferrite. The dielectric permittivity of all these powder samples in the nanoregime was evaluated and the effect of grain size on the permittivity has been correlated. It has been found that in all the three systems namely nickel ferrite, lithium ferrite and cobalt ferrite, the dielectric permittivity increases consistently with decrease of particle size. Typical value of around 14 was found for nickel ferrite and 10 for cobalt ferrite and 9 for lithium ferrite at a high frequency of 8 MHz. Ac conductivity of all the samples is also studied as a function of frequency, temperature and particle size. Nickel ferrite and cobalt ferrite did not exhibit any marked dispersion, while lithium ferrites exhibited a dispersion.

Microwave absorbers based on ferrites can be prepared by incorporating high frequency ferrites in various rubber matrixes. The rubber

ferrite composites consisting of various loadings of the filler for various particle sizes are prepared according to a specific recipe. For applications, mouldability and processability are essential requirements and these have been evaluated by determining the cure characteristics. It has been found that composites based on nitrile rubber have negligible aging effects and are processable and mouldable with the added advantages like oil resistance and stability. The dielectric permittivity of these composites also have been evaluated and it has been found that the permittivity is dependent on the volume fraction of the filler and also a function of particle size of the incorporated filler. At low frequency upto 8 MHz, a semi empirical relation of the form

$$\varepsilon^* = \frac{\varepsilon_1 \varepsilon_2}{\varepsilon_1 y_2 + \varepsilon_2 y_1}$$

was employed to model the dielectric permittivity for various loadings. These composites were tested upto a temperature of 393K and found to be very stable.

In applications involving microwave absorption at high frequencies, the evaluation of dielectric permittivity and magnetic permeability in the X band (8-12 GHz) is estimated in order to model microwave absorbers and to determine the bandwidth of absorption. This is based on eth surface impedance equation

$$Z = \sqrt{\frac{\mu_r}{\varepsilon_r}} \tanh \left[j \frac{2\pi}{\lambda} \sqrt{\mu_r \varepsilon_r}\, t \right],$$

With this objective in mind, the dielectric permittivity of RFCs in the frequency range 8-12 GHz was determined. Both real and imaginary components of the permittivity was determined and their variations with

respect to frequency, loading and particle size were found out. These values could be fitted to an existing model based on Bergmann's relationship which is of the form

$$\varepsilon_c = \frac{\varepsilon_m\{1 - 2V_f \frac{(\varepsilon_m - \varepsilon_f)}{(2\varepsilon_m + \varepsilon_f)}\}}{\{1 + V_f \frac{(\varepsilon_m - \varepsilon_f)}{(2\varepsilon_m + \varepsilon_f)}\}}$$

The fitted values are in good conformity with the observed values. The evaluation of tanδ for all eth composites in various loadings indicates that there are absorption maxima at around 9 GHz and 11.2 GHz, which is an indication of the bandwidth of absorption. However it must be mentioned here that the inability to evaluate the magnetic permeability of these composites at these frequencies due to instrument limitations were one of the handicaps in utilising the surface impedance equation for modelling an absorber having a minimum thickness.

Scope exists to undertake a thorough study to synthesise composites with active fillers like carbon black. The incorporation of carbon black along with the magnetic fillers of appropriate grain sizes could well enhances the bandwidth of absorption. Stealth application necessitates thin coatings. So emulsions based on ferrites, carbon black and rubber latex can be prepared and tested for microwave absorption.

Application of composites demand good mechanical properties. In our study on RFCs, the various parameters like tensile strength, modulus at different percentage and elongations at break were estimated. It has been found that fine particles in nitrile matrix are reinforcing in nature. The absence of crystallite sites in nitrile rubber and high porosity of fine particles

is an ideal combination in enhancing the mechanical properties and also in tuning the properties in general.

Most of the envisaged objectives have been fulfilled to a certain extent. There is always scope for further studies, improvement and innovation. Though the anomaly observed in the magnetic properties could be explained satisfactorily, conclusive evidence for specific system are necessary. This is an area, which is wide and open.

Perhaps, targets of fine particles of nickel ferrite, cobalt ferrite, lithium ferrites with and without impurity could be synthesised. Thin films could be grown on substrates using RF sputtering or pulse laser deposition technique. A systematic study on these films will surely throw more light on the surface properties exhibited by these materials in the thinfilms form. This will be another good proposition from the physics point of view and also from the application point of view. This is because magneto-optical devices or magneto-optical sensors could be prepared based on these films. Recent observations in systems like lithium ferrites have been revisited because of potential applications in microwave regime. If phase pure, and structure stabilised lithium ferrite with and with out flux like bismuth can be prepared, they could well open a plethora of possibilities of further applications in the form of wave guides etc.

Though there has been 'more room at the bottom' but the exploration have been shallow and there is a huge scope for exploring the 'bottom' further and there is more more hidden truths at the "bottom"!

Publications

1. On the Incorporation of Magnetic Fillers in Elastomer Matrices. M.R.Anantharaman. Philip Kurian, B.Banerjee, E.M.Mohammed and ***M. George***. Kautschuk Gummi Kunststoffe (Germany) 49, 424, 6/96
2. Microwave absorption studies of rubber ferrite composites. ***M. George***, E.M.Mohammed, M.R.Anantharaman, P.Kurian and K.Vasudevan Presented at the National Symposium on Advances in Polymer Technology held at Cochin University of Science and Technology during 1998